USAARL Contract Report No. CR-98-01

Development of a Standard for the Health Hazard Assessment of Mechanical Shock and Repeated Impact in Army Vehicles Phase 5

By

James Morrison
Daniel Robinson
George Roddan
Jordan Nicol
Marguerite Springer
Steven Martin
Barbara Cameron

B.C. Research Inc.
Vancouver, B.C., Canada

February 1998

19980311 110

DTIC QUALITY INSPECTED 8

Approved for public release, distribution unlimited.

U.S. Army Aeromedical Research Laboratory
Fort Rucker, Alabama 36362-0577

Notice

Qualified requesters

Qualified requesters may obtain copies from the Defense Technical Information Center (DTIC), Cameron Station, Alexandria, Virginia 22314. Orders will be expedited if placed through the librarian or other person designated to request documents from DTIC.

Change of address

Organizations receiving reports from the U.S. Army Aeromedical Research Laboratory on automatic mailing lists should confirm correct address when corresponding about laboratory reports.

Disposition

Destroy this document when it is no longer needed. Do not return it to the originator.

Disclaimer

The views, opinions, and/or findings contained in this report are those of the author(s) and should not be construed as an official Department of the Army position, policy, or decision, unless so designated by other official documentation. Citation of trade names in this report does not constitute an official Department of the Army endorsement or approval of the use of such commercial items.

Human use

Human subjects participated in these studies after giving their free and informed voluntary consent. Investigators adhered to AR 70-25 and USAMRMC Reg 70-25 on Use of Volunteers in Research.

Reviewed:

JOHN P. ALBANO
MAJ, MC, SFS
Director, Aircrew Protection
Division

Released for publication:

JOHN A. CALDWELL, Ph.D.
Chairman, Scientific
Review Committee

CHERRY L. GAFFNEY
Colonel, MC, SFS
Commanding

REPORT DOCUMENTATION PAGE

Form Approved
OMB No. 0704-0188

1a. REPORT SECURITY CLASSIFICATION Unclassified	1b. RESTRICTIVE MARKINGS
2a. SECURITY CLASSIFICATION AUTHORITY	3. DISTRIBUTION / AVAILABILITY OF REPORT Approved for public release, distribution unlimited
2b. DECLASSIFICATION / DOWNGRADING SCHEDULE	
4. PERFORMING ORGANIZATION REPORT NUMBER(S) USAARL Report No. CR-98-01	5. MONITORING ORGANIZATION REPORT NUMBER(S)
6a. NAME OF PERFORMING ORGANIZATION U.S. Army Aeromedical Research Laboratory 6b. OFFICE SYMBOL (*If applicable*) MCMR-UAD	7a. NAME OF MONITORING ORGANIZATION U.S. Army Medical Research and Materiel Command
6c. ADDRESS (*City, State, and ZIP Code*) P.O. Box 620577 Fort Rucker, AL 36362-0577	7b. ADDRESS (*City, State, and ZIP Code*) 504 Scott Street Fort Detrick, MD 21702-5012
8a. NAME OF FUNDING / SPONSORING ORGANIZATION 8b. OFFICE SYMBOL (*If applicable*)	9. PROCUREMENT INSTRUMENT IDENTIFICATION NUMBER DAMD17-91-C-1115
8c. ADDRESS (*City, State, and ZIP Code*)	10. SOURCE OF FUNDING NUMBERS PROGRAM ELEMENT NO.: 62787A PROJECT NO.: 30162787A878 TASK NO.: FA WORK UNIT ACCESSION NO.: DA336192

11. TITLE (*Include Security Classification*)
Development of a standard for the health hazard assessment of mechanical shock and repeated impact in Army vehicles, Phase 5 (U)

12. PERSONAL AUTHOR(S)
J.Morrison, D.Robinson, G.Roddan, J.Nicol, M.Springer, S.Martin, and B.Cameron

13a. TYPE OF REPORT	13b. TIME COVERED	14. DATE OF REPORT (*Year, Month, Day*)	15. PAGE COUNT
Final	FROM TO	1998 February	181

16. SUPPLEMENTAL NOTATION

17. COSATI CODES			18. SUBJECT TERMS (*Continue on reverse if necessary and identify by block number*)
FIELD	GROUP	SUB-GROUP	mechanical shock, repeated impact, vibration exposure, jolt, jolt standards, biomechanic modeling

19. ABSTRACT (*Continue on reverse if necessary and identify by block number*)
This study describes a health hazard assessment (HHA) method for evaluating exposures to repeated mechanical shocks in tactical ground vehicles (TGVs). This method will predict the risk of injury to the crew of a TGV given its seat acceleration signature. The HHA will identify both acute and chronic health risks resulting from either a few large amplitude shocks, or from prolonged exposure to travel over rough terrain. The HHA is based on experimental data obtained from volunteers exposed to a range of repeated shock exposures. The HHA consists of four components: dynamic response models which predict seat-to-spine transmission of acceleration; a biomechanical model which computes the compressive force in the lumbar spine in response to acceleration; a dose model for exposure to repeated shocks based on material fatigue characteristics; and an injury risk model based on the probability of failure. The output of the HHA method is used to determine the appropriate risk assessment code (RAC) as defined in the U.S. Army Health Hazard Assessment protocol. A software version of the HHA method with a graphical user interface (GUI) has been developed in MATLAB . The components of the HHA are outlined and some test results are presented.

20. DISTRIBUTION / AVAILABILITY OF ABSTRACT ☒ UNCLASSIFIED/UNLIMITED ☐ SAME AS RPT. ☐ DTIC USERS	21. ABSTRACT SECURITY CLASSIFICATION Unclassified
22a. NAME OF RESPONSIBLE INDIVIDUAL Chief, Science Support Center	22b. TELEPHONE (*Include Area Code*) (334) 255-6907 22c. OFFICE SYMBOL MCMR-UAX-SS

Executive summary

This report represents Phase 5 of a study entitled "Development of a Standard for the Health Hazard Assessment of Mechanical Shock and Repeated Impact in Army Vehicles", Contract No. DAMD17-91-C-115.

This report describes the final phase of a six year study consisting of the following 5 phases:

Phase 1: a comprehensive review of the literature, including field measurements of vehicle vibration, epidemiological data, experimental indices or health effects, dynamic response models, dose-effect models, and existing standards;

Phase 2: analysis of acceleration data obtained from military vehicles under a variety of operational conditions, development of unique methods for motion characterization, and development of appropriate motion simulations for the experimental phase;

Phase 3: pilot study conducted at the Multi-axis Ride Simulator (MARS) in Fort Rucker, Alabama, to develop suitable measures of human response to shock;

Phase 4: measurement of human response to individual shocks of different duration and amplitude, and to daily exposures to repeated mechanical shocks during experiments at the MARS in Fort Rucker, Alabama;

Phase 5: development of a health hazard assessment method based on the information gathered in the previous phases of the project.

Individual reports were provided detailing the analysis within each phase of the project. This report summarizes the outcome of Phase 5 and presents the proposed health hazard assessment (HHA) method for evaluation of exposure to repeated mechanical shocks in Army vehicles.

The HHA method developed in Phase 5 incorporates objective measures of human response to acceleration, and a clearly defined dose-effect relationship between the tactical ground vehicle (TGV) seat acceleration history and risk of injury to the operator and crew of a TGV. The complete HHA method includes test conditions, types of measurements, data reduction and analysis techniques, as well as the predictive models necessary to translate measurements into an estimation of health risk.

The predictive models that comprise the HHA method include:

- biodynamic response models that predict spinal acceleration in response to acceleration input at the seat;
- regression models that predict forces at the L4/L5 lumbar joint, given spinal acceleration;
- a fatigue based model to quantify the cumulative effect of repeated mechanical shocks; and
- an injury probability function which relates the cumulative dose to the probability of spinal injury within a normally distributed population.

The output of the HHA method is used to determine the appropriate Risk Assessment Code (RAC) as defined in Army Regulation 40-10. A description of the models and their development is included in this report. A software version of the HHA method, complete with a graphical user interface (GUI), has been developed to run under MATLAB™ software.

The HHA method can be applied to the identification of both acute and chronic health risks resulting from either a few large amplitude shocks, or from prolonged exposure to repeated shocks due to travel over rough terrain. Within this context, the HHA method should have applications outside of the military environment. In particular, the HHA method is relevant to the evaluation of shock exposures encountered by vehicle operators in mining, forestry and construction.

Table of contents

List of illustrations

List of tables

Introduction

Background

The purpose of Phase 5 was to develop a health hazard assessment (HHA) method which is suitable for evaluating the risk of injury from exposure to repeated mechanical shocks in tactical ground vehicles (TGVs). The operation of modern TGVs over rough terrain produces repetitive mechanical shocks which are transmitted to the soldier primarily through the seat. Repetitive shocks from military vehicles are typically low frequency (2 to 20 Hz) waveforms with amplitude up to 5 g (49 $m \cdot s^{-2}$) and separated by approximately 0.25 seconds or more (Roddan et al., 1995; U.S. Army Health Hazard Assessor's Guide, 1996).

The existing method of HHA for whole-body vibration (WBV) is based on International Organization for Standardization (ISO) 2631 (1985), which uses a root mean squared (rms) measure of vibration amplitude at the seat. This standard was not intended for the evaluation of repeated shocks. There is, therefore, a requirement for an improved method of HHA which is specific to repeated mechanical shock exposure in TGVs. This includes the HHA for exposure to vibration with high crest factors (or the ratio of peak acceleration to the rms acceleration).

Within this report, the term "shock" has been used to refer to a transient acceleration event imparted by direct transmission of vehicle motion through the seat. The direction of shocks and acceleration are expressed according to the basicentric coordinate system of ISO 2631 (1985). Therefore, in the upright seated posture, the x axis refers to fore-aft motion (where fore is the positive direction), the y axis refers to lateral motion (where left is the positive direction), and the z axis refers to vertical motion (where up is the positive direction).

Phase 5 objectives

The main objective of Phase 5 was to develop a HHA method for evaluating exposure to mechanical shocks and repeated impact.

Human response models

The first step in the development of a HHA method was to review and evaluate existing standards and biodynamic models. Low back pain and chronic degeneration of the spine have been associated with exposure to WBV and repeated shock (Dupuis and Zerlett, 1987; Hansson and Holm, 1991; Sandover, 1986a; Hulshof and van Zanten, 1987). Epidemiological studies suggest that the lumbar spine is more susceptible to damage and discomfort in response to vibration and repeated mechanical shock than the thoracic and cervical regions. However, the thoracic spine may be more susceptible to damage in response to a single impact of higher magnitude (Jones, Madden and Leudeman, 1964). The proposed HHA method for evaluating exposure to repeated shock is, therefore, focused on the risk of injury to the lumbar spine.

Biodynamic models have varied from relatively simple mass spring models containing one degree of freedom (Payne, 1992) to highly complex representations of the human body containing multiple degrees of freedom (Orne and Liu, 1971; Hopkins, 1972) or which are capable of simulating 3-dimensional motion (Belytschko and Privitzer, 1978; Amirouche and Ider, 1988).

A spinal model that has gained popularity is the dynamic response index (DRI) developed by Payne (1965), and revised as Payne (1992) to predict the effect of vertical (z axis) acceleration. The DRI was developed from the response of a single mass-spring-damper system, and the index is proportional to the peak compressive force developed in the spring and damper. A similar model was proposed by Fairley and Griffin (1989), based on data from humans exposed to lower amplitude vibrations. The Fairley-Griffin model contains a lower natural frequency (fn = 5 Hz) and higher critical damping ratio (ζ = 0.48) than the DRI (fn = 11.9 Hz and ζ = 0.35). Payne (1984) proposed similar models for the response to fore-aft (x axis) acceleration (fn = 10 Hz; ζ = 0.15) and lateral (y axis) acceleration (fn = 7.2 Hz; ζ = 0.15).

A more physiological approach was reported by Blüthner, Hinz and Seidel (1986) and Seidel, Blüthner and Hinz (1986). The authors describe a biomechanical model in which the compressive load at the L3/L4 disc was calculated from measures of trunk acceleration, upper torso mass and EMG activity. At 3 $m \cdot s^{-2}$, and frequencies of 1 to 7 Hz, the computed disc compressive forces

ranged from 2 to 4.5 kN. The authors concluded that compressive force does not correlate uniformly with vibration intensity. Hinz et al. (1994) applied a revised version of this model to estimate compressive force at the L3/L4 joint in response to 4 $m \cdot s^{-2}$ transient accelerations.

A number of limitations are apparent in existing human response models. Most models are based on a limited range of experimental data, and have not been tested with repeated mechanical shocks or validated against measured data. Few models include prediction of chronic health effects or tissue damage. Many of the models, including some of the more complex mathematical models, are restricted to uniaxial acceleration. Despite these criticisms, there have been several important contributions to biodynamic modeling which have direct relevance to the development of a HHA method.

Standards

A number of standards have been published for evaluation of WBV and shock. The most commonly used is the ISO 2631 (1974, 1985). It uses frequency weighting filters and the rms acceleration level to evaluate the health effects of exposure. The ISO 2631 (1985) is restricted to vibrations having a maximum crest factor of 6, and thus excludes exposures containing shocks. Nevertheless, this standard has been used in most reports of vehicle acceleration data. The newly revised ISO 2631 (1997) includes analysis of vibrations with crest factors up to 9.

The British Standards (BS) 6841 (1987) recommends that exposures containing shocks should be evaluated using a vibration dose value (VDV) of the form:

$$VDV = \left(\int_0^T a(t)^4 dt\right)^{1/4} \qquad (1)$$

where a(t) represents the frequency weighted seat acceleration. The VDV does not provide limits for health effects. However, a VDV of 15 is said to cause severe discomfort (BS 6841, 1997), and is approximately equivalent to the health exposure limit of the ISO 2631. A revision of ISO 2631 (1997) includes methods of evaluating repeated shocks, including the VDV, but exposure limits and risk of injury are not cleary defined.

An alternative method of evaluating repeated shocks was reported by the Air Standardization Coordinating Committee (ASCC,

1982). It was based on the work of Allen (1977) and Payne (1978) who further developed the DRI model to account for the health effects of multiple shocks. The ASCC used a fatigue-failure model in which the number of shocks required to cause failure was a function of the predicted stress level (or DRI) of a single shock and the estimated static failure stress (or DRI_{MAX}). The health hazard assessment was based on a small amount of data (mainly spinal injury data from air crew ejection) at relatively high DRI values, and was limited to positive z axis shocks. Payne, Brinkley and Sandover (1994) have shown that the DRI provided a good correlation with subjective perception of shocks. However, Anton (1986) examined 223 air crew ejections and found the DRI to be a poor predictor of injury. Despite these limitations, the DRI model output is related to injury data, and some validation data have been reported. Thus, at the present time, the ASCC offers the best available guide to the health hazard assessment of repeated impacts.

Only the ASCC standard provides a prediction of severe discomfort and percent injury level. However, these limits are based on the output of a model which is a poor predictor of spinal transmission. In addition, the suggested dose level for severe discomfort contained in the BS 6841 (1987)(i.e., VDV less than or equal to 15) does not appear to be applicable to a military population. The Phase 4 experiments proved that most soldiers are capable of tolerating a daily VDV of approximately 60. It should be noted that at this level of exposure, some subjects experienced a high level of discomfort and residual stiffness post exposure. However, due to the non-linear nature of the VDV model, a VDV of 60 represents more than 250 times the number of shocks required to attain a VDV of 15.

Other Phase 4 results showed that existing standards are inadequate to describe the human response to shock. Specifically:

- the magnitudes of shock transmission determined by the BS 6841 (1987) frequency weighting filters and the ASCC biodynamic model (DRI) do not accurately reflect spinal transmission of shocks;

- in the z axis, there is a very distinct non-linear magnitude effect that cannot be simulated by current linear models such as the DRI;

- the BS 6841 (1987) and ISO 2631 (1985) use the same frequency weighting function for x and y axes, yet measured transmission ratios differ in the x and y axis; and

- subjective ratings of shock exposures do not correspond with exposure doses as measured by the VDV.

The above findings support the need to develop a new and separate standard for exposure to mechanical shocks. The basis for such a standard has been developed and is presented in the format of an HHA method.

Military significance

The U.S. Army has established a HHA Program to evaluate and control health hazards in support of the Army's military capabilities and performance. Overall, the HHA Program is an integrated effort that supports all areas and mission needs. Its specific objectives which are relative to this contract are to: preserve and protect the health of individual soldiers; enhance soldier performance; reduce readiness deficiencies related to health hazards; and reduce personnel compensations claims by eliminating or reducing injury or illness caused by health hazards associated with the use of Army systems (Liebrecht, 1990).

Health hazard assessment refers to the process of identifying, evaluating, and controlling risks to the health and effectiveness of personnel who test, use, service, or support Army systems. Many of the effects of health hazards are not immediate and may appear only after months or years of exposure. Such delayed effects may limit long-term contributions to the Army and may develop into serious health problems in the future, although the short-term impact the soldier's performance may be minimal (Liebrecht, 1990).

The HHA program utilizes resources to apply biomedical knowledge and principles to support the development of military material systems (Liebrecht, 1990). A variety of health hazards can directly affect the soldier operating military systems. In relation to this project, soldiers who operate or are transported in tactical ground vehicles (TGVs) are exposed to mechanical forces which are considered health hazards, including vibration and shocks.

With the continuing emphasis on increased mobility and firepower, new TGVs developed by the U.S. Army are generally lighter in weight and capable of considerably higher speeds than their predecessors. This combination of lower weight and higher speed over rough terrain produces repetitive mechanical shocks which are transmitted to the soldier primarily through the seating system. Anecdotal evidence indicated that 50 percent of a company reported blood in the urine following operation of fast attack vehicles (USAARL, unpublished). Under certain motion environments, exposure to shock and vibration poses health and safety threats to the crew and performance degradation due to fatigue (Larson, Well and Kaplan, 1973; Heslegrave et al., 1990).

There is a requirement to develop exposure standards for repetitive whole-body shocks which are relevant to the environment of soldiers operating modern tactical vehicles and weapon systems. Currently the Army relies on standard guidelines to assess the effects of repeated shock and vibration on performance, fatigue, and health and safety of the soldier while operating or being transported by TGVs. Most standards cited in MIL-STD 1472D are predicated on ISO 2631 (1985). The ISO standard is largely based on subjective measurements of fatigue and comfort, rather than health, and does not adequately account for the health effects of repeated shock (Village and Morrison, 1989). It is essential that cause-effect relationships between the mechanical environment and injury (acute and chronic) be determined for quantification of a health hazard assessment.

Overview of the health hazard assessment (HHA) method

Any HHA method capable of predicting the risk of injury from repeated mechanical shocks must be based on data from a wide range of studies encompassing human response, injury incidence, material properties and theoretical models. Therefore, the approach adopted in this study was to construct a HHA method which is based on components selected from existing models, human response data, tissue characteristics and injury data.

From a review of the literature, it was established that there was insufficient experimental data on human response to repeated shocks to either test existing models or develop a new HHA method. Thus, a number of experiments were performed during Phases 3 and 4 in which volunteers were exposed to a range of shock profiles and prolonged repeated shock exposures typical of those measured in TGVs (Village et al., 1995; Cameron et al., 1996).

The Phase 4 experiments provided seat acceleration, spinal acceleration, displacement (Optotrak), internal pressure, and muscle activity data. In Phase 3 and Phase 4, these data were utilized in the development and validation of the proposed HHA method. No objective evidence of injury to organ systems or tissues was apparent in the biochemical measures and little evidence of muscle fatigue was observed after exposure to severe motion. However, there was consistent subjective feedback regarding degraded physical status and perception of motion severity, fatigue, and discomfort.

It was clearly demonstrated that the motion conditions in these experiments could result in extreme soreness and pain. Given the lack of objective evidence of injury and the relatively low levels of muscle activity indicated by electromyography (EMG), it was likely that this soreness was related to inflammation or damage to spinal structures (i.e., vertebrae, intervertebral discs, ligaments). Furthermore, long-term exposure to vehicle motion has been associated with degenerative changes and injury to these structures (e.g., Boshuizen, Hulshof and Bongers, 1990; Wikström, Kjellberg and Landström, 1994). Hence, an estimate of stress in the spine, combined with known material properties of vertebrae and discs (e.g., Brinckmann, Biggeman and Hilweg, 1988) and existing models of mechanical fatigue of vertebrae (Lafferty, 1978; Sandover, 1983, 1986a; Seidel, Blüthner and Hinz, 1986; Hansson, Keller and Spengler, 1987) may provide a good estimation of the probability

of acute injury. Although not a component of the present HHA methodology, incorporation of a recovery model with material fatigue principles could extend the model to the case of cumulative damage or degeneration over the longer term.

Ideally, the structure of the HHA method should include the following features:

- a means of predicting human spinal response (acceleration) in 3 axes;
- a biomechanical model capable of computing internal forces in response to shocks;
- a means of relating biodynamic response (acceleration) to force (or tissue stress) within the body;
- the ultimate (compressive) strength of the L4/L5 vertebral joint and the fatigue properties of cyclic loading;
- a means of predicting the cumulative effect of repeated mechanical shocks (a fatigue based dose model);
- a means of assessing probability of injury, based on the population variance in the data related to maximum strength of vertebrae and/or acute injury.

A review of existing models and standards established that none satisfies all of the above criteria. From the above requirements, a new HHA structure was developed which integrates information from four distinct models:

- biodynamic response models which predict acceleration of the lumbar vertebrae in the x, y and z axes in response to mechanical shocks input at the seat;
- a biomechanical model which analyzes spinal compressive force at the L4/L5 joint in response to shocks input at the seat;
- a dose model for exposure to repeated shocks based on prediction of spinal compressive forces and material fatigue failure theory; and
- an injury risk model based on the compressive strength of vertebrae, population variance and the probability of failure.

A brief overview of these four component models is provided below, followed by a more detailed account of their development.

Biodynamic response models

As a first step, the characteristics of existing dynamic response models and filters were compared with the spinal acceleration data collected in Phase 4 (Cameron et al., 1996). During Phase 4 experiments, seated subjects were exposed to a series of shocks input at the seat in the x, y and z axes. Each shock was in the form of a single damped sinusoid, having a fundamental frequency between 2 to 20 Hz and amplitude of $\pm$ 0.5 to $\pm$ 4 g. Acceleration was measured at the seat and at the skin surface over the lumbar vertebrae. It was found that the BS 6841 (1987) filter and DRI (Payne, 1992) z axis models underestimated spinal transmission of the larger amplitude (2, 3 and 4 g) shocks in the z axis, and did not accurately reproduce the spinal response to negative z axis shocks. In addition, the spinal response in the z axis was non-linear with amplitude. Although the response to seat accelerations in the x and y axes was approximately linear, the DRI (Payne, 1992) x and y axis models overestimated transmission in these axes. Details of these findings are provided in the Phase 4 Report (Cameron et al., 1996).

Based on these findings, a series of dynamic response models were developed and tested using system identification techniques and the experimental data collected in Phase 4. The models (described in detail in a later section of this report: pages 35-47)provide a continuous (time series) prediction of the x, y and z axis acceleration of the lumbar spine in response to the x, y and z axis input accelerations at the seat.

In the x and y axes, two separate strategies were investigated. The spinal response was modeled in the form of linear difference equations, (equations 24 and 25, page 41) using MATLAB™ systems identification software, and in the form of a mechanical analog, similar to that of the DRI. The latter consisted of a mass, spring and damper. The natural frequency, fn, and critical damping ratio, ζ, of the models were adjusted to provide a best fit between the experimental data and the model output. Although the linear difference equations gave slightly better results in terms of both rms and rmd error, the analog models provided a more stable frequency response over the range

of testing (0 to 80 Hz). Hence, in the HHA method the spinal response to acceleration in the x and y axes is modeled using a second order linear model having the parameters fn = 2.125 Hz and $\zeta = 0.22$.

As the z axis response was found to be non-linear (Cameron et al.,1996), a different strategy was used to model the response in this axis. A recurrent neural network (RNN) was developed and trained to represent the system dynamics using the acceleration data measured in Phase 4. The RNN predicted acceleration output at the lumbar spine based on the previous acceleration inputs at the seat and previous predicted outputs. Although more difficult to train, the RNN proved to be more desirable than a linear difference equation because it predicted the spinal response more accurately over the range of shock amplitudes tested (Nicol, 1996). A series of neural networks with different parameters were trained using samples of input-output data selected from a typical subject and then tested using unseen data. The best RNN developed consisted of 12 input processing elements (PEs), 7 hidden layer PEs and 1 output PE. The quality of the output wave forms achieved using the RNN were superior to those predicted by the DRI or the BS 6841 frequency weighting filters. The rms and rmd error between the predicted lumbar spine acceleration and the measured lumbar spine acceleration was smaller for the RNN than the BS 6841 frequency weighting filter, the ASCC (1982) DRI, or the revised DRI (Payne, 1991). Further details of RNN development are provided in the section entitled, "Development of the health hazard assessment method - Biodynamic response models".

Biomechanical model

A biomechanical model was developed to calculate the compressive force at the L4/L5 lumbar joint. The model utilizes measured human response data as input. Thus, it is not a predictive model, and a detailed biomechanical analysis using data measured form the vehicle operator does not form part of the HHA method. However, the results of the biomechanical model were integrated into the HHA method in the following manner. The biomechanical model was applied to the experimental data obtained from Phase 4 to provide information on the compressive forces generated at the lumbar L4/L5 joint in response to mechanical shocks in the x, y and z axes. This information was then used to relate the peak spinal accelerations predicted by the dynamic

response models (above) to the compressive force acting on the L4/L5 lumbar vertebral joint.

Input to the biomechanical model consisted of position and acceleration data of the upper body in the x, y and z axes, as well as abdominal pressure. These data were collected in Phase 4. Abdominal pressure was measured by a specially designed rectal probe housing a miniature pressure transducer. Displacement was measured by infrared emitting diodes placed over the cervical (C7), thoracic (T4, T6, T8, T9, T10 and T12) and lumbar (L1 and L5) vertebrae using an Optotrak system. The Optotrak data were used to determine the position and acceleration of the upper body centre of mass.

The initial biomechanical model developed considered the upper body mass as a rigid body as in the model of Seidel, Blüthner and Hinz (1986) and Hinz et al. (1994). The results obtained using this model proved that it was impractical for large amplitude (i.e., greater than 1 g) shocks (Robinson et al.,1995). The mass of the upper torso was therefore partitioned into two compartments representing the spine and soft tissues. The two compartments were each further subdivided into three spinal levels in order to accomodate the effects of spinal flexion on acceleration forces.

The new biomechanical model computed forces and moments due to the linear and angular acceleration of the upper body mass and due to intra-abdominal pressure. Abdominal and spinal muscle force and the resultant lumbar compressive and shear forces (at the L4/L5 joint) were then determined using an anatomical model and the principle of dynamic equilibrium. This model is described in detail in a later section of this report: pages 47-58.

The human response data collected during Phase 4 were used as inputs to the model, with output being the compressive (Cz) and shear (Cx, Cy) forces at the L4/L5 lumbar joint. Peak forces were calculated for a series of shocks ranging from negative 4 g to positive 4 g in the x axis, positive 0.5 to positive 4 g in the y axis and negative 2 g to positive 4 g in the z axis. Compressive and shear forces resulting from z axis shocks were larger than those for x or y axis shocks. These estimates of joint force, together with cadaver data of the ultimate strength of vertebrae, were subsequently used in a repetitive stress dose model in order to establish risk of injury.

Repetitive stress dose model

A dose model was developed which incorporates both a theory of fatigue failure and the material properties of the human L4/L5 vertebral joint. The dose model was based on the fatigue theory of Miner (1945) and the proposals of Payne (1976), Allen (1977) and Sandover (1983) that damage to the vertebrae due to repetitive shocks can be predicted using the concept of fatigue failure.

Miner (1945) proposed that the degree of fatigue (D) of a material subject to repeated stress can be expressed by the ratio (n_i/N_i), where n_i is the number of cycles completed at stress S_i and N_i is the number of cycles required to cause failure. Thus, failure occurs when D = 1. This approach to modeling fatigue has been extended to include biological materials, based on the experimental data of several researchers (see Sandover 1986b). This relationship can be generalized to any number of stress levels and cycles and expressed in the form:

$$D = \sum(n_i/N_i) \qquad (2)$$

In addition, the experimental results of Lafferty (1978) and Carter et al. (1981) show that when bone is repeatedly stressed, the number of cycles (N_i) required to cause failure can be modeled as:

$$N_i = (S_u/S_i)^x \qquad (3)$$

where S_u = static failure stress, S_i = applied repetitive stress level, and x is a constant for each material (Sandover, 1986b). The equivalent static stress level, S_e, which will produce a fatigue of D from a single loading can be written as:

$$S_e = \{\sum[n_i(S_i)^x]\}^{1/x} = S_u \cdot D^{1/x} \qquad (4)$$

The equivalent stress value S_e can be considered as the stress "dose" applied to the material. This relationship has a similar form to the existing DRI dose function (Payne, 1991).

By substituting Cz_i (the compressive force estimated from the biomechanical model) for S_i (stress) in the above equation, a spinal compressive force "dose value" (Cz_e) was obtained for the lumbar vertebrae in which Cz_i represented the peak lumbar compressive force due to shock i, and Cz_u represented the

ultimate compressive strength of the lumbar L4/L5 joint (i.e., the compressive force required to cause injury). An exponent of x = 6 was chosen for the dose model based on the available literature for fatigue failure of bone (Lafferty, 1978; Carter et al., 1981; Brinckmann, Biggeman and Hilweg, 1988; Hansson, Keller and Spengler, 1987). The ultimate strength of the L4/L5 spinal unit, Cz_u, was defined as 10,093 N, based on the combined experimental data of Hutton and Adams (1982) and Porter, Adams and Hutton (1989). Details of this model are provided in the section: "Repetitive stress dose function".

Integration of the biodynamic and biomechanical models with the repetitive stress dose function

In order to develop an HHA method that could be related to existing knowledge of tissue properties, a biomechanical model was applied to estimate internal vertebral loading in response to individual shocks. This model is described in the section "Three segment eccentric segregated mass model". The biomechanical model offers the advantage of a detailed analysis of lumbar compressive forces. However, it is an inverse dynamic model that requires displacement and acceleration data measured from the soldier as input. Hence, it is not a predictive model in the same manner as the dynamic response models discussed above. In these models the human acceleration response is predicted directly from the acceleration data input at the seat (i.e., the vehicle shock signature). Therefore, the biomechanical model was implemented in conjunction with the dynamic response models to determine the peak compressive force generated at the L4/L5 joint in response to shocks measured from a vehicle.

The output of the biomechanical model obtained from the Phase 4 data was compared with the outputs of the dynamic response models developed for the HHA. Regression functions were computed which related the peak compressive force developed at the L4/L5 joint to the corresponding lumbar spine acceleration response to shocks in each axis. With the aid of these relationships, the peak spinal accelerations predicted by the dynamic response models (in response to shocks input at the seat) can be used to estimate the corresponding peak lumbar compressive forces. These compressive force values are then used by the repetitive stress dose model (equation 48) to obtain an accumulated compressive force dose (Cz_e) measured in Newtons of force. Further detail on the dose model is provided in the secton entitled, "Development of the health hazard assessment method - Repetitive stress dose model".

Injury risk model

The output of the dose model provides a single compressive dose value for any given seat acceleration time series input to the dynamic response models. In accordance with normal biological variation, there will exist a range of dose values at which individual operators might be expected to experience injury or health effects. Hence, rather than associating the presence or absence of injury with a discrete dose value of 10,093 N (i.e., $Cz_e = Cz_u$), it is more practical to express the health effect of any dose in terms of the probability of sustaining injury. This can be achieved by relating the computed dose value to a cumulative probability function, conceptually illustrated in Figure 1.

The probability of injury (or compressive failure) is based on the distribution of a normal variable, which can be calculated using the relationship:

$$\Phi = f\ (Cz_e,\ Cz_u,\ \sigma) \qquad (5)$$

where Φ = probability of injury due to material failure and σ = standard deviation of ultimate strength Cz_u. The variance (σ) of the underlying probability density function can be derived from cadaver data on the static strength of the vertebra-disc complex. The injury risk model was implemented using a mean compressive strength value of Cz_u = 10,093 N and a standard deviation of σ = 1,926 N derived from Hutton and Adams (1982) and Porter, Adams and Hutton, (1989). These data were considered to be the most reliable information available in terms of measurement technique and the age range (19 to 46 years) of cadaver specimens. Details of the injury risk model are provided in the section entitled "Development of the health hazard assessment method - Injury risk model".

Integration of model components

The dynamic response models, biomechanical model output, dose model and injury risk model were combined to produce HHA method. Given input seat acceleration time series in the x, y and z axes, the model computes the probability of injury for a specified exposure duration.

A fundamental requirement of the HHA method is that it must be integrated into the existing U.S. Army Health Hazard Assessment Program (AR 40-10, 1991). The probability of injury predicted by the HHA method, therefore, is used to determine the hazard severity level on a scale of I to IV. The hazard severity level is combined with the probability of hazard occurrence (determined by the operational definition of the vehicle) to determine the corresponding Risk Assessment Code (RAC) as defined in the AR 40-10 (1991).

A software version of the HHA method with a graphical user interface (GUI) has been developed using MATLAB™ software. The HHA GUI allows for the selection of input data files of vehicle seat acceleration in the x, y and z axes, the intended exposure duration (days, hours, minutes, seconds), and the expected probability of occurrence of this exposure (ranked A to E according to whether the particular exposure is likely to be frequent, occasional or improbable). The HHA GUI program then calculates the spinal acceleration response, the compressive force dose value, and injury probability. The resultant hazard severity level and RAC value are then reported on the HHA GUI. The HHA GUI also provides options to display the seat and spinal acceleration, the lumbar compressive force dose value and the probability of injury as a function of exposure time.

The HHA method was tested using a selection of repeated shock profiles and exposure durations varying from 6 hours to 20 years. The input data for this simulation were obtained from experimental data collected in Phase 3 and Phase 4. Results indicated that the most severe exposure containing 2 and 4 g z axis shocks would cause marginal injury in one day, but could lead to severe injury if soldiers were exposed on a daily basis for a prolonged period. By comparison, exposure to rms vibration levels equivalent to the ISO 2631 (1985) health guidance limit provided negligible to marginal injury risk, depending on shock content, when accumulated over a period of 20 years.

Military vehicle HHA test protocol

A test protocol was developed for evaluation of military vehicles using the HHA method. It is the intention of the vehicle test and evaluation procedure to apply a standard method for evaluating the health risk associated with the vibration and impact environment of any Army vehicle. Knowledge of the health

risk associated with specific operating situations can be applied during vehicle design and acquisition, or for planning operations and exercises to minimize both chronic and acute injuries to the soldier.

The test protocol includes:

- operating conditions under which a vehicle is to be tested;
- types of measurements to be made;
- methods of data reduction and analysis; and
- assessment of health hazard using risk assessment codes.

Details of the military vehicle HHA test protocol are provided in the section "Military vehicle test protocol" and in the Phase 5 report (Morrison et al., 1997).

Development of the health hazard assessment method

The development of an HHA method for exposure to repeated mechanical shock involved an evaluation of existing methods, models and standards, followed by the development of a series of novel models to sequentially relate seat acceleration to spinal acceleration (biodynamic models), spinal acceleration to internal spinal forces (biomechanical model), the cumulative effect of repeated spinal loading (dose model), and the associated health risk (injury probability model). The review of existing models and the development of the novel models that comprise the proposed HHA method are outlined below.

Existing models and methods

A fundamental objective in the development of the biodynamic models was to predict the physical behaviour of the human body (or individual tissues). The output of the model may be expressed in terms of displacement, acceleration, force, material stress or physiological response. Thus, a well developed biodynamic model can be an ideal tool for assessing the health effects of mechanical shock and vibration.

To evaluate the applicability of using existing biodynamic models to predict health effects from repeated mechanical shock, an understanding of the human response to shock is required. Although very little has been published regarding the human response to low level (less than 5 g) shocks, some valuable data can be gained by studying the more readily available data regarding human response to vibration. One of the more important applications of knowledge of the human response characteristics and biodynamic models which predict human response is the development of standards and guidelines designed to promote health and prevent injury.

This section provides a brief review of the current status of the literature with respect to human response to vibration and shock, biodynamic models of the human response, and standards that apply this information.

Human response to vibration and mechanical shock

When the human body experiences a disturbance, as in exposure to vibration or shock, it demonstrates a dynamic response. External displacements applied to the body may be amplified or attenuated in different tissues, resulting in local stresses. The potentially harmful effects of vibration or shock can be assessed by measuring the transmitted acceleration (and hence stress) of different sub-systems of the body in response to an acceleration input. Transmission of acceleration through the body can then be expressed in terms of a transfer function. The acceleration transfer function provides insight into the behaviour of a body sub-system and enables the investigator to assess the magnitude and frequency of input acceleration at which a particular tissue is likely to suffer damage.

Numerous researchers have investigated the transmission of acceleration from the seat to different levels of the spine. Panjabi et al. (1986) measured accelerations of the lumbar vertebrae at an input level of 1.0 and 3.0 $m \cdot s^{-2}$ at the seat. A resonant frequency of 4.4 Hz and mean transmission factor of 1.6 was measured in the z axis. The x axis accelerations at the seat displayed transmission factors of 0.2 to 0.8 with no obvious resonant frequency.

Donati and Bonthoux (1983) reported a maximum seat-to-thorax transmission in the z axis at 4 Hz, with a transmission factor of approximately 2.3. Mechanical driving impedance measures showed resonances at 4 Hz and 8 Hz, which were slightly lower than those at 5 Hz and 11 Hz measured in the z axis by Coermann et al. (1960).

The characteristics of the vibration response have also been described in the form of apparent mass, m_{app}, representing the complex ratio between applied force and acceleration.

$$m_{app} = \frac{\text{Force transmitted at seat}}{\text{Acceleration at seat}} \qquad (6)$$

Selection of apparent mass as a method of displaying the system response provides an output function which is more readily interpreted by the experimenter, and which can be normalized to the body weight of each subject. At zero frequency, the apparent mass in the z direction simply represents the body mass of the subject (Fairley and Griffin, 1989).

Fairley and Griffin (1989; 1990) measured apparent mass in different postures and at different levels of acceleration in the x, y and z axes. Acceleration of the seat in the x axis produced a heavily damped response, with resonant frequencies at 0.7 Hz and 2.5 Hz. When provided with a backrest, a single, more pronounced resonance occurred at approximately 3.5 Hz. The authors suggest that the lower resonant frequency represents body sway, while the secondary resonance represents linear translation rather than rotation of the torso. It was observed that without a backrest, body sway was controlled by voluntary or involuntary muscle contraction (Fairley and Griffin, 1990). Lateral motion produced a less well defined response of apparent mass, with resonant frequencies of 0.7 Hz and 2 Hz without back support, and a single resonance at approximately 1.5 Hz when supported by a backrest. The effect of the backrest was much less pronounced in the lateral direction (y axis).

The resonant frequency of the apparent mass function in the z axis decreased as acceleration amplitude increased from 0.25 to 2.0 $m \cdot s^{-2}$, whereas, resonant frequency increased in response to muscle tension. This finding contradicts the expectation that muscle tension, and hence resonant frequency, would increase with acceleration magnitude, and suggests that the dynamic response of the body is non-linear.

To compare the data of different authors using a variety of units, Sandover (1982) converted z axis impedance data to apparent mass. Results typically show a flat response at low frequencies, resonance at 4 to 6 Hz, and a rapid attenuation of the apparent mass function at higher frequencies. A resonant frequency of 5 Hz has been attributed to the spinal column and pelvis (Sandover, 1982). However, the intervertebral discs have been shown to be too stiff in axial compression to attenuate low frequency shocks associated with vehicle motion (Markolf, 1970; Belytschko and Privitzer, 1978; Smeathers, 1989). Belytschko and Privitzer (1978) concluded that the resonance of driving point impedance shown at 5 Hz resulted from a combination of pelvic, visceral and spinal elements, and reflected the elastic properties of the buttocks, abdominal wall and spinal flexion respectively. This conclusion is supported by Sandover (1982), who reported the pressure response in the lower intestine of upright seated subjects to z axis acceleration to be similar to that of apparent mass, having a peak pressure at 5 to 6 Hz.

Although measures of driving point impedance and apparent mass provide useful indications of the response of the body, these measures do not provide sufficient detail to determine the behavior or stresses within individual systems such as the abdomen or spine. In particular, there is a lack of experimental data regarding non-linearities of individual systems, particularly in response to mechanical shocks and impacts.

Biodynamic response models

During the past 40 years, attempts have been made to model the biodynamic characteristics of the human body. These models have varied from relatively simple mass spring models containing one degree of freedom (Payne, 1992) to highly complex representations of the human body containing multiple degrees of freedom (Hopkins, 1972) and capable of simulating 3-dimensional motion (Amirouche and Ider, 1988). Few models have been validated with experimental data and this is typically only for low amplitude rms vibration (ISO/DIS 2631-1, 1995). Few validated models have been designed to simulate the effect of shock or impact. These would include the DRI (Payne, 1975; 1992) and the models of Belytschko and Privitzer (1978). However, none of the models have been tested for their ability to predict human resopnse to repeated shocks with amplitudes commonly seen in off-road vehicles (± 0.5 g to ± 4 g).

The inability of uniaxial lumped parameter models to provide direct insight into spinal injury mechanisms was highlighted by the work of Orne (1969) and Orne and Liu (1971). Orne and Liu (1971) investigated the effect of simultaneous impact accelerations on the spinal column in three independent motions (z axis translation, x axis translation, and y axis rotation) using a discrete parameter model with viscoelastic elements for discs. Large bending moments occurred in the thoracic region which, together with axial force, produced a high compressive stress in the anterior aspect of the thoracic vertebrae. These results were similar to injury data from pilot ejections (Hirsch and Nachemson, 1961). The three dimensional whipping motion, in response to an x axis acceleration component, increased shear and bending stresses in the lumbar region and decreased the axial response (Orne, 1969). The analysis was repeated using a uniaxial model (z axis) which produced substantially different results.

Prasad and King (1974) developed a discrete parameter model of the spine in which each vertebra had 3 degrees of freedom in the sagittal plane (z and x axis translation and y axis rotation). A new feature introduced in the model, which differentiates it from those of Orne and Liu (1971) and Braunbeck and Wilkinson (1981), is the transmission of load through the articular facets, based on experimental work using cadavers (Prasad, King and Ewing, 1974). Results of the model provided a good correlation with experimental results for different impact accelerations and spinal postures.

A sophisticated discrete parameter model of the spine was also developed by Belytschko and Privitzer (1978). Their model included the head, vertebrae and ribs interconnected by deformable elements representing the discs, ligaments and viscera. Outputs from the models gave good agreement when compared with human impedance data. The model was further developed to include an injury criterion based on stresses in the vertebral bodies resulting from axial compression and bending. This model and the corresponding injury criterion were primarily concerned with destructive impact and compressive fracture of the vertebrae. Hence, it does not address the risk of fatigue-induced injury due to repetitive mechanical shock experienced in vehicle operation.

Muksian and Nash (1974) reported a uniaxial lumped parameter model of a seated human. Individual elements represented the head, vertebral column, upper torso, thorax, diaphragm, abdomen and pelvis. This model included non-linear stiffness and damping properties for the torso, thorax and abdomen complex. The authors were obliged to assume linear properties for frequencies less than 10 Hz, and introduce non-linear properties for frequencies greater than 10 Hz. The model represents a mathematical fit of experimental data rather than a physiological model including active muscle properties.

Most spinal models, regardless of sophistication, treat the musculature as passive viscoelastic elements. A more physiological approach is reported by Blüthner, Hinz and Seidel (1986) and Seidel, Blüthner and Hinz (1986). The authors describe a biomechanical model in which the compressive load at the L3/L4 disc is calculated from measures of trunk acceleration, upper torso mass and EMG activity. The transmissibility between T5 and the seat are measured at peak (maximum and minimum) accelerations. An output of muscle force, ligament force and disc compressive force with time is provided by the model.

At 3 $m \cdot s^{-2}$, and frequencies of 1 to 7 Hz, the computed disc compressive forces ranged from 2 to 4.5 kN. The main conclusions of this study are that muscle activity does not protect the intervertebral disc from stress at most frequencies, and that the magnitude of compressive forces does not correlate uniformly with vibration intensity. The authors also calculated that the magnitude of stress at this vibration amplitude was sufficient to cause fatigue fractures of the cartilaginous end plates. A more thorough presentation of this model and its applicability to the evaluation of shocks is provided below in the section entitled "Biomechanical Modeling".

The single degree of freedom model employed by the DRI has gained considerable attention since initially presented by Payne (1965) to predict the response to vertical acceleration. The parameters for the vertical model have been modified several times, with the most recent version (Payne, 1992) defined by its undamped natural frequency (fn = 11.9 Hz) and damping ratio (ζ = 0.35). Payne (1984) extended the DRI model to the x and y axes, deriving model parameters (y axis: fn = 7.2 Hz and ζ = 0.15; and x axis: fn = 10 Hz and ζ = 0.15) based on chest acceleration data from Brinkley (1971). Although this model has been used for repetitive shock evaluation (ASCC, 1982) and is useful for the evaluation of discomfort (Payne, 1996), Anton (1986) found the DRI to be a poor predictor of injury for pilot ejections.

Mechanics of the Spine

In the development of biodynamic models, an understanding of the mechanics of the spine is important. The spine is a complex structure consisting of a series of rigid elements (vertebrae) connected by flexible viscoelastic elements (intervertebral discs). Compressive, bending and shear loading can be transmitted by a combination of forces in the intervertebral discs, apophyseal facet joints, ligamentous structures and active muscle contractions.

Two mechanisms have been proposed to relate vibration exposure to degenerative changes of the spine: impairment of nutrition; and mechanical fatigue due to repetitive loading (Dupuis and Zerlett, 1987; Hansson and Holm,1991; Brinckmann, 1985; Sandover, 1988).

Hansson and Holm (1991) identified molecular diffusion through the tissue matrix and fluid transfer due to the pumping action of loading and unloading the disc as two mechanisms that enable spinal nutrition. Kraemer, Kolditz and Gowin (1985) demonstrated that the disc acts as an osmotic system, releasing fluid under load until an equilibrium point is reached, and reabsorbing fluid as the load is released. This pumping action is thought to play an important role in nutrition of the disc.

Holm and Nachemson (1983) studied the effects of canine spinal movement during exercise on transport and metabolic parameters of the disc. They concluded that movement gives rise to positive nutritional variations. In a later study, these authors observed a reduced nutrient supply and loss of disc height in the spines of pigs exposed to vibration (Holm and Nachemson, 1983).

The role of mechanical fatigue as a factor in chronic degeneration of the spine was proposed by Sandover (1983), who outlined two hypotheses to relate fatigue induced failure of vertebral tissue to disc degeneration. In the first, dynamic compressive loading of the joint leads to fatigue induced microfractures of the end plate or subchondral trabeculae. Calluses formed during the repair process lead to reduced nutrient diffusion. This hypothesis is supported by Brinckmann (1985), who states that although fresh end plate fractures are not readily seen on radiograms, ossifications within the vertebral body as a late indicator of these events show that end plate fractures are rather frequent. In the second hypothesis, dynamic shear, bending or rotational loading of the joint leads to fatigue induced failure within the annulus, either as tensile failure of the collagen fibres, or as failure of cohesion between fibres or lamellae. Sandover also suggests that this process may relate to the annular lamellae already weakened by impaired nutrition as described in his first hypothesis.

Sandover (1983; 1986a) proposed a model of fatigue-induced failure of the intervertebral joint in response to cyclic loading. The data of Lafferty (1978) and others (Carter et al., 1981; Weightman, 1976) were utilized to develop the following relationship for fatigue:

$$N_i = (S_u/S_i)^x \qquad (7)$$

where N_i = number of cycles to failure, S_u = static failure stress, S_i = applied repetitive stress, and x = constant.

Sandover (1983) noted that the value of exponent x varied between biological tissues and test methodologies from x = 5 for cortical bone (Carter et al., 1981)) to 20 for cartilage (Weightman, 1976). Sandover (1983) proposed an exponent value of 9.95 based on Lafferty (1978). This value was revised to 7.7 in a later paper (Sandover, 1986a). Sandover (1983; 1986a) estimated the spinal loading in response to whole-body vibration at 2.0 $m \cdot s^{-2}$ rms and 5 Hz to predict the fatigue failure life of the vertebral joint. Fatigue failure was predicted to occur at 1000 working days for an exponent of 8, and following a single day of exposure for an exponent of 5.

Sandover (1986a) extended his concept of fatigue induced failure by application of the Palmgrem-Miner hypothesis to obtain a dose-response relationship. This hypothesis (Miner, 1945) states that the degree of fatigue damage is given by the summation of n_i/N_i, where n_i is the number of cycles at a particular stress level, S_i, and N_i is the number of cycles to failure at that stress. The effect of a particular vibration environment can then be estimated in terms of a "dose" value as:

$$D = n_i(S_i/S_u)^x \qquad (8)$$

where D = fatigue dosage index. In this system, a dosage value of D = 1.0 represents the accumulated exposure at which fatigue failure is expected.

Standards and guidelines

Standards exist for a variety of purposes and applications. Ideally a standard governing environmental exposures, such as shock and vibration, should address three questions:

1. Who is at risk to which particular health conditions?

2. What combination of exposure times and environmental factors will produce these conditions?

3. What are tolerable, accepted, or optimal environmental conditions in view of the effects? (Sandover, 1979).

Although a variety of guidelines exist, the main standards for human response to vibration have been developed by the International Organization for Standardization (ISO) and the British Standards Institution (BSI). The only existing standards with direct relevance to the evaluation of repeated shock are

BS 6841 (1987) and ASCC (1982). An overview of some of the standards and guidelines governing vibration and shock is presented below. Where appropriate, a discussion of the limitations and revisions to the standard is included.

ISO 2631 (1985): Mechanical vibration and shock - Evaluation of human exposure to whole-body vibration

In an attempt to set standards which limited exposure to WBV, ISO 2631 (1985) was published in 1974. Revisions to this standard were implemented in 1978, 1985 and 1997. The 1997 revision was published on July 19, 1997, and was therefore unavailable at the time this report was prepared. Therefore, the Draft International Standard (ISO/DIS 2631-1, 1995) which preceeded this revision has been presented as the most recently available information.

ISO 2631 (1985) was based on the results of early investigations on subjective tolerance and discomfort relative to sinusoidal WBV. It provided limits for exposure to WBV, in relation to the effects on comfort, performance and health (Griffin, 1990). Although useful for assessing passenger comfort involving steady-state WBV, the ISO 2631 (1985) contains certain limitations which are addressed in ISO/DIS 2631-1 (1995). The dependency of health, working proficiency and comfort on exposure time had been assumed in early versions of this standard. This concept was not well supported by research, and therefore was been removed from ISO/DIS 2631-1 (1995). The limits for performance decrement were also considered to be dependent on the particular tasks involved and have therefore also been excluded from ISO/DIS 2631-1 (1995). Health guidance caution zones were provided based on the following two equations:

$$a_{w1} \cdot (T_1)^{1/2} = a_{w2} \cdot (T_2)^{1/2} \qquad (9)$$

where a_{w1} and T_1 are the weighted rms magnitude of vibration and exposure time, respectively for the first exposure period and, a_{w2} and T_2 are the weighted rms magnitude and exposure time for the second period.

The second equation is similar but based on a fourth root relationship:

$$a_{w1} \cdot (T_1)^{1/4} = a_{w2} \cdot (T_2)^{1/4} \qquad (10)$$

The health guidance caution zones for these two equations essentially identical for durations from 4 to 8 h, for which most occupational observations exist.

The measurement of acceleration must be performed during a period of exposure which is indicative of the typical exposure. This meets with increasing difficulty when non-stationary exposures, or exposures with high amplitude transients, are assessed. The rms method of evaluation underestimates the influence of high amplitude pulses or impacts, indicating that an exponent of 2 is not appropriate for motion containing mechanical shocks (Griffin and Whitham, 1980; Hoddinott, 1986; Hall, 1987). In order to address this limitation, ISO/DIS 2631-1 (1995) provides specific measurement procedures for vibration with a crest factor greater than 9. In conjunction with this change, the rms method is extended to a crest factor of 9. Previous versions of ISO 2631 had limited the application of the rms method to a crest factor of 6. The crest factor is defined as:

$$\text{Crest Factor} = \frac{\text{peak acceleration}}{\text{rms acceleration}} \tag{11}$$

For exposures with a high crest factor (i.e., greater than 9) and containing mechanical shocks, ISO/DIS 2631-1 (1995) proposes the use of either the running rms method or the fourth power VDV. The running rms is expressed as:

$$a_w(t_0) = \left[\frac{1}{\tau} \int_{t_0-\tau}^{t_0} a_w^2(t)dt \right]^{1/2} \tag{12}$$

where: $a_w(t)$ is the weighted instantaneous acceleration, τ is the integration time for running averaging, t is the time (integration variable), and t_0 is the time of observation (instantaneous time).

The VDV, as defined in BS 6841 (1987), is more sensitive to peaks and is expressed as:

$$\text{VDV} = \left(\int_0^t \left[a_w^4(t)dt \right] \right)^{1/4} \tag{13}$$

An estimated VDV (eVDV) is included as a simplified dose calculation in ISO/DIS 2631-1 (1995):

$$eVDV = 1.4a_w \cdot (t)^{1/4} \qquad (14)$$

where: a_w is the frequency weighted rms acceleration in $m \cdot s^{-2}$, and t is the duration in seconds.

When the vibration exposure consists of two or more periods of exposure to different acceleration magnitudes, the normalized VDV for the total exposure is calculated from the fourth root of the sum of the fourth powers of individual dose values.

Annex A of ISO 2631 (1985) states that insufficient data are available to show a quantitative relationship of the probability of health risk. However, guidance caution zones are provided, with a VDV of 15 recommended as the maximum daily dose.

Limitations of ISO 2631

The revisions contained in ISO/DIS 2631-1 (1995) appear to be an improvement over the previous ISO 2631 (1985), since they incorporate a wider variety of exposures. However, the decision to remove limits from the main body of the standards was not acceptable to all researchers. There was resistance to eliminating the rms measure since it makes future comparison with past research difficult. There is also a lack of evidence to substantiate the new weighting curves and the fourth power analysis (Boileau, 1988). For some vibration environments, the new draft is stricter by a factor of four (Boileau, 1988). The concept of an accumulating vibration dose measure for health effects is an improvement. However, it does not characterize the temporal nature of shocks which may be linked to long term health effects.

British Standard 6841: British Standards Guide to Measurement and Evaluation of Human Exposure to Whole-Body Mechanical Vibration and Repeated Shock

The philosophy of BS 6841 (1987) was to improve methods provided in ISO 2631 (1985), simplify methods that were unnecessarily complex, and extend the scope of standards to new situations and conditions. The main function of BS 6841 (1987) was to provide superior measurement procedures for evaluating vibration rather than to determine limits of exposure.

This standard is applicable to motion transmitted to the human body through the buttocks of a seated person, feet of a standing person and the supporting area of a recumbent person. It can also be applied to x axis motions of a backrest. Frequency weightings are applied to the appropriate accelerometer signals in the same manner as ISO/DIS 2631-1 (1995). Five different weightings (W_b, W_c, W_d, W_e, and W_g) are specified for the frequency range of 0.5 to 100 Hz. These weightings correspond to the following axes and applications: namely z-seat (W_b); x-back (W_c); x and y-seat (W_d); rotational x, y, z (W_e); and z-seat relative to hand control and vision (W_g). A sixth frequency weighting (W_f) was specified for the z component in the frequency range 0.1 to 0.5 Hz for assessing motion sickness. Band-limiting filters were also specified to remove signal components outside the frequency range of interest. The band-limiting and frequency weighting are presented as realizable filter characteristics (i.e., magnitude and phase) which can be implemented in analog or digital form. Vibration exposure in more than one axis is evaluated using the VDV, recently adopted into ISO/DIS 2631-1 (1995).

Appendix A of BS 6841 is designed to account for the effects of repeated shocks. The BS 6841 does not specify limits of comfort or safe exposure, as it was considered that there was insufficient data on which to base these limits.

The VDV is to be obtained, where possible, through a vibration measurement consisting of the full vibration exposure. The VDV method has the advantage that it is applicable to intermittent vibration exposures, repeated shocks and exposures consisting of periods of vibration at different levels. When the vibration conditions are constant (or regularly repeated) a single representative period may be measured and the VDV becomes:

$$VDV = \left(\frac{t_0}{t_1} \cdot VDV_1^4 \right)^{1/4} \qquad (15)$$

where: t_0 is the total vibration exposure and t_1 is the duration of a representative time period. In addition, if there are N measurements of VDV for a single exposure, then the total VDV is expressed as:

$$VDV = \left(\sum_{n=1}^{n=N} VDV_n^4 \right)^{1/4} \qquad (16)$$

This standard states that VDV in the region of 15 $m \cdot s^{-2}$ will usually cause severe discomfort (Appendix A).

Limitations of BS 6841

The limitations of this standard are similar to those for ISO/DIS 2631-1 (1995). Additionally, the VDV dose measure does not fully account for the effect of repeated cycles (i.e., material fatigue) that may be a factor in long term health effects. For example, two weighted sinusoidal signals with identical amplitude and duration but different frequencies will have similar VDVs, yet a different number of cycles for a given time period. If damage to the body is a function of the number of stress cycles, the VDV will not appropriately characterize this.

Dynamic Response Index (DRI)

The Dynamic Response Index (DRI) was developed to characterize the severity of vertical shocks and potential for spinal injury resulting from aircraft ejections (Payne, 1968; Payne, 1975; Payne, 1978). The DRI is based on a single degree of freedom dynamic model of the spine and upper body. The model consists of a single spring, mass and damper. The undamped natural frequency, ω, is 52.9 $rad \cdot s^{-1}$, and the damping ratio, ζ, is 0.224. Input to this model is the z axis acceleration at the seat. The DRI was originally defined as the ratio of the peak force in the spring to the mass of the model, which has the units of acceleration. This was then made dimensionless by dividing by the acceleration of gravity (g). Thus:

$$DRI = \frac{(\text{Peak force in the spring})}{(\text{Mass of the mod el} \cdot g)} \qquad (17)$$

The DRI method requires determination of the peak deflection of the spring, using the complex transfer function of the model. The DRI is then related to the peak value of the spring deflection by the following equation:

$$DRI = \frac{(\omega^2 \delta)}{(g)} \qquad (18)$$

where: ω is the undamped natural frequency ($rad \cdot s^{-1}$); g is the acceleration of gravity, 9.81 $m \cdot s^{-2}$, and δ is the maximum deflection of the model.

The DRI can be interpreted as the maximum equivalent acceleration, in units of g, produced by a shock or oscillation. An unaccelerated subject possesses a DRI of 0.

Pilot ejection seat data were used to calibrate the injury rate based on the calculated DRI. A DRI of 21.5 corresponds to a 50% injury rate, while a DRI below 12 corresponds to an injury rate of less than 2%.

Limitations of the DRI

The simple compression model of the spine and upper body does not adequately describe the real physical situation, which may include large bending stresses induced by rocking motions of the spine and pelvis (Sandover, 1982). The original DRI model applies only to the vertical axis. The DRI only considers positive shocks (i.e., compression loading) and does not consider loading of the spine in tension. In addition, the method does not account for complicated time histories or variations in the rate of application of the acceleration (jerk). A slow rate of loading can produce the same DRI as a sudden shock. The DRI model attenuates frequencies greater than 10 Hz, since they were not considered important in spinal injury. This results in excessive allowable levels at high frequencies compared with curves developed from subjective data (Griffin, 1990). The original DRI did not account for repeated shocks.

Air Standards Coordinating Committee guideline (ASCC, 1982)

The Air Standards Coordinating Committee (ASCC) developed a guideline to give provisional guidance regarding criteria for exposure of aircraft crew and ground support personnel to repeated shocks (ASCC, 1982). This guideline is based upon work by Allen and Payne (Allen, 1977). It was surprising that only three years after the ISO 2631 (1974) was originally published, a public plea was made for more data on mechanical shock and development of better standards (Allen, 1977). The ASCC (1982) guideline used the DRI procedure and accounted for repeated shocks by arranging them into an exceedance format similar to that used to calculate cumulative fatigue damage in metals (Miner, 1945). Proposed criteria were provided in the form of curves. One family of three curves plots the DRI as a function of the number of shocks per day, and was thus appropriate for assessing repeated daily exposures. The upper curve in this family defines high amplitude shocks requiring recovery. The injury limit and severe discomfort boundary were based on a small

amount of data from seat ejections, Mirage aircraft, and German tank crew maneuvers. Healthy men in aerobatic maneuvers sustained DRIs of 5 or 6 up to 100 times per day with few, if any, reports of spinal injury (Allen, 1977).

Limitations of the ASCC guideline

The ASCC guidelines are concerned only with acceleration in the vertical direction and assume that damage is a linear function of accumulated loads. The standard applies only to seated healthy men and is based on a small amount of data. The ability of the DRI to predict the long term effects of repeated shocks typical of those experienced in vehicles has not been tested. The effect of repeated shocks on soft tissue may be important in this range (Forshaw and Ries, 1986).

Summary

The most recognized standard for human response to whole-body vibration is ISO 2631 (1985). Recent revisions in ISO/DIS 2631-1 (1995) appear similar in many respects to BS 6841 (1987). These newer approaches incorporate root mean quad (rmq) and VDV as the main method of characterizing vibration with shocks and repeated impacts. Limits of over-exposure have been removed from the body of the standards and placed in Appendices as guidelines. Both ISO/DIS 2631-1 (1995) and BS 6841 (1987) state that epidemiological evidence supports the 4 to 8 hour vertical acceleration limit of the previous ISO 2631 (1985), which is roughly equivalent to a VDV of 15. Little evidence exists to support use of these guidelines for signals with repeated shocks of high magnitude.

Two guidelines were identified which address exposure to repeated shocks. Both of these use the DRI (ASCC, 1982; Kanda et al., 1982). The ASCC (1982) curves of severe discomfort plot the number of shocks in 24 hours as a function of the DRI. Kanda's (1982) tentative daily exposure is based on a study of spinal disorders among crew members of high speed ships. It is not clear from the study how the authors derived the limit curve. Although validated with health data, both guidelines are limited to models of spinal injury for repeated shocks in the vertical axis. No standards explicitly consider recovery in their models.

Conclusions

A number of shortcomings exist in the biodynamic models reviewed. Although many models are available to predict the transfer function of one or more body sub-systems, these models do not extend to the prediction of chronic health effects or tissue damage as a result of exposure to WBV or repeated shocks.

Second, most models are mathematical rather than physiological in nature. Therefore, they consist of mechanical analogues of the human body which are tuned to match known experimental data. This undermines the validity of the model because it is no longer independent of the experimental data with which it is compared (Amirouche, 1987). In this respect, these models represent mathematical solutions of human body response. They provide no information regarding the underlying physiological or biomechanical effects on the body sub-systems or tissues. To achieve this, a physiological or biomechanical model is required in which the parameters are based on known tissue properties.

Third, most models have been validated on the basis of a single output response such as seat to head transfer function (Muksian and Nash, 1974; Braunbeck and Wilkinson, 1981). Such response functions can be adequately represented by a simple one or two degree of freedom system. Thus, this type of testing is inadequate to properly validate a more complex model in which the various subsystems of the body are represented (Muksian and Nash, 1974). In this context, the complexity of current modeling has exceeded the capacity for experimental validation (Soechting and Paslay, 1973; Panjabi, 1973; Rizzi, Whitman, and DeSilva, 1975).

Fourth, many of the models, including some of the more complex mathematical models, are restricted to uniaxial displacement (Payne, 1965; Muksian and Nash, 1974; Demic, 1989). While this may be acceptable in representing impulse response, such as pilot ejection analysis, it places a serious constraint on attempts to represent human response to WBV and repeated shock experienced by all-terrain vehicle operators. Axial impact loading typically results in damage to the thoracic vertebrae (Jones, Madden, and Luedeman, 1964), whereas epidemiological data indicate that vehicle operators usually experience damage at the lumbar vertebrae (Dupuis and Zerlett, 1987; Hansson and Holm, 1991). The latter effect may result from the introduction of an anterior-posterior component of acceleration, creating a flexor torque, and hence increased compression at the lumbar joints.

Despite the criticisms, there have been several important contributions to biodynamic modeling which have direct relevance to the development of a health hazard assessment method.

- Orne (1969) has shown that the introduction of anterior-posterior input forces and the presence of bending moments (and hence flexion) within the spine substantially alters the prediction of compressive stresses acting on the thoracic and lumbar motion segments.

- Prasad and King (1974) have shown that the articular facets play an important role in the transfer of compressive forces during axial impact loading.

- Sandover (1983) has proposed a model based on fatigue failure of materials. Sandover selected data on the fatigue characteristics of bone and cartilage to model fatigue failure of tissue in response to cyclic loading. Models of both vertebral end-plate and the disc annulus suggested the possibility of fatigue failure in those structures.

- Seidel, Blüthner and Hinz (1986) constructed a model of stress in the lumbar spine based on anthropometric data, EMG activity and accelerations of the upper trunk (measured at the thoracic vertebra). The predictions of this model also supported the possibility of fatigue failure at the end plates of lumbar vertebrae after long term exposure to WBV.

- Hinz and Seidel (1989) have shown that any fatigue model based on rms values of acceleration as an estimate of input stress will underestimate the health effects of vibration. This is due to the non-linear nature of the transfer function between the input acceleration at the seat and the output acceleration response of the human.

In the development of guidelines for prediction of health effects of vibration, there are two possible approaches to be considered: subjective response models, and biodynamic response models.

The ISO Standards (2631,1985; ISO/DIS 2631-1, 1995) are based primarily on subjective response. This is due, in part, to the limitations of early biodynamic models. However, subjective

response models have also been widely criticised for their inability to accurately describe the chronic health effects of vibration and repeated shock. In particular, there is little evidence to support the time dependence of a subjective response model, and hence the time dependency of ISO 2631 (1985). Although a subjective response model may be acceptable for steady state vibration exposure, it becomes increasingly difficult to apply with confidence in the presence of multiaxial vibration or vibration with repeated shocks. In these circumstances, it is probable that a biodynamic model can provide a more versatile prediction of human response.

The DRI, designed to assess health effects of impact loading, is based on a simple biodynamic model. The advances achieved since the introduction of the DRI offer the potential of a more sophisticated biodynamic index incorporating the important features of more recent models, such as the consideration of compression, torque and shear forces, muscle activity, non-linear stiffness and damping, material properties and fatigue characteristics.

Biodynamic response modeling

Evaluation of existing models

The objective of a biodynamic model is to predict the dynamic behavior of the human body ((or individual tissues) in response to a disturbance. In this study, the objective was to develop a biodynamic model (or models) capable of predicting acceleration at the lumbar vertebrae in the x, y, and z axes when provided with measured seat acceleration as input data. Using the experimental data collected during Phase 4, separate approaches were investigated for modeling the response to vertical (z axis) and horizontal (x and y axis) shocks. These data included shocks in the ±, +y, and ±z directions with amplitude of 0.5 g to 4 g and frequencies of 2 to 20 Hz.

Biodynamic models and filters were considered for their suitability in modeling the x and y axis data (Table 1). The DRI linear models of human response to acceleration in the x and y axes (Payne, 1984) and the W_d filter of BS 6841 (1987) were considered for their potential to represent the human response characteristics for mechanical shocks in the range ±0.5 g to ±4 g as described in the Phase 4 Report (Cameron et al., 1996).

The mean transmission from the seat to the lumbar (L2) and thoracic (T1) spine of both positive and negative x axis shocks was compared to the frequency response of the DRI (10 Hz) x axis model (Payne, 1984) and the W_d filter (BS 6841, 1987)(Figure 2).

The DRI (10 Hz) response curve consistently overestimated the magnitude of acceleration transmitted to the spine by 2 to 3 fold. The undamped natural frequency of the DRI (10 Hz) model is also much higher than suggested by the measured spinal acceleration (see Figure 2).

The frequency response of the DRI (7.2 Hz) y axis model was compared to the measured mean transmission from the seat to the L3 and T2 vertebrae in response to y axis shocks (Figure 3). As was observed in response to x axis shocks, the DRI model overestimated the amplitude of y axis acceleration transmitted to the spine. The natural frequency of the DRI model (7.2 Hz) is also much higher than suggested by the measured spinal acceleration data in the y axis.

A better approximation of the Phase 4 data was achieved by the output of the BS 6841 filter. However, as shown in Figure 3, the BS 6841 filter consistently produced a slight overestimation of shock transmission at both the lumbar and thoracic levels. When compared with measured data in the y axis, the BS 6841 filter considerably underestimated shock transmission at the lumbar level for low frequency shocks (2 to 6 Hz), and had a slower decay rate with increasing shock frequency than the measured y axis spinal transmission data.

Overall, neither the DRI or the W_d filter adequately represented the experimental data for x and y axis shocks input at the seat. In order to address this limitation, new biodynamic models were developed.

Biodynamic models and filters used in existing standards were also considered for their ability to model the z axis data. These are summarized in the previous section entitled "Existing models and methods". It was determined that existing standards did not adequately represent lumbar acceleration response to z axis shocks. In particular it was found that existing standards such as ASCC 1982 and BS 6841 (1987) did not match the frequency dependency of spinal response to shocks. Second the z axis response to shocks was found to be non-linear over the input amplitude range of -4g to +4g whereas existing standards assume a linear response. Details of theses findings are presented in the results of the Phase 4 experiments (Cameron et al., 1996). Based

on these findings, a new non-linear dynamic response model was developed to represent z axis spinal response to shock.

Biodynamic modeling background

A biodynamic model may be developed using two fundamental approaches. From an analytical approach, the model is based on physical principles such as conservation of energy or the balance of forces. For example, the body may be modeled as a system consisting of a mass, spring and damper (Payne, 1984). A differential equation can then be written which describes this system. The analytical approach suffers when the system is overly complex, not well understood, or highly nonlinear. In any of these situations it is difficult to develop a model based on first principles.

An alternative modeling approach is to identify the system based solely on measured input and output data. Over the past five decades, considerable mathematical tools have been developed for analyzing and designing systems. Most of these tools are based on linear algebra, complex variable theory, and the theory of ordinary, linear differential equations (Narendra and Parasarathy, 1990). As a result, well-developed techniques for the analysis of linear systems exist. A similar set of tools does not exist for nonlinear systems. Consequently, modeling such systems is considerably more difficult. The model of a system may be defined by a mathematical operator, P, which maps the input space U into the output space Y. P may be realized in a variety of mathematical forms, such as differential equations, difference equations, or as a transfer function.

Figure 4 depicts a single-input, single-output (SISO) system to be modeled, where u(t) is the input signal, w(t) is additive system noise, r(t) is the unobservable system output, n(t) is measurement noise, and y(t) is the observable system output. Given a set of measured input data, u(t), and output data y(t), the objective is to determine the predictive model operator, $\hat{P}$, such that

$$\|y - \hat{y}\| = \|P(u) - \hat{P}(u)\| \leq \varepsilon \qquad u \in U \tag{19}$$

for some error, $\varepsilon > 0$ and some defined norm, denoted by $\|\cdot\|$, such as the root mean squared error (rmse).

Therefore, the system is identified by assuming a parametric model of some suitable structure and then adjusting the parameters so that the discrepancy between the model output and the system output is minimized. The model accuracy will depend on a number of factors such as the choice of model structure, the parameter estimation method, the type of input signal, the complexity of the system, and the nature of the disturbances, $w(t)$ and $n(t)$.

When identifying a system based on input-output data, a common approach is to express the system as a function of delayed inputs and output. This formulation of the modeling problem may take one of two forms: the series-parallel model or the parallel model. In the series-parallel model, the predicted output, $\hat{y}(t)$ is expressed as a function of previous input, u, and previous measured outputs, y, as expressed by

$$\hat{y}(t) = \hat{P}[u(t-1), \ldots, u(t-l), y(t-1), \ldots, y(t-m)] \qquad (20)$$

where l and m are the orders of the input-output model, respectively; and $\hat{P}$ is the model operator (a linear or nonlinear function). This model is appropriate for applications in which a one step prediction is required. In other words, the model is intended for use on-line (when the system's output is available in real-time).

In some applications, the model is required to be used off-line (i.e., when the system's output is not easily obtained in real-time). In this case, the parallel model must be used in which the measured outputs in Equation 20 are replaced by the model's predicted output. Thus, the parallel model is expressed as

$$\hat{y}(t) = \hat{P}[u(t-1), \ldots, u(t-l), \hat{y}(t-1), \ldots, \hat{y}(t-m)] \qquad (21)$$

where $\hat{P}$ is the approximation of the system operator, $u(t)$ is the sampled input, $\hat{y}(t)$ is the model's output, and l and m represent the model orders. Since Equation 21 is a recursive equation, the parallel model has the capacity to represent dynamic systems whose output depends on the current input and current system state. The model orders are indicative of the system's capacity to store information about past behavior. The model order can often be estimated based on knowledge of the system. When this knowledge is not available, the values of l and m can be found through iterative trial and error.

When P is a linear operator, Equation 21 may be described by a generalized linear difference equation of the form

$$\hat{y}(t) = \sum_{i=0}^{l} a_i u(t-i) - \sum_{i=1}^{m} b_i \hat{y}(t-i) \qquad (22)$$

The model parameters consist of the coefficients a_i, and b_i. These parameters are normally chosen based on the input-output data in order to satisfy condition Equation 19. The model structure is specified by setting two parameters; m, the number of previous outputs, and l, the number of previous inputs. Models of this form were developed and tested to predict the spinal response to x and y axis shocks.

In Phase 4 of this study, the amplitude dependence of the spinal response to shocks in the z axis clearly demonstrated non-linearity. Hence, in the development of models to predict spinal response in the z axis, a non-linear function was required in the parallel model of equation 21. When P is a nonlinear operator, the parallel model may be implemented in the form of a recurrent neural network.

Recurrent neural networks

Artificial neural networks (ANN) are a class of computational structures which, in some respects, emulate biological neural networks. An ANN consists of elementary processing units analogous to biological neurons in function, but far less complex (Figure 5).

A network of interconnected processing elements (PEs) may be implemented as a computer program or as an electronic circuit. Connections between PEs are unidirectional communication channels with a scalar gain factor called the connection weight. Inputs to each PE are amplified or attenuated by the weight of each connection, and then summed. The sum of these weighted inputs is then passed through a non-linear activation function, resulting in an output which is distributed to other PEs. The input-output characteristics of the PE depend on the particular activation function chosen. A common choice is the hyperbolic tangent function described by

$$\tanh(x) = \frac{e^{x} - e^{-x}}{e^{x} + e^{-x}} \qquad (23)$$

ANN adapt through modifications of the connection weights according to a pre-defined adaptation algorithm, or training rule. The training rule and arrangement of PEs (network architecture) are what distinguish different types of artificial neural networks.

ANN architecture may be classified as either static or dynamic. A static network performs a nonlinear transformation of the form $y=G(x)$. Static networks are systems without memory, since the current output is a function of only the current input. These networks are usually referred to as feedforward neural networks (FFNN) because information flows unidirectionally, from input to output PEs without any cycles.

Dynamic networks contain feedback connections. Thus, their output is a function of both the current input and the current network state. Because the output must be calculated recursively, these networks are usually referred to as recurrent neural networks (RNN). In signal processing terminology, recurrent neural networks are equivalent to nonlinear infinite impulse response (IIR) filters.

Recurrent neural networks, introduced in the works of Hopfield (1982), are recognized for their powerful mapping and representational capabilities. A number of different architectures have been developed, including Hopfield networks (1982), recurrent multi-layer perceptrons (Fernandez, Parlos and Tsai, 1990), and Elman networks. These variations fall into one of three categories: externally-recurrent; internally recurrent; and fully-recurrent. In an externally-recurrent network (Figure 6), information from the output layer feeds back to PEs in the input layer. This structure makes the RNN ideal for implementing the parallel system identification model to define systems capable of predicting the non-linear spinal response to z axis shocks.

Methodology

The mechanical response of the lumbar spine due to seat acceleration was divided into components along the biodynamic x, y and z axes. In order to simplify the modeling procedure the response in each of these axes was modeled separately. The acceleration was measured on the spinous processes of the L2, L3, and L4 vertebrae (x, y and z respectively) during Phase 4.

The lumbar spine exhibited a linear response to seat acceleration in the x and y axes. It was, therefore, possible to model the response using a linear model of the form described in Equation 22. In contrast, the response in the z axis exhibited nonlinear characteristics (Cameron et al., 1996). The inadequacy of a linear modeling approach further indicated that a nonlinear model was required. Therefore, a recurrent neural network was chosen to model the lumbar response in the z axis.

x and y axis linear model development

Two methods were considered for the development of the x and y axis linear models. Linear difference equations and single degree of freedom lumped parameter models were developed for both x and y axes. In order to select the most appropriate model for the final HHA method, a comparison was then made between the results of these methods.

x and y axis linear difference equations

X and y axis linear models were developed using linear difference equations of the form given in Equation 22. The coefficients were determined using the method of linear least squares (Sinha and Kuszta, 1983). The model orders, l and m, were determined through trial and error, based on minimizing prediction error. The lumbar response in the x axis was modeled with a 15th order difference equation described by

$$y_x(t) = \sum_{i=o}^{15} a_i u_x(t - i) \qquad (24)$$

Equation 24 represents a moving average (MA) model in that the predicted output is a weighted sum of a moving window of previous input samples. Since m = 0, the difference equation is not dependent on previous outputs and is non-recursive.

In contrast, the y axis response was modeled by a 20th order recursive difference equation described by

$$y_y(t) = \sum_{i=o}^{20} a_i u_y(t - i) - \sum_{i=1}^{20} b_i y_y(t - i) \qquad (25)$$

This equation is often referred to as an auto-regressive model with exogenous inputs (ARX model).

Single degree of freedom lumped parameter model development

A single degree of freedom (lumped parameter) model was optimized to fit measured spinal response data obtained in Phase 4 for both x and y axis mechanical shocks. The model parameters which include the damping ratio (ζ) and undamped natural frequency (fn), were adjusted using an iterative procedure. The damping coefficient was adjusted between 0.1 and 0.7 and the natural frequency was adjusted between 1 Hz and 10 Hz. Each model was then used to predict a lumbar response to measured seat input data and compared to the measured lumbar data. The decision criteria used in this optimization were the rms error and rmd error given in Equations 26 and 27 respectively.

$$\mathrm{rms}(\Theta) = \left[\frac{\sum_{t=1}^{N} [y(t) - \hat{y}(t, \Theta)]^2}{N} \right]^{1/2} \tag{26}$$

$$\mathrm{rmd}(\Theta) = \left[\frac{\sum_{t=1}^{N} [y(t) - \hat{y}(t, \Theta)]^{10}}{N} \right]^{1/10} \tag{27}$$

where Θ is the set of model parameters, $\hat{y}(t)$ is the measured output, $\hat{y}(t, \Theta)$ is the model's predicted output, and N is the number of data samples.

The rmd error was included in the analysis to ensure that the model provided a good fit to high amplitude shock peaks. In a non-stationary signal it is possible to obtain a small rms error without accurately predicting transient peaks. In the present analysis the rms error reflects predominantly the model fit to the background vibration signature. A data file containing a subset of the full range of shock magnitudes (± 0.5, 1, 2, 3, and 4 g) and frequencies (2 to 20 Hz) measured during experiment ST1 of Phase 4 (Cameron et al., 1996) was used for the optimization. The results of the optimization are presented in Table 2.

The model parameters were also optimized using ST1 data containing shocks of a single magnitude of either ± 0.5, 1, 2, 3, or 4g. It was found that results for each magnitude were reasonably consistent, $1.0 < fn < 2.125$ and $0.22 < \zeta < 0.46$, for the x axis and $1.0 < fn < 2.125$ and $0.22 < \zeta < 0.58$ for the y axis. For the x axis, the damping ratio tended to be higher for low amplitude and negative shocks, while the natural frequency remained consistent for all shock magnitudes. Similarly, for the Y axis, the damping ratio tended to be higher for low amplitude shocks, while the natural frequency was consistent for all shock magnitudes. However, the determination of the final model was based on the optimization results of the combined shock magnitudes.

z axis model development

A nonlinear operator was required to adequately characterize the system in the z axis. The z axis model was therefore implemented as an externally recurrent network. Inputs to the network consisted of delayed samples of the system input and delayed network predictions. The input to each hidden layer processing element (PE) was a weighted summation of outputs from the previous layer. The output of a hidden layer PEs was a nonlinear transformation of its weighted inputs, in the form of a hyperbolic tangent function described in Equation 23. In the output layer, the output of each PE was a linear summation of its weighted inputs. The hidden and output layers also included a bias unit which added a constant value to each PE.

In order to adequately represent the system, an appropriate RNN structure had to be chosen. It has been demonstrated that one hidden layer is sufficient to uniformly approximate any continuous function (Narendra and Parasarathy, 1990). The number of PEs in this layer was determined through trial and error.

The network was trained and tested for different numbers of hidden PEs. Only one output PE was required for this application since the network predicts only one variable. The model orders, l and m, were determined using an iterative approach, while the model coefficients were determined using least squares estimation (Sinha and Kuszta, 1983).

The final developed model can be expressed by a composition of the following analytical functions:

$$y_p(t) = \sum_{j=1}^{7} W_j x_j(t) + W_{j+1} \qquad (28)$$

$$x_j(t) = \tanh\left[\sum_{i=1}^{8} w_{ji} u(t-i) + w_{j9}\hat{y}(t-1) + w_{j10}\hat{y}(t-2) + w_{j11}\hat{y}(t-3) + w_{j12}\hat{y}(t-4) + w_{j13}\right] \qquad (29)$$

for $j = 1,\ldots,7$

The number of terms in these equations was determined experimentally. Input data shocks ranged in amplitude between - 2 g and + 4 g and in frequency between 2 Hz and 20 Hz. A simulated noise function was also appended to the measured input and output signals in order to ensure an appropriate frequency response for the neural network above 20 Hz. The model parameters (w's and W's) were estimated from measured input-output data using the Levenberg-Marquardt version of nonlinear least squares (Fletcher, 1987).

Results

Model selection and validation

Each model developed was tested with unseen data. A pure simulation (i.e., using only the input) was performed to generate the model predicted output. Input data contained seat shocks with a similar waveform but different amplitudes and frequencies compared to those contained in the training data. These shocks were selected from the data obtained during the ST1 experiments of Phase 4 (Cameron et al., 1996). The performance of the models on these data indicated how well the models represent the true system as opposed to merely fitting the training data. Models were also tested using a continuous swept sinusoidal signal containing frequencies from 2 to 20 Hz to evaluate their frequency response.

Model output was evaluated in terms of the rms error, rmd error and visual inspection of the plotted output relative to the measured lumbar response data. The rms error was used to evaluate the model's ability to predict low level vibration, whereas the rmd error was used to evaluate the ability to predict high amplitude shocks. A summary of the rms and rmd error results are given in Tables 3 and 4. Visual inspection was used to evaluate the overall dynamics of the system.

x and y axis linear difference equations

A sample response to a 4 g, 8 Hz seat shock obtained using the unseen test data as input to the x axis (non-recursive) model was superimposed upon the measured lumbar acceleration data in Figure 8. A sample of the y axis recursive model output obtained using unseen test data was superimposed upon the measured lumbar data in Figure 9. These plots clearly indicate that there is a good fit between the predicted and measured lumbar acceleration. The model output does not appear to contain as much high frequency energy as the measured data. However, in response to both negative and positive seat shocks, the model outputs were generally representative of the measured response in terms of shape, peak acceleration and phase.

The frequency response of the x and y axis linear difference equations were compared to measured frequency response data obtained in Phase 4 of this study, using a continuous swept sinusoidal signal containing frequencies from 2 to 20 Hz. The frequency response of both the x and y axis models significantly differed in both magnitude and shape from the measured response.

X and y axis single degree of freedom lumped parameter models

A summary of the results of the optimization process is given in Table 2 and the respective rms and rmd errors of the lumped parameter and other models are provided in Tables 3 and 4. In Figure 10, a sample of the x axis lumped parameter model output was superimposed upon the measured lumbar data for a 4 g, 8 Hz seat shock. A similar example of the y axis lumped parameter model output, was superimposed upon the measured lumbar data, is illustrated in Figure 11 for a 4 g, 4 Hz seat shock.

These figures illustrate a good fit between the predicted and measured lumbar acceleration. The lumped parameter model output does not appear to contain as much high frequency energy as the measured data. However, in response to both negative and positive seat shocks, the model outputs were generally representative of the measured response in terms of shape, peak acceleration and phase.

The frequency response of the x and y axis lumped parameter models were compared to measured frequency response data obtained in Phase 4. A continuous swept sinusoidal signal containing frequencies from 2 to 20 Hz was provided as input. The frequency response was found to be similar in shape to the measured

lumbar response. However at the resonant frequency, the peak acceleration response exceeded the measured response by a factor of approximately 2.

z axis RNN model

Examples of the predicted lumbar acceleration obtained from the RNN model in response to z axis shocks are shown in Figures 12 to 18. In these figures, the measured lumbar acceleration data were compared to output from the RNN.

Figures 12 to 18 indicate a fairly good fit between the model output and the measured L4 z axis acceleration. The model response is similar to the measured response in terms of shape, although the peak amplitudes are not matched exactly. The model's performance is very satisfactory with respect to its frequency response and satisfactory with respect to its amplitude response. Although the model was capable of predicting the secondary shock observed in measured data in response to large amplitude shocks input at the seat, it was inconsistent in representing the high frequency component of this response (e.g., compare Figure 15 to Figure 18).

Both the rms error and rmd error between the predicted lumbar spine acceleration and the measured lumbar spine acceleration was smaller for the RNN (rms error = 3.3; rmd error = 20.4) than the BS 6841 frequency weighting filter (rms error = 6.9; rmd error = 33.7), the ASCC (1982) DRI (rms error =6.7; rmd error = 31.3), or the revised DRI (Payne, 1991)(rms error = 6.6; rmd error = 32.2).

Summary

The lumped parameter models were selected for use in the HHA method for predicting the linear lumbar spine response in the x and y axes. A RNN model was selected to predict the spinal response to z axis shocks at the seat.

The linear difference equations slightly outperformed the lumped parameter models in terms of the rms and rmd error for the x axis, while the opposite was true for the y axis. However, the lumped parameter model had a more consistent frequency response. Therefore, the overall performance of the lumped parameter model was considered to be superior to the linear difference equations. Both the linear difference equations and the lumped parameter models outperformed the BS 6841 in both the x and y axis filters.

The z axis RNN model provided an adequate estimation of vertical acceleration in the lumbar vertebrae. The model was trained to predict the response to input shocks measured at the seat for amplitudes between - 2 g and + 4 g, and frequencies between 2 and 20 Hz.

As the x and y axis models are linear, they can theoretically be extended to shock magnitudes beyond the range of verification (± 4 g) with a degree of caution. However, due to the non-linear nature of the RNN model, prediction of lumbar response to shocks outside of the training data is likely to be inaccurate. Testing with simulated shocks with amplitude greater than 6 g demonstrated that the model tended to saturate (i.e., stabilize at a maximum value). Hence, the application of the RNN should be limited to z axis shocks at the seat in the range of - 2 g to + 4 g. Shocks of this magnitude are typical of those measured in TGVs.

Biomechanical modeling

Biomechanical model development

Several existing biomechanical models were investigated with respect to their ability to adequately estimate vertebral forces in response to shocks. Although none of these models were appropriate, their contributions to the structure of the current biomechanical model are discussed briefly below.

Spinal loading in response to whole body vibration or mechanical shock has been estimated using a variety of dynamic models, ranging from simple lumped parameter models (Payne, 1978) to complex discrete parameter models (Belytschko and Privitzer, 1978; Amirouche and Ider, 1988) and finite element models (Shirazi-Adl, 1994). The discrete parameter Head-Spine Model of Belytschko and Privitzer (1978) was obtained from Wright-Patterson AFB because it had been applied previously to the assessment of impact and buffeting scenarios in aircraft. However, this model was limited by the complexity of the computer program, poor usability and lack of documentation. In addition, dynamic models are based on a prediction of the system response to an input acceleration at the seat, rather than the measured response of the system (inverse dynamics). The response of linear dynamic models do not adequately represent the non-linear relationship between the input seat acceleration and the spinal

acceleration response that was observed in the experiments of Phase 4 (Cameron et al., 1996). Therefore, inverse dynamic models were investigated as an alternate approach to analyze the forces generated by the spinal response.

Seidel, Blüthner and Hinz (1986) developed an inverse dynamic model to predict stress at the spine in response to sinusoidal WBV, given anthropometric data, EMG and acceleration of thoracic vertebrae. Hinz et al. (1994) used a simplified version of this model to estimate spinal loading in response to transient vibrations up to 0.4 g. The success of this model in its initial application to whole body vibration and low amplitude impacts suggested that it may also be valuable in estimating spinal compression for larger impacts, such as those observed in tactical ground vehicles (Roddan et al., 1995). The experimental measures collected during Phase 4 included all of the parameters required for input to the model of Seidel, Blüthner and Hinz (1986). A representation of this model was programmed in MATLAB™ and modified to include internal (abdominal) pressure. Spinal compression estimates from this model indicated a number of difficulties that could not be alleviated using the model structure.

The development of a novel biomechanical model based on inverse dynamics was therefore undertaken. The objectives of the biomechanical model were to account for the complexities of the observed response and provide a realistic estimate of spinal compression due to impacts up to 4 g. Details of model development that were important to arriving at the current status of the biomechanical model are outlined below. This model is a three segment, inverse dynamic model of the upper torso which calculates both compression and shear force at the L4/L5 joint in response to mechanical shocks input at the seat. The model has been tested using shocks of 0.5 to 4 g magnitude with waveform durations of 0.05 to 0.25 seconds (4 to 20 Hz) in the x, y and z axes.

Application of the "Seidel Model" concept

The original model of Seidel, Blüthner and Hinz (1986), with the additional contribution of internal pressure, was tested with data measured during Phase 4 to determine its ability to estimate lumbar compressive forces in response to mechanical shocks. This included 0.5, 1, 2, and 4 g, 5 Hz, positive z axis shocks. A brief overview of the model is provided below, and a schematic of the model components is shown in Figure 19A.

Based on Seidel, Blüthner and Hinz (1986), the mass of the upper body above the L3/L4 joint was estimated to be 57 percent of total body mass, and the center of mass was assumed to be 0.125 m horizontal from the center of the L3/L4 disc. Linear acceleration was measured over the spinous process at T3 and corrected prior to analysis to remove skin motion artifacts using the inverse skin transfer function method described by Morrison et al. (1995). This acceleration (a) was then attributed to the upper body mass (B) at a horizontal distance (b) from the L3/L4 joint. The torque (B·a·b) generated at the L3/L4 joint was calculated from its three component terms.

The moment generated by intra-abdominal pressure (P) was calculated assuming an equal distribution of pressure over the cross-sectional area of the abdomen (SA), and a moment arm (p) of 0.125 m, which placed the associated force directly below the mass of the upper torso. Cross sectional area was assumed to be 2/3 that estimated as the abdominal cross sectional area for each subject. Abdominal cross sectional area was calculated using abdominal girth as circumference and assuming circular geometry. With these assumptions, the axial force (P·SA) applied to the spine by the intra-abdominal pressure moment (P·SA·p) is then equal to the product of the pressure and the surface area of the abdomen. Because internal pressure was measured at the base of the abdomen, a propagation delay of 20 msec was assumed. This delay approximates the time observed for the acceleration to transmit from the lumbar spine (L4) to the thoracic spine (T3), and was assumed to be a good estimate of the time required for propagation of a pressure wave to the level of the center of mass of the upper body.

EMG signals measured over the erectors spinae at the level of the L3 vertebra were rectified and then filtered using a zero-phase shift finite impulse response (FIR) filter with a 50 msec Hanning window. The muscle force was calculated using the slope and intercept of the EMG-force calibration to convert integrated EMG activity to a muscle force time series. The muscle force (M) was calculated assuming a distance (m) of 0.05 m between the muscle belly and the center of the L3/L4 disc. An electromechanical delay of 50 msec was incorporated between peak EMG activity and peak muscle force generation (Seidel, Blüthner and Hinz, 1986).

To satisfy the condition of moment equilibrium (see Figure 19A), the imbalance resulting from the upper torso moment (B·a·b), the opposing muscle moment (M·m) and the moment

due to internal pressure (P·SA·p) was assigned to the ligaments. It was assumed that the ligaments could represent tension (L) in either anterior or posterior ligaments with an estimated moment arm (l) of 0.025 m, thus producing a balancing moment (L·l), where:

$$L \cdot l = B \cdot a \cdot b - P \cdot SA \cdot p - M \cdot m \qquad (30)$$

The compressive load (C) acting at the center of rotation of the L3/L4 disc was assumed to be the result of calculated upper torso force (B·a·cos(v)), muscle force (M), ligament force (L), and intra-abdominal force (P·SA). Thus:

$$C = B \cdot a \cdot \cos(v) + M + L - P \cdot SA \qquad (31)$$

where v is an approximate angle of 10 degrees between the spinal axis and vertical at the L3/L4 level. The absolute value of the estimated ligament moment was used to calculate ligament force, since either posterior or anterior ligament moments would contribute to compression.

Hinz et al. (1994) reported dynamic compressive loads, above the static compressive force associated with sitting, of 185 N to 991 N (maxima) in response to 0.4 g, 5 Hz sinusoidal vibration in the z axis. In the present analysis, the dynamic compressive force in response to a 0.5 g, 5 Hz shock was estimated at approximately 500 N above the mean static force (Figure 19(B)). This confirmed that our version of this model produced results of similar magnitude to those observed by Hinz et al. (1994) for low amplitude transient vibrations.

However, the peak compressive force estimated by this model for higher amplitude shocks (Figure 19(C)) was much larger than anticipated (28 kN). Lumbar forces of similar magnitude have only been reported from biomechanical analysis of power lifters (Cholewicki, McGill and Norman, 1991; Granhed, Jonson and Hansson, 1987). Although the reported ultimate strength of lumbar vertebrae varies considerably between studies, a liberal estimate of 10 kN based on Porter, Adams and Hutton (1989) and Hutton and Adams (1982) is less than half of that estimated in response to a 4 g shock. The compression estimated for both 2 and 4 g shocks exceeded the yield point for lumbar vertebrae reported by Kazarian and Graves (1977). The conclusion is similar from data reported by Brinckmann (1988), where ultimate strength of lumbar vertebra was estimated at anywhere from 3 kN to 12 kN. The lumbar forces calculated by the Seidel model in

response to large shocks, and the lumbar forces of similar magnitude reported by Cholewicki, McGill and Norman (1991) and Granhed, Jonson and Hansson (1987) are difficult to reconcile with material properties of vertebrae, particularly given the absence of any evidence of injury to the spine.

A large component in the compressive force estimated by the Seidel model was associated with a high frequency acceleration spike superimposed on the T3 acceleration response to the underlying 2 or 4 g shock. Large values of compressive loading were associated with these high frequency acceleration responses. A large component of the compressive force was due to the relatively large ligament moments (and small moment arm) that were required for the condition of equilibrium. Therefore, alternate modeling methods were investigated to address the effect of the high frequency acceleration components.

Segmented mass model

Several observations lead to a partitioning of the upper torso mass to accommodate the effects of high frequency acceleration events. A time delay in the transmission from one spinal level to the next was observed in both the accelerometer and Optotrak data collected in Phase 4. It was believed that a multi-segment model may distribute peak transient forces in time across several mass segments, rather than acting as a single peak force involving the entire mass of the upper torso. In addition, high frequency spikes were not reported in the response of the multi-segment discrete parameter model of Belytschko and Privitzer (1978) to large shocks. It was therefore believed that the progressive transmission of acceleration from one segment to the next along the spine may reduce the effect of the high frequency components on lumbar compression. The upper torso mass was divided into six segments as illustrated in Figure 20, based on the mass distribution used by Belytschko and Privitzer (1978).

The vertical acceleration (a_i) of each mass segment was estimated as a partial sum of the accelerations measured at T3 and L4 vertebrae, as follows:

$$a_i = x_i \cdot a_{T3} + y_i \cdot a_{L4} \qquad (32)$$

where:
$y_i = (d_{T3} - d_i)/(d_{T3} - d_{L4})$
$x_i = 1 - y_i$
d_i = vertical position of segment i,

d_{T3} = vertical position of T3
d_{L4} = vertical position of L4
x_i and y_i = weighting coefficients
a_i = acceleration of segment i
a_{T3} = acceleration of T3
a_{L4} = acceleration of L4

Compressive force at L4 (F_6) due to the acceleration of the upper body mass was calculated as the cascade sum of forces from segment 1 downwards.

$$F_n = \sum_{n=1}^{i} m_i \cdot a_i \qquad (33)$$

Figure 21 illustrates the response of this model to a positive z axis, 4 g, 5 Hz shock. Although the absolute estimate of compressive force was considerably reduced, no significant improvement over single segment models was achieved with respect to the contribution of high frequency acceleration spikes. The difference in compression magnitude relative to that estimated by the Seidel model was due to the absence of muscle or ligament forces and the lack of moments, since the mass was located directly above the spine. The perceived weaknesses in this segmented mass model are characteristics of other lumped parameter models such as the DRI. In biomechanical models that utilize the more realistic geometry of an offset mass, the muscle forces required for moment equilibrium contribute significantly to compressive forces at the spine. Therefore, a model with offset geometry and muscle forces was required to represent spinal forces in response to shocks.

Eccentric segregated mass model

The high frequency spikes measured in the spinal response to large amplitude shocks were not observed in the internal pressure response. Spectral analysis confirmed that the high frequency components present in the spinal response were not translated into an increase in internal pressure, as illustrated in Figure 22.

This observation suggested that the high frequency acceleration transmitted through the spine was not transmitted to the soft tissues of the abdomen. The logical assumption was the existence of a low-pass filter effect between the relatively stiff tissue of the spine and the softer tissue of the remaining

upper torso. Therefore, it is logical that only the mass of the spine experiences these high frequency acceleration events. The possibility that spinal structures may be excited at frequencies that are considerably higher than whole body resonance is supported by Markolf (1970) and Markolf and Steidel (1970) who reported intervertebral disc resonance at 240 Hz, with spinal resonance modes at 76 Hz for torsion and 37 Hz for bending in both the sagittal and coronal planes. Hence, whole-body resonance that is generally considered to occur between 4 and 6 Hz may not reflect the specific dynamic response of spinal structures in the axial direction. Instead, it may reflect the response of the relatively large soft tissue mass in the upper torso.

These observations and assumptions were incorporated into a biomechanical model which divided the upper torso mass into two components: one component representing the spinal mass and a second component representing the remaining upper torso mass. This eccentric segregated mass model (ESMM) utilized a mass distribution that was based on data reported for the Belytschko and Privitzer (1978) isolated ligamentous spine model, in which the ligamentous spinal mass was approximately eighteen percent of the total upper torso mass. This mass distribution was based upon tissue densities and cross sectional areas from cadaver studies, which agreed well with more recent data from magnetic resonance imaging (MRI) scans (Pearsall, Reid and Livingstone, 1996).

The acceleration measured at the spinous process was then assumed to act on the spinal mass. The remaining torso mass was assumed to be influenced only by the lower frequency components of the measured (spinal) acceleration. Therefore, acceleration of the remaining torso mass was determined by low-pass filtering the measured spinal acceleration with a cut-off frequency determined by comparing the power spectral density of internal pressure with spinal acceleration. The spinal acceleration was assumed to contain frequency components in the range of 0.5 to 150 Hz, while the remaining torso was assumed to experience acceleration in the range of 0.5 to 20 Hz. The general structure of the model is illustrated in Figure 23.

The ESMM was also developed to account for three dimensional acceleration and rotational motion, enabling estimation of forces at the spine from accelerations in the x, y, or z axes. Several additional improvements were made to the ESMM model, including:

- the incorporation of cross-axis response (i.e., x axis response to z axis shock);
- the incorporation of angular acceleration;
- dynamic correction of spinal accelerometer data to correct for accelerometer orientation (relative to a global coordinate system);
- dynamic location of the torso center of mass, derived from Optotrak data of spinal displacement; and
- inclusion of lateral muscle forces in response to y axis shocks.

Spinal position data (Optotrak) were measured in Phase 4 experiments at nine locations (C7, T4, T6, T8, T9, T10, T12, L1, and L5 spinous processes). These data were used to establish the orientation of the spine relative to vertical. This allowed for the correction of both accelerometer orientation and center of mass position relative to the L5 vertebra. Angular acceleration about the center of mass was estimated from the difference between linear accelerations measured at lumbar and thoracic locations.

The ESMM calculated the lumbar spine compressive force (F_c) due to the combined effect of spinal muscle force (F_{ext}), abdominal muscle force (F_{flex}), vertical acceleration ($a_i(z)$) of the spinal and soft tissue masses (m_i), and the force exerted by pressure in the abdomen (F_p). Thus:

$$F_c = F_{ext} + F_{flex} + \sum_{i=1}^{2} m_i \cdot a_i(z) - F_p \qquad (34)$$

where i = 1, 2 represents spinal and soft tissue masses, respectively.

Angular acceleration estimates from this model were large and resulted in unrealistic torques at L5. This was due, in part, to the assumptions required to estimate angular acceleration for a single segment model from linear accelerations at two points along the segment. Treatment of the upper torso as a single rigid mass requires uniform rotation of the entire upper torso. However, observation of spinal position data suggested

a process of spinal flexion and extension with bending in the mid-thoracic region.

Three segment eccentric segregated mass model

To represent the complexity of spinal flexion and extension in response to mechanical shocks, a three segment version of the ESMM was developed. In order to provide direct input data for each segment, spinal position data (Optotrak) were used to define the position, angle relative to vertical, and accelerations. Angles were determined using Euclidean geometry between two defining markers. Table 5 summarizes the characteristics of each segment. Linear accelerations of the spinal mass were computed from Optotrak displacement data as the double differential of position and band-pass filtered between 0.5 and 80 Hz. Accelerations of the soft tissue masses were calculated by low pass filtering spinal accelerations at 20 Hz. Angular acceleration about the center of mass of each segment were computed from the change of spinal angle and band-pass filtered between 0.5 and 20 Hz.

Moments were computed for each segment relative to the L4/L5 joint center (Mxj) based on the linear (aij)and angular ($\ddot{\Theta}$) accelerations of the segment masses and their respective horizontal and vertical distance (lxif, lzij) from the L4/L5 joint center. Segmental moments and the moment associated with intra-abdominal pressure (Mp) were summed to estimate the net muscle moment ($Mx_{L4/L5}$) required for equilibrium. Thus:

$$Mx_j = m_{ij} \cdot az_{ij} \cdot lx_{ij} - m_{ij} \cdot ax_{ij} \cdot lz_{ij} + I_j \cdot \ddot{\Theta}_j, \text{ and} \quad (35)$$

$$Mx_{L4/L5} = \sum Mx_j - M_p \quad (36)$$

where: i= 1, 2 represents spinal and soft tissue masses respectively, and j= 1, 2, 3 represents segments 1, 2, and 3.

It was then assumed that a positive muscle moment required force from the posterior muscles (e.g., erectors spinae) and that a negative muscle moment required force from the anterior muscle (e.g., rectus abdominus). A similar approach was applied independently to the y axis data to establish the muscle moment associated with lateral muscles, where:

$$My_{L4/L5} = \sum My_j \quad (37)$$

Compressive (Cz) and shear (Cx, Cy) forces were then calculated as vector sums of the component forces in the axes of the spine at the L4/L5 level. Vectors were calculated using the flexion/extension (θ_3) and lateral (ϕ_3) angles of the lumbar segment.

The compressive (Rz) and shear (Rx, Ry) forces were first calculated in absolute coordinates, as:

$$Rz = \sum (m_{ij} \cdot az_{ij}) + F_{ext} \cdot \cos(\theta_3) + F_{flex} \cdot \cos(\theta_3) + F_{lat} \cdot \cos(\theta_3) - F_p \quad (38)$$

$$Rx = \sum (m_{ij} \cdot az_{ij}) - F_{ext} \cdot \sin(\theta_3) - F_{flex} \cdot \sin(\theta_3) - F_{lat} \cdot \sin(\theta_3) \quad (39)$$

$$Ry = \sum (m_{ij} \cdot ay_{ij}) - F_{ext} \cdot \sin(\phi_3) - F_{flex} \cdot \sin(\phi_3) - F_{lat} \cdot \sin(\phi_3) \quad (40)$$

In spinal coordinates, relative to L5, this was expressed as:

$$Cz = Rz \cdot \cos(\theta_3) - Rx \cdot \sin(\theta_3) - Ry \cdot \sin(\phi_3) \quad (41)$$

$$Cx = Rz \cdot \sin(\theta_3) + Rx \cdot \cos(\theta_3) \quad (42)$$

$$Cy = Rz \cdot \sin(\phi_3) + Ry \cdot \cos(\phi_3) \quad (43)$$

The data from one volunteer were used to calculate the forces resulting from the shocks in the Phase 4 ST1 experiment. This volunteer was identified as a typical subject, since his spinal acceleration response was close to the average response for the entire ST1 subject pool (Cameron et al., 1996). The resultant forces computed by the biomechanical model were consistent with known material properties of the spine. Figures 24 to 33 contain frequency response curves of peak lumbar spine compressive force and peak A-P shear force estimated for all shock directions (± x, + y, ± z) and shock amplitudes (0.5, 1, 2, 3, and 4 g) in the ST1 experiment. In addition, frequency response curves were generated for lateral shear in response to positive y axis shocks (Figure 34).

The overall pattern of compressive and shear forces generated at the L4/L5 joint in response to shocks of different amplitude and frequency was very similar. The results indicated trends related to shock direction, amplitude and frequency. Trends related to shock direction included:

- the forces estimated in response to z axis shocks were larger than those for x or y axis shocks;
- compressive force was greater in response to y axis shocks than x axis shocks; and
- A-P shear in response to an x axis shock was similar to lateral shear in response to a y axis shock.

Trends related to shock amplitude and frequency included:

- the amplitude of the resultant peak compressive force was nonlinearly related to shock amplitude;
- at frequencies greater than 10 Hz, there was little difference between the responses to shocks of different amplitude;
- the larger amplitude shocks produced a greater increase in force as shock frequency decreased, as illustrated by greater steepness in the frequency response curves; and
- the frequency response curves for larger amplitude shocks begin to increase rapidly at a higher frequency.

The compressive and shear force responses for a given shock had approximately the same relative proportion of ultimate strength, indicating that this model would predict similar probability of failure in compression as it would in shear.

Interpretation of the biomechanical model within the HHA method

The final biomechanical model used the displacements and accelerations of the upper body, together with an anatomical model of the torso, to estimate the compressive forces acting at the L4/L5 joint. The predicted spinal accelerations output from the dynamic response models (described above in the section "Biodynamic response modeling") were regressed against the compressive force estimated by the biomechanical model at the L4/L5 vertebral level. The correlational analysis is described in the section entitled, "Integration of the biodynamic and biomechanical models with the repetitive stress dose function".

The relationship between spinal acceleration and forces at the L4/L5 joint, along with knowledge of the compressive strength of vertebrae, were used within the context of the HHA to estimate the number of submaximal shocks that would result in fatigue

failure. Therefore, transformation of acceleration data to force data allowed for the prediction of vertebral damage (injury) due to repetitive shocks by relating the measured motion at the seat to the ultimate strength of the vertebra. This application of the biomechanical model is described in detail in the section entitled "Integration of the biodynamic and biomechanical models with the repetitive stress dose function".

Repetitive stress dose model

Although compression fracture is the common failure mode of the vertebra-disc complex in severe axial impact loading, this mechanism does not apply to repetitive loading which is considered to be within the linear portion of the stress-strain curve. Low back pain and back disorders which have been associated with exposure to WBV and repeated shocks point to a chronic degeneration of tissues rather than acute failure (Sandover, 1981).

Two hypotheses have been proposed to relate vibration exposure to degenerative changes of the spine: impairment of nutrition and mechanical fatigue due to repetitive loading (Dupuis and Zerlett 1987; Hansson and Holm 1991; Brinckmann 1985; Sandover 1988). The role of mechanical fatigue as a factor in chronic degeneration of the spine was proposed by Sandover (1983), Dupuis and Zerlett (1987) and Brinckmann (1985). Brinckmann (1985) suggested that disc herniation is caused by some type of fatigue failure of the disc structure rather than by a single mechanical overload. In support of this argument, Brinckmann (1985) observed that clinical symptoms of disc herniation are caused by large pieces of annular material and sometimes fragments of cartilaginous end plate.

Experimental data of Carter et al. (1981) and Lafferty (1978) indicates that when subjected to repetitive loading, bone exhibits fatigue (i.e., a reduction in the ability to carry a load) in a manner that follows a similar relationship to material fatigue in metals proposed by Miner (1945). Sandover (1983; 1986b) proposed a model of fatigue-induced failure of the intervertebral joint in response to cyclic loading, and extended his concept of fatigue-induced failure by application of the Palmgrem-Miner hypothesis to obtain a dose-response relationship. Simply put, if the number of cycles, N_i, in relation to a given stress, S_i corresponds to a failure criterion, then a lower

number of cycles, n_i, to the same stress level, S_i, produces a partial fatigue proportional to n_i/N_i. If successive loadings occur at various stress levels so that there are n_1 loadings to S_1, n_2 loadings to S_2 etc., then the cumulative fatigue can be described as:

$$D = \sum_{i=1}^{m} (n_i / N_i) \qquad (44)$$

where: n_i is the number of cycles at the i^{th} stress level; N_i is the number of cycles to failure at the i^{th} stress level; m is the number of stress levels. In this form, the value D represents the fraction of fatigue life of the material, where failure is expected to occur when D = 1.0.

Payne (1976) and Allen (1977) also proposed a fatigue failure model for repeated impacts similar to the relationship for metals proposed by Miner (1945). In this model, based on the Dynamic Response Index (DRI), the peak values of DRI obtained for a series of individual impacts were summed to obtain a DRI dose value representative of the equivalent static stress level.

Repetitive stress dose function

Having reviewed the available literature, it was determined that a fatigue-based dose model offered the best approach to evaluation of repetitive mechanical shocks. A model of this type was developed and incorporated into the HHA method. The model is based on the fatigue theory of Miner (1945) and the proposals of Payne (1976), Allen (1977) and Sandover (1986b) that damage to the vertebrae due to repetitive shocks can be predicted using the concept of fatigue failure. The model differs from previous dose models in that it relates the mechanical shock input at the seat to compressive forces calculated at the L4/L5 lumbar joint and the ultimate strength of the joint. Peak compressive forces are obtained from the relationship between the spinal accelerations predicted by the biodynamic models and the output of the biomechanical model described in the previous section. Material properties of the joint are obtained from cadaver data. The format of the compression dose model is described below.

The experimental results of Lafferty (1978) and Carter et al. (1981) show that when bone is repeatedly stressed, the number of cycles to failure N_i can be modeled as:

$$N_i = (S_u/S_i)^x \qquad (45)$$

where S_u = static failure stress, and S_i = applied repetitive stress level. Miner (1945) further proposed that the degree of fatigue, D, can be expressed by the ratio n_i / N_i , where n_i is the number of cycles completed at stress S_i, and failure occurs when D = 1. This relationship can be generalized to any number of stress levels (m) and cycles, and expressed as a dose function in the form:

$$D = \sum(n_i/N_i) \quad \text{for } i = 1, m. \tag{46}$$

A significant feature of the cumulative fatigue concept is the hypothesis that failure occurs when D = 1.0. Hence values of D < 1.0 indicate the fraction of fatigue life which has been consumed.

As the number of cycles to failure (N_i) can be expressed as a function of the applied stress S_i, and the ultimate stress S_u (as described in Equation 45), the fraction of fatigue life of the material consumed can be expressed as a function of the number of cycles at each stress level and the ultimate strength (Sandover, 1986a):

$$D = \sum[n_i \cdot (S_i/S_u)^x] \quad \text{for } i = 1, m. \tag{47}$$

From this relationship it can be deduced that the equivalent static stress level, S_e, required to produce dose D from a single loading can be written as:

$$S_e = \{\sum[n_i \cdot (S_i)^x]\}^{1/x} = S_u \cdot D^{1/x} \quad \text{for } i = 1, m. \tag{48}$$

It should be noted that whereas dose function "D" (defining the fatigue life consumed) increases linearly with the number of cycles n_i, the dose function "S_e" (based on equivalent stress) has a curvilinear increase with the number of stress cycles n_i, due to the logarithmic relationship between stress level and the number of cycles to failure. Although a dose function based on fatigue life was proposed by Miner (1945) and Sandover (1986a) the concept of "equivalent stress" (Equation 48) is utilized in the DRI dose function described by Payne (1976) and Allen (1977) and adopted in the ASCC Standard (1982). The growth of this dose (DRI_e) as a function of number of shocks is similar in form to that of the VDV proposed in BS 6841 (1987). However, the two dose functions differ in that the DRI is based on the peak output force (or DRI value) of the model, and uses an exponent of x = 8, whereas the VDV is based on the integral of acceleration and uses an exponent of x = 4.

Applying the above relationships together with knowledge of the material properties of the vertebra and inter-vertebral discs, and loading information from biomechanical models, an estimate of the accumulated fatigue dose can be made.

By substituting the compressive force, Cz_i (obtained from the biomechanical model described above in the section entitled "Three segment eccentric segregated mass model") for stress, S_i, a spinal compression dose value "Cz_e" was obtained for the lumbar vertebrae, in which Cz_i represents the peak lumbar compressive force due to the ith shock, . In this model, failure will occur when Cz_e achieves a value equal to the ultimate compressive strength, Cz_u, of the L4/L5 joint (i.e., the equivalent static force required to cause injury). The ultimate strength of the L4/L5 spinal unit Cz_u was defined as 10,093 N, based on the combined experimental data of Hutton and Adams (1982) and Porter, Adams and Hutton (1989). The analysis of ultimate strength data used in the HHA is described in the section below, entitled "Injury risk model".

An exponent of x = 6 was chosen for the dose model based on the available literature for fatigue failure of bone (Lafferty, 1978; Carter et al., 1981; Hansson, Keller and Spengler, 1987; and Brinckmann, Biggeman and Hilweg, 1988 and 1989). The value of this exponent was subject to validation using repeated mechanical shock and rms vibration data collected during Phase 3 and Phase 4, together with selected epidemiological data of spinal damage and vehicle ride characteristics reviewed in Phase 1. This process is described in detail in a later section entitled "Validation of the HHA method".

Integration of the biodynamic and biomechanical models with the repetitive stress dose function

Three biodynamic models were implemented for the prediction of acceleration at the lumbar vertebrae of a seated soldier in response to mechanical shocks. These models are described above in the section entitled "Biodynamic response modeling". For the x and y axes, a single degree of freedom lumped parameter model was implemented. For the z axis, a non-linear recurrent neural network model was implemented. Each of these models predicted acceleration in the lumbar region of the spine. The x, y, and z axis biodynamic models predicted acceleration at the L2, L3, and L4 vertebrae respectively, in response to mechanical shocks input at the seat.

The output of the biomechanical model, Cz_i, obtained from the Phase 4 experimental data was compared with the outputs of the x, y and z axis dynamic response models using the same data. The relationships between the outputs of the models were approximately linear. Regressions were computed between lumbar compressive forces, Cz_i, and predicted lumbar spine accelerations, a_x, a_y, and a_z in response to shocks in each of the x, y and z axes. The data sets used in these analyses included shocks of nominal magnitude 0.5, 1, 2, 3, and 4 g, having a damped sinusoidal waveform, and fundamental frequencies of 2, 4, 5, 6, 8, 11, 15, and 20 Hz (Cameron et al. 1996). A separate regression was computed to relate compressive force to the predicted lumbar acceleration in each direction (positive and negative) in the x axis. These relationships are shown in Figures 35 to 38, and the corresponding regression equations are given in Table 6.

With the aid of these relationships, the peak spinal accelerations predicted by the three dynamic response models (in response to data measured at the seat) are used to estimate the corresponding peak lumbar compressive forces, Cz_i. The compressive force values due to shocks in all three axes are then inserted into the repetitive stress dose model of Equation 48 to obtain a repetitive stress dose in terms of lumbar compressive force (measured in Newtons). These relationships and knowledge of material properties are used in the HHA method to estimate whether a particular exposure to repeated mechanical shocks will result in fatigue failure of the lumbar joint.

A similar set of regression equations were also developed for shear force at the L4/L5 vertebral level. These data are presented in Table 7 and the relationships between predicted lumbar acceleration and shear force are shown in Figures 39 to 42. Again, knowledge of the material properties may be used to estimate fatigue failure of the lumbar joint due to cyclic shear stress. As the HHA is based on fatigue due to spinal compressive force, these data are not currently implemented as part of the HHA method. The equations were obtained using lumbar shear force and predicted lumbar acceleration in each of the x and y axes.

Injury risk model

The output of the dose model provides a single value dose estimate, Cze, for any given series of shocks input at the seat.

This represents the average response expected from the population of soldiers. Similarly the equivalent static force, Czu, at which failure is expected to occur represents an average value based on a number of cadaver samples. In accordance with normal biological variation, a range of dose values exist at which individual soldiers might be expected to experience injury or health effects. Hence, rather than associating the presence or absence of injury with a discrete dose value (i.e., a binary output), it is more practical to express the health effect of any dose in terms of the probability of sustaining an injury (i.e., as a continuous variable). This can be achieved by relating the computed dose value to a cumulative probability function based on the population variance. When probability of injury is based on the distribution of a normal variable, it can be calculated using the relationship:

$$\phi(Cz_e) = 0.5 * \left[1 + \mathrm{erf}\left(\left(1 / \sqrt{2}\right) \cdot (Cz_e - Cz_u) / \sigma\right)\right] \qquad (49)$$

where: Φ is probability of injury; Cz_e is the calculated dose; Cz_u is the mean of the dose distribution; σ is the standard deviation of the dose distribution; and erf is the error function.

As the dose value (Cz_e) is, in effect, a fraction of the ultimate compressive force (Cz_u) required to cause system failure, the distribution (σ) of the underlying probability density function can be derived from experimental data on the fatigue failure of the vertebra-disc complex.

Henzel, Mohr and von Gierke (1968) provided a comprehensive review of vertebral compression due to axial loading based on in vitro observations. The authors identify the following four distinct events in the load deformation data of the spinal unit:

- end plate fractures;
- proportional limit;
- yield point; and
- total failure.

End plate fractures occur within the linear portion of the load deformation curve (Perey, 1957). The proportional limit defines the limit of linear elastic behaviour, beyond which load

deformation becomes non-linear and there is a reduced stiffness. It represents the point at which a material begins to fail, but on release is able to recover its preload form. The yield point defines the ultimate or maximum load beyond which irreversible deformation occurs. Total failure defines the point at which the structural integrity is lost and the material collapses.

The strength of spinal units (vertebra-disc complex) and isolated vertebra in axial compression have been measured by Ruff (1950), Perey (1957), Gozulov et al. (1966), Yamada (1970), and Kazarian and Graves (1977), Hutton and Adams (1982), Brinkmann (1988) and Porter, Adams and Hutton (1989). Ruff (1950) reported yield points of 5,800 N to 10,500 N for thoracic and lumbar vertebrae (T8 to L5) with a progressive increase in strength with descending position in the vertebral column. These values are approximately 50% greater than those reported by Yamada (1970) and Kazarian and Graves (1977), but lower than those of Gozulov et al. (1966). The large variance in the strength of vertebrae reported in the literature is due partly to experimental technique (e.g., measuring either yield point or ultimate strenth; testing a single vertebra or a spinal unit). It has also been shown that strength varies with strain rate, body mass, bone density and age. However, many samples used in these studies are from elderly cadavers, and thus the data are inappropriate to compare to a military population.

Tolerance of the spine to G_z impact acceleration has been estimated by Stech (1963) from a combination of in vitro data of yield strengths of individual vertebrae, biomechanical analyses of the spine, and probability theory. Stech (1963) reanalysed the data of Ruff (1950) and Perey (1957) to construct injury probability curves as a function of z axis acceleration level. Data included probability of end plate fracture, proportional limit deformation, and compression fracture at different vertebral levels. Stech and Payne (1963) also calculated the combined injury probability function of compressive fracture of a vertebra for the complete spinal column. Results indicated a 0.5 probability of fracture at an acceleration of 18 g at age 20, reducing to 13 g at age 40. By comparison, the 0.5 probability of end plate fracture in the lumbar region was calculated to occur at approximately 10 to 12 g which represented about half the acceleration level for vertebral fracture.

There are several weaknesses in the analytical approach of Stech (1963) to the assessment of injury risk. The analysis does not include the effects of dynamic response, acceleration

profile, pulse duration, spinal flexion, or loading of the articular facets, which will influence the probability of spinal injury (Henzel, Mohr, and von Gierke, 1968; Prasad, King, and Ewing, 1974; Glaister, 1978; Payne, 1991). Thus, although the predictions of Stech (1963) for individual vertebrae provide reasonable agreement with epidemiological data (Henzel, Mohr, and von Gierke, 1968; Jones, Madden, and Luedeman, 1964), in general the epidemiological data indicates a higher tolerance level than the injury probability functions for the complete spinal column (Stech, 1963; Stech and Payne, 1963).

The most appropriate data for estimating Cz_u in the HHA method was determined to be that of Hutton and Adams (1982) and Porter et al. (1989). These authors used complete spinal units and provided the anatomical level, age and sex of each sample. In order to determine the ultimate strength, Cz_u, a total of 34 experimentally determined values were selected from 17 male cadavers with an mean age of 27 $\pm$ 9 yr. Results are shown in Table 8. The lumbar level of these specimens varied from L1/L2 to L5/S1. Hence, the percent gain in strength at each lumbar level was determined using paired data from the same cadaver. A mean gain of 5.45% was observed at each descending vertebral joint. Therefore, the data of each specimen was corrected to the level of L4/L5 and a mean ultimate strength, Cz_u, and standard deviation, σ, were computed using all 34 data points (Table 9). A mean value of Cz_u = 10,093 N with a standard deviation of σ = 1,926 N was obtained. For the purpose of the HHA method, these values were incorporated into the probability of injury model to define the population distribution of injury.

Similar data for ultimate strength in shear (Cx_u) were not as available as the compressive strength data. However, a mean value of Cx_u = 2700 N with a standard deviation of σ = 400 N was estimated from Begeman et al. (1994). The proposed HHA method does not incorporate shear forces into the repetitive stress dose; however, these data have been provided to allow for future revisions to the method. The corresponding regression equations required to relate spinal acceleration to shear forces at the L4/L5 joint are provided in Table 7.

Integration of model components

The biodynamic response models, biomechanical model output, the lumbar compressive force dose model and injury risk model

were combined to produce a HHA method. The initial input to these models consists of seat acceleration time series in the x, y and z axes. The HHA method output is the probability of injury calculated for a specified exposure duration.

The data analysis required to estimate risk of injury from seat acceleration follows several steps that sequentially utilize the models described above. Seat acceleration data, measured in the vehicle, are transformed into spinal acceleration time series estimates by the biodynamic models. Spinal acceleration peaks that exceed the prescribed minimum threshold are transformed into compressive force utilizing the regression equations that relate biomechanical model output to spinal acceleration. The dose model calculates a cumulative dose based on the data set of peak compressive forces. The cumulative dose allows for the estimation of the probability of injury, based on the normal distribution represented by the injury risk model. The integrated application of these models has been simplified in the HHA GUI software program.

A fundamental requirement of the HHA method is that it must be integrated into the existing U.S. Army Health Hazard Assessment protocol (AR 40-10). For this purpose the probability of injury predicted by the HHA method determines the hazard severity level on a scale of I to IV. The hazard severity level, combined with the probability of occurrence (determined by the vehicle type, and its operating environment), is used to determine the appropriate Risk Assessment Code (RAC). Details of the integration of the HHA method output with AR 40-10 are provided in the section entitled "Risk assessment codes - integration of the HHA method with RACs" of this report.

A software version of the HHA method with a graphical user interface (GUI) was developed in MATLAB™. The HHA GUI selects the input data files of vehicle seat acceleration in the x, y and z axes, the intended exposure duration (days, hours, minutes and seconds), and the expected probability of occurrence of this exposure (ranked A to E according to whether the particular exposure is likely to be frequent, occasional or improbable). The program then calculates the spinal acceleration response, the compressive dose value and injury probability, and reports the resultant hazard severity level, and RAC value to the HHA GUI. The HHA GUI also provides options to display the seat and spinal accelerations, the lumbar compression dose value and the probability of injury as a function of exposure time.

The HHA was tested using a selection of repeated shock profiles and exposure durations varying from 6 h to 20 yrs. The input data for this simulation was obtained from experimental data collected in Phase 3 and Phase 4. Results of this analysis are presented in the section "Validation and limitations". A typical output from the injury risk model is shown in Figure 43 for exposure to large amplitude repetitive shocks (2 and 4 g) in the z axis over a 6 h period at a shock rate of 64 ±2 g and two +4 g per 5 min.

Risk assessment codes

Background

The process of health hazard assessment falls under the umbrella of the Manpower and Personnel Integration (MANPRINT) program. MANPRINT is intended to ensure the operability and supportability of materiel systems by ensuring that human factors are an integral part of the design and development cycle (AR 602-2). Six domains are included within the MANPRINT program and are each guided by their own policy documents: Health Hazard Assessment Program (AR 40-10); Human Factors Engineering (AR 602-1); System Safety (AR 385-16); Manpower (AR 570-5); Training (AR 350-35); and Personnel (AR 71-2). The HHA method proposed by B.C. Research Inc. (BCRI) must be implemented within the scope of the MANPRINT program and according to the policy documents of the HHA program. Therefore, the HHA method must be based on realistic, empirical data that can be applied during system development and during life cycle evaluation of the total system.

The HHA Program is intended to 1) bolster warfighting capabilities by conserving or enhancing fighting strength, and 2) to ensure successful Army modernization in a safe, efficient, and cost-effective manner. These goals are accomplished by (a) preventing combat casualties and performance decrements caused by routine operation of Army combat systems, (b) enhancing soldier performance and system effectiveness, (c) reducing health-related readiness deficiencies, (d) reducing system retrofit requirements, and (e) reducing disability compensation liabilities. The HHA program attempts to meet these objectives by performing a systematic and militarily relevant HHA to identify, evaluate and control risks to the health and effectiveness of personnel who test, use, service, or support Army systems.

Health hazards are considered to be existing or likely conditions, inherent to the use of materiel, that can cause death, injury, acute or chronic illness, disability, and/or reduced job performance of personnel. In the interest of systematic evaluation, health hazards are classified into five major categories: mechanical forces, chemical substances, biological substances, radiation, and environmental extremes.

Within each category, several types of health hazard are specifically addressed. The present research is intended to generate a standard method for the HHA of exposure to repeated mechanical shock in tactical ground vehicles. "Shock" falls within the health hazard category of "mechanical forces", along with noise, blast overpressure, vibration, and trauma. Given that both vibration and repeated shock are motion characteristics, it was the intention of the present research to develop a HHA method that was specific to repeated shock, yet not inconsistent with the existing test protocol for vehicle vibration. The current criteria for the HHA of whole body vibration are defined by the measurement and analysis methods of ISO 2631 (1985), as outlined in MIL-STD-1472D, and interpreted according to the risk assessment codes (RACs) outlined in AR 40-10. Specifications for the HHA of individual hazards are detailed in the United States Army Health Hazard Assessor's Guide (1996).

The HHA protocol presented for the evaluation of repeated mechanical shocks defines the measurement and analysis methods, hazard severity criteria (defined from injury probability), and corresponding RACs. In defining the RAC, it is also necessary to specify the probability of hazard occurrence for each test condition. The hazard probability is assigned based on the intended vehicle use, anticipated employment scenarios or mission profiles. The proposed HHA protocol is described in the section below entitled "Military vehicle HHA test protocol".

The HHA process and risk assessment

The process of HHA is intended to identify possible health hazards, quantify their severity and probability of occurrence, and recommend actions for the control of potential health hazards for a materiel system within the intended environmental and operational context of the system. This assessment is formally documented in a Health Hazard Assessment Report (HHAR) under the direction and review of the Office of the Surgeon General. Two types of HHAR are specifically defined by AR 40-10: the Initial HHAR (IHHAR), and the regular HHAR. An IHHAR identifies potential hazards and relevant health standards during concept exploration and early demonstration phases of materiel development. Hence, the IHHAR is based on gross system descriptions or test data from predecessor systems. The regular HHAR provides a quantitative assessment of existing or potential

health hazards, usually based on test data from the system to be assessed.

The HHAR provides a complete background of the system, which includes detailed analysis of the physical system and the intended usage scenarios throughout the life cycle of the system. This system analysis is used to generate an inventory of potential hazards which could reasonably be expected to place personnel at risk. Each identified potential hazard is then assessed using available quantitative data. These data are analyzed and interpreted by comparison with relevant health standards within the context of the intended operations. If the quality, completeness or operational validity of the existing data are deficient, recommendations for further data collection or analysis are provided.

The criticality of an identified hazard is quantified using a Risk Assessment Code (RAC). The relative criticality is used to establish priorities for control actions. The RAC incorporates the hazard severity and the probability of hazard occurrence into a ranking of risk from 1 to 5. A RAC of 1 reflects a high degree of criticality (a severe hazard with a high probability of occurrence) and an RAC of 5 reflects either a negligible hazard or a minor hazard with a very low probability of occurrence. The RAC is determined from a matrix of severity and hazard probability, illustrated in Table 10.

In general, hazard severity is categorized from catastrophic (I) to negligible (IV). This categorization is based on existing health standards and is intended to define the degree of illness or injury which could result from exposure to the hazard. For some hazards, a well established dose-response relationship that can relate hazard intensity and duration to a range of illnesses or injuries is not available. Many existing health standards (e.g., ISO 2631, 1985) provide "safe exposure limits" that define a hazard dose believed to present a risk to health. In these cases, hazard severity has been categorized by the duration of safe exposure (DSE) at a specified hazard intensity, rather than the degree of illness or injury. Use of DSE to rate hazard severity relies on the underlying assumption that exceeding the safe exposure limit will result in a serious injury or decrement in the functional status of the soldier. The evaluation of hazard severity for whole body vibration excludes category I, which is associated with death or the loss of a bodily system.

Hazard probability ranks the likelihood that the specified hazard (e.g., repeated mechanical shock exposure) will be encountered during the intended operational conditions. This ranking, summarized in Table 11, is based on relating the test conditions and existing data to the thoroughly defined environment that the system is anticipated to operate within. In the specific case of HHA for vehicle shock or vibration, the operational definition should include the expected range of terrain types, vehicle speeds, loading conditions, and mission profiles. From this information, motion signatures can be ranked according to the likelihood of occurrence during the intended operation of the vehicle.

The level of risk (RAC) is assigned for a specific test condition, combining the parameters of hazard severity and hazard probability. Based on the RAC for each hazard, recommendations are formulated to reduce, control, or eliminate hazards with an unacceptable risk level. Risk mitigation options may include: engineering modifications (e.g., isolation, source modification), protective equipment, administrative controls (e.g., personnel selection, health monitoring), or operating controls (e.g., operating cycle/timing, crew positioning, system configuration, training).

Integration of the HHA method with RACs

The HHA method developed for the assessment of exposure to repeated shocks allows for the prediction of injury probability from a three axis (x, y, and z) seat acceleration profile. Therefore, injury probability can be defined for any acceleration signature and exposure duration, or for a mission profile that contains several motion signatures with anticipated durations for each. This method can be implemented within the MANPRINT program to define the RAC and to assist in the selection of mitigation strategies.

Assignment of the RAC requires that the probability of injury (provided by the HHA method) associated with a given exposure to repeated mechanical shocks must be related to a hazard severity rating, shown in Table 10 from AR 40-10. This assignment is described below. The probability of hazard occurrence, as described in Table 11, will be dependent on the vehicle type and its operational role. Hence, the probability of hazard occurrence must be defined by the user through analysis

of vehicle specifications and intended operating conditions, as described in the section on "Military vehicle HHA test protocol". Therefore, the RAC will be determined by the injury probability (i.e., the output of the HHA model) and by the system analysis (i.e., the operating environment of the vehicle).

Once it has been established that the level of risk is sufficient to warrant control actions, the injury probability (as a function of dose) provides valuable information that can be used in the intelligent selection and establishment of hazard mitigation measures. The injury probability curve is a sigmoidal function with a relatively steep slope on the rising portion of the curve ($0.2<\Phi<0.8$). Control measures will have the greatest influence on injury probabilities that fall within this region of the curve. The effect of control measures that reduce the cumulative dose can be directly assessed in terms of injury risk.

The HHA method can also be applied by field or command operations during the planning phase of a maneuver to establish the relative health risk associated with aspects such as vehicle selection, route planning, or operation timing. The ability to assess complex mission profiles with a variety of vehicle speeds and terrain conditions allows for operationally relevant assessment of the injury risk presented by individual missions. This could be accomplished through the utilization of a motion signature database for a variety of terrain, speed, and loading conditions. The construction of a vehicle ride profile for a specific mission would allow for the direct estimation of injury risk due to repeated shock.

Definition of hazard severity

Hazard severity levels have been defined for repeated shock exposure, based on the probability of injury, as summarized in Table 12. Probability of injury is estimated from measured seat acceleration data by applying a series of mathematical models. These models are briefly described in the section "Overview of the health hazard assessment (HHA) method", with full details of each model provided in the subsections of "Development of the health hazard assessment method". A graphical user interface (HHA GUI) has been developed to allow the integrated application of human response models, a dose model, and a probability density function to predict the likelihood of injury. An example HHA using the HHA GUI is provided below.

The probability of injury defines the likelihood of experiencing a spinal injury (end-plate fracture or disc prolapse) during an exposure duration specified by system analysis. This injury is considered catastrophic, since the soldier may be rendered incapable of using the lower limbs. Lower injury probabilities are still associated with a more remote possibility of spinal injury, but may also be associated with a higher probability of soft tissue injury and soreness (i.e., a less critical type of injury).

The hazard severity levels assigned in Table 12 have been incorporated into the HHA GUI. At hazard severity level I (catastrophic) more than 50 percent of soldiers who experience a particular repeated shock exposure (or mission profile) may be expected to sustain spinal injury. At hazard severity level II, more than 10 percent of soldiers may experience injury. At hazard severity level III (marginal) less than one soldier in ten is likely to be injured, and at level IV (negligible) less than one soldier in 100 is likely to sustain serious injury. These hazard severity levels are suggested on the basis of military acceptance of risk. These levels are clearly higher than would be acceptable in non-military environments (e.g., industrial exposures), and may be considered high for military training exercises. The probability bands provided in Table 12 may be easily readjusted in the HHA GUI to meet the acceptance levels of the U.S. Army in peace time and warfare, or any other use.

The procedures for establishing an operationally relevant test matrix, instrumentation, data acquisition and analysis, and definition of exposure duration are outlined in the section below entitled "Military vehicle HHA test protocol".

Example of a HHA using the HHA GUI

The data from the Phase 4 LT3/LT4 experimental conditions with 2.0 and 4.0 g shocks will be used for the purpose of this example. Acceleration at the seat was measured in each of the x, y and z axes during a five minute test segment and sampled at 500 Hz to data files named SEATX.dat, SEATY.dat and SEATZ.dat. The repeated shock exposure represented by these signals was found to be close to the daily (8 h) tolerance of soldiers.

The HHA GUI program is started from within MATLAB™ by typing "hha_gui", which starts the program and brings up a graphical user interface (Figure 44). Using the Browse buttons to view the available data files, select the respective data files for input x, y and z acceleration data (SEATX.dat, SEATY.dat and SEATZ.dat). Enter the Sampling Frequency (500 Hz), Minimum Threshold (3 $m \cdot s^{-2}$), Extrapolation Time (000:06:00:00), and Hazard Probability (C). These selections assume that an exposure of six hours duration to a repeated shock environment of this magnitude would occur only a few times in the life of the vehicle. Select the Output plots that are desired (Probability of Injury). Once the input parameters have been confirmed, use the mouse to click on the START button. The green progress bar along the bottom of the screen will provide information regarding progress of the data analysis.

The HHA GUI will sequentially:

- model the lumbar spine acceleration response in each of the biodynamic axes, using the dynamic response models;
- detect and quantify the acceleration peaks that exceed the prescribed minimum threshold;
- display the number of peaks detected;
- estimate the peak compressive force at the L4/5 joint for each shock, based on regression equations relating predicted spinal acceleration to the corresponding compressive force;
- calculate an accumulated lumbar compression dose value, based on the predicted peak compressive forces;
- extrapolate the dose to the prescribed duration of exposure (6 h) and display the resultant dose (in this case, 8448);
- calculate and plot (Figure 45) the probability of injury, by relating the extrapolated dose to the mean value and population variance of ultimate compressive strength of the lumbar L4/L5 spinal unit (in this case, $\Phi = 0.1962$);
- assign and display the hazard severity (in this case, II), based on probability of injury;

- assign and display the Risk Assessment Code (RAC), based on the assigned hazard severity and hazard probability (in this case, RAC = 2).

The HHA predicts a 0.196 chance of injury from a daily exposure of 6 hours, which corresponds to a hazard severity of "II". In other words, one would expect 20 soldiers out of 100 to sustain an injury as a result of this exposure. Given a hazard probability of "C", this test condition rates a RAC of "2". This is considered to be a "high" risk level within AR 40-10. This example also illustrates the importance of accurately assigning the hazard probability, since the alternate assignment of "E" (improbable) would result in a RAC of "4" (low risk level).

Application of the HHA method

The HHA method described above predicts the risk of injury and assigns the RAC for a specified test condition, exposure duration and hazard probability. This approach provides the risk of acute injury from a well defined single exposure condition that may last a few hours or a few days. Two other exposure scenarios may be of interest for the evaluation of health hazard: chronic injury from regular exposure to repeated shocks during a number of years; and complex mission profiles that may involve exposure to multiple acceleration conditions. The RAC can be determined for either of these scenarios if the appropriate exposure duration and probability of occurrence are defined.

Evaluation of chronic exposure scenarios requires that the total number of hours of actual exposure time is known. For example, during a single year of driving a vehicle for 6 hours per day, 5 days per week, and 48 weeks per year, the equivalent exposure time would be 1,440 hours (i.e., 6·5·48=1,440). This duration (Tnew) can then be used as the input exposure duration to the HHA GUI, or used to calculate an extrapolated dose (Δnew) based on a previously calculated dose (Δprev) for another known exposure duration (Tprev), by applying the following equation:

$$\Delta new = \left[(Tnew / Tprev) \cdot \Delta prev^{6}\right]^{\frac{1}{6}} \qquad (50)$$

Because the dose function is a sixth power function, the dose value will double when the exposure time is increased by a factor of 64.

The evaluation of mission profiles can be performed utilizing a set of dose values that describe the individual doses, Δ_j (where $\Delta_j=(Cz_e)_j$) resulting from defined exposures (j= 1 to n). This requires that the representative test conditions have been evaluated, with the corresponding dose values and exposure durations recorded. The mission profile is then defined by a sequence of acceleration conditions (based on vehicle speed and terrain), with a duration for each condition. The individual dose associated with each acceleration condition (Δnew) can be calculated using the above relationship, based on the ratio of the exposure duration during the mission (Tnew) to the duration recorded for the test condition (Tprev), to establish the set of dose values, Δ_j. The dose value for the entire mission profile can then be calculated by:

$$\text{Dose} = \left[\sum_{j=1}^{n} \Delta_j^{6} \right]^{\frac{1}{6}} \qquad (51)$$

The probability of injury for long term exposures or complex mission profiles can then be calculated from the dose value by utilizing the error function and probability distribution defined in the section "Development of the health hazard assessment method - Injury risk model", or by reading the value directly from Figure 46. Figure 46 illustrates the relation between the dose value and the probability of injury that is defined by the injury probability model, with a mean compression failure value of Cz_u= 10,093 N and standard deviation of 1,926 N.

The injury probability can be converted to hazard severity using Table 12. Assuming the health hazard assessment is for a planned mission or specified lifetime exposure, the hazard probability would be "A". Table 10 can then be used to derive the RAC, based on the hazard severity and hazard probability.

Military vehicle HHA test protocol

Background

New tactical ground vehicles (TGVs) commissioned by the U.S. Army are generally lighter in weight and capable of higher speeds than their predecessors. This combination of lower weight and higher speed over rough terrain produces repetitive mechanical shocks that are transmitted to the soldier primarily through the seat system. The modern soldier may experience a wide range of vibration and impact exposure, resulting from the variety of military vehicles in use, the varied terrain in which they operate, and the wide range of speeds at which they travel. It is the intention of the vehicle test and evaluation procedure to apply a standard method for evaluating the health risk associated with the vibration and impact environment of any Army vehicle. Knowledge of the health risk associated with specific operating situations can be applied during vehicle design and acquisition, or for planning operations and exercises to minimize both chronic and acute injuries to the soldier.

The following guideline for evaluation of exposure to repeated mechanical shocks can be implemented in parallel with existing methods of evaluating vibration exposure and as a general extension of existing Test Operations Procedures (e.g., TOP 2-2-808(2)). The guideline includes recommendations for:

- operating conditions under which a vehicle is to be tested;
- types of measurements to be made;
- methods of data reduction and analysis; and
- assessment of health hazard using risk assessment codes.

Methodology

In order to characterize and evaluate the health hazard associated with the vibration and shock environment of a military tactical ground vehicle, it is necessary to obtain reliable seat acceleration data for a wide range of operating conditions.

The data set should contain an authentic and realistic range of continuous (background) vibration, and a representative number of mechanical shock signatures in the three biodynamic axes (i.e., x, y, z). The test protocol should be determined based upon a detailed System Description.

System description

A System Description includes physical machine parameters, performance parameters, and strategic uses of the vehicle. Machine description should include all relevant physical variables such as: vehicle type, weight, installed power, speed range, off and on road tire pressures, fuel level and arsenal load. An operational study of the vehicle in question must be carried out to quantify performance parameters and the full range of conditions in which the vehicle will be expected to operate during both field exercises and battle conditions. Tables 13 to 15 provide sample worksheets for a complete System Description.

Health hazard assessment requires knowledge of the probability of a specific test scenario during the life of the vehicle. This Hazard Probability is determined based on a well defined operational study that details terrain type, vehicle speed, and payload. Table 16 provides a format for defining operational conditions during a typical mission profile. Several such mission profiles may need to be documented to provide a full System Description.

Test protocol

A vehicle test protocol should be designed to cover the full range of conditions and speeds as determined from the operational study. The selected test tracks should accurately simulate the range of expected conditions. Table 17 shows the ride courses available at the Aberdeen Proving Ground. This range of test courses should be adequate to represent most of the typical conditions that military vehicles would encounter.

If there is a high probability of occurrence of a terrain condition that is not in the above list, it is recommended that such a course be located or constructed for test purposes.

The test program should be well planned and documented using a test matrix. This can be used to identify any deficiencies in the test program and to systematically document data analysis.

Vehicle speed should be incremented in 5 mph steps to the expected full speed of the vehicle. Each vehicle load condition should be tested over the full speed range. Table 18 provides an example of a Vehicle Test Data Sheet.

Environmental factors will also need to be recorded, such as outside temperature and inside vehicle temperature, operating noise levels (may be speed dependent), and prevailing weather conditions.

For new vehicles that have never been evaluated, it is recommended that ethical approval of the test program be obtained from the appropriate authorities. Tests should be performed in a "walk up" design with the least severe tests run first (this would normally mean slowest speeds and smoothest ground). The results of each subsequent test should be evaluated for Hazard Severity and RAC, prior to proceeding to a test condition that is anticipated to be more severe. This approach will minimize the probability of inadvertently injuring test personnel.

Selection of personnel

Test personnel should have experience operating a similar military vehicle. This will ensure that vehicles are operated in a realistic fashion during maneuvering exercises. Test personnel should also fall within approximately one standard deviation of the median for body size and weight to ensure that the response of the seat system is within normal range.

Instrumentation and data acquisition

Mechanical shocks will be quantified in terms of acceleration, expressed in units of $m \cdot s^{-2}$. All relevant seat locations of the vehicle will be instrumented with three linear accelerometers or a triaxial accelerometer aligned with the biodynamic axes and mounted in a seatpad which conforms to the Society of Automotive Engineers (SAE) (1974) seatpad standard. Accelerometers should have a range of $\pm$ 200 $m \cdot s^{-2}$ ($\pm$ 20 g) and frequency bandwidth 0 Hz to 200 Hz. In cases where there are an excessive number of seats, as in a troop carrier, it is not practical to measure at all seat locations. Representative data should be acquired by instrumenting fore and aft locations as well as both sides of the seating configuration.

The data acquisition system must be capable of reliable operation within the motion environment to be tested. At present (1997), a typical portable system capable of handling data acquisition and analysis functions consists of a notebook computer (Pentium or 486DX processor) with 32 MB ram, 500 MB hard drive, PCMCIA type 3 12-bit A/D card and associated data acquisition software.

Signal conditioning units will provide a stabilized power supply and appropriate amplification and filtering for each acceleration channel. Amplification factors should be chosen in order that the expected range of acceleration, nominally $\pm$ 100 $m \cdot s^{-2}$, represents about 50 percent of the input range of the A/D card. To avoid problems of noise and aliasing the amplifier for each acceleration channel should be fitted with a low pass filter (4-pole butterworth) at approximately one half of the sampling frequency. Calibrations of the data acquisition system is necessary to maintain and validate the integrity of data. It is recommended that a dynamic calibration be performed and recorded for each accelerometer using a standard commercial dynamic calibrator.

Digital sampling rates should be not less than 160 hz on all channels, in order to fully capture and define shock signatures.

Data records should be a minimum of 5 minutes in length to provide sufficient statistical sample. Shorter sampling times may be used where test runs cannot be configured to provide a 5 minute sample, provided the acceleration signal is representative of longer exposures.

A test and operating procedure checklist should be used to ensure that all standard procedures have been followed and are repeatable, as well as to reduce training time for new personnel. Fully document all tests, including: calibrations, locations of all seatpads, vehicle type, weight, speed, track, data file names, sampling frequency and data directories, etc.

Data analysis

Data should be documented by plotting acceleration time histories to confirm integrity of the data, and by performing the HHA using the HHA GUI, as outlined in the example provided in the section above on "Risk assessment codes". The HHA should be documented by reporting the test conditions, exposure duration, resultant dose, hazard severity, hazard probability, probability

of injury and RAC. This allows future reanalysis of the results for a different exposure duration or for a different hazard probability. It also allows for future analysis of a mission profile that is comprised of combinations of test conditions, where the cumulative dose during the mission and the associated probability of injury are calculated as outlined in the section above ("Risk assessment codes").

Validation and limitations

Validation of the HHA method and the component models is seriously limited by the lack of available information regarding the human response to repeated mechanical shocks. There are very few well documented experiments that have measured both the input shock acceleration at the seat and the response in terms of spinal acceleration or injury. No research could be located that measured the internal spinal forces in response to low level or repeated mechanical shocks. Therefore, the validation procedures detailed below are based on utilizing the data that were measured during the Phase 3 and 4, as well as the few epidemiological studies of relevance.

The majority of available data cover the two extremes of WBV and impact, represented by low amplitude steady state vibration and large amplitude single impacts (e.g., pilot ejection). This information has been used to rationalize the end-point outcomes of the HHA method. However, this provides limited validation of the predictive ability of the HHA method for the range of mechanical shocks typical of TGVs. There is a need for consistently documented field data and epidemiological data to validate and fine tune the proposed HHA method.

Validation of the biodynamic response models

Three biodynamic response models are incorporated into the HHA method of data analysis. This includes a simple lumped parameter model for the x and y axes, as well as a nonlinear difference equation for the z axis response. To validate each model, a pure simulation with unseen data (i.e., using only the input and not the measured output) was performed to generate the model predicted output. The validation data sets were comprised of seat shocks which had not been used during model development. These seat shocks were of similar wave form, but different amplitudes and frequencies, than those contained in the training data. The model output was evaluated in terms of the rms error, rmd error and visual inspection of the plotted output compared to the corresponding measured data. The rms error was used to evaluate the ability of the model to predict low level vibration and small shocks whereas the rmd error was used to evaluate the model's ability to predict the peak acceleration of high amplitude shocks. Visual inspection (viewing the plotted output compared with the measured lumbar output) was used to evaluate

the overall dynamics of the system. The performance of the models on these data indicate how well the biodynamic response models represent the true system. In addition, the response of the BS 6841 filter was compared with the model response to determine whether any advantage was gained by utilizing a dynamic response model. A detailed description of the validation analysis of the biodynamic models is provided in the "Results - Model selection and validation" section of "Biodynamic response models".

The overall performance of the x and y axis lumped parameter model were considered to be superior to the models developed using linear difference equations and to the BS 6841 Wd filter for both the x and y axes. The strength of the predictive ability of the lumped parameter model was evident in the analysis of rms and rmd error (Tables 3 and 4). Therefore, the x and y axis lumped parameter models were confirmed for use in the HHA program.

The z axis non-linear difference equation (RNN model) also outperformed the BS 6841 filter, and provided an adequate estimation of vertical acceleration in the lumbar vertebrae for seat shocks that ranged in amplitude from - 2 g to + 4 g and in frequency from 2 to 20 Hz. The RNN model was capable of representing the acceleration spike in response to the larger shocks (+ 3 g and + 4 g), and in some cases represented the secondary impact. The RNN model predicted the secondary impact (positive acceleration) in response to a large amplitude negative shock. This capability to represent the non-linear characteristics of the lumbar response to z axis shocks is a significant improvement over the predictive ability of linear models (e.g., DRI) and filters.

Validation of the biomechanical model

The biomechanical model was provided with experimentally obtained spinal acceleration and displacement data to estimate forces at the L4/L5 joint in response to mechanical shocks. Confidence in the ability of this model to evaluate the response to shocks is based on an evaluation of the compressive forces estimated for the end point conditions of static sitting and compressive failure from a single shock, and a comparison of the forces estimated in response to submaximal shocks with compressive strength data for the lumbar spine and with forces estimated for lifting and carrying tasks in industry.

The static forces at the L4/L5 joint, represented by the intercept in the regression equations of Table 6, fall within the range anticipated to support the upper torso in the absence of motion (Andersson, Örtengren and Nachemson, 1977). The regression equations for the compressive and shear force response to z axis shocks predict failure of the L4/L5 spinal unit in response to spinal accelerations of 17 to 20 g. This compares well with single impact studies and pilot ejection analyses. Vertebral damage is reported to occur most frequently in the lower thoracic and upper lumbar region in the form of anterior wedge fractures at impact accelerations of 13 to 25 g (Fryer 1961; Hirsch and Nachemson 1961; Laurell and Nachemson 1963; Stech 1963; Jones, Madden and Luedeman 1964; Myklebust et al., 1983). These reports are based on the input acceleration at the seat. The reference acceleration for the biomechanical model is acceleration at the spine. Nevertheless, these comparisons tend to support the validity of the biomechanical model for estimation of forces in response to mechanical shocks.

During Phase 4 experiments, mechanical shock exposure did not result in spinal injury to the volunteers. The peak compressive and shear forces estimated by the biomechanical model for these exposures were considerably less than the ultimate compressive strength data reported by Porter, Adams and Hutton (1989) and Hutton and Adams (1982) for young male subjects (see Tables 8 and 9), and well below the ultimate shear strength reported by Begeman et al. (1994). A negative z axis 4 Hz 4 g shock resulted in a compressive force estimate of approximately 6,000 N. This shock condition was considered by most subjects to represent the most severe that they would voluntarily tolerate without concern of injury.

Biomechanical analyses of occupational lifting tasks have indicated that most workers cannot tolerate L5/S1 disc compression forces in excess of 6,400 N (Chaffin and Andersson, 1991), which corresponds to the Maximal Permissible Limit of the National Institute for Occupational Safety and Health (NIOSH) Work Practices Guide for Manual Lifting (1981). While the response to mechanical shock is not directly comparable to the stress associated with manual lifting, the consistency between these maximum values tends to support the predicted output of the model.

Validation of the HHA method

Evaluation of the dose model and of the injury probability model was based on an overall evaluation of the proposed HHA method. Validation was based on an analysis of the end point conditions (i.e., large single mechanical shocks and steady state WBV), experience during the Phase 3 and Phase 4 experiments, and comparison with the available epidemiological data.

The upper end point was established using cadaver studies. Predictions were compared with fracture data obtained from pilot ejection studies, which indicate that a single large mechanical shock of approximately 13 to 20 g should result in a probability of injury of approximately 0.5 (Fryer 1961; Hirsch and Nachemson 1961; Laurell and Nachemson 1963; Stech 1963; Jones, Madden and Luedeman 1964; Myklebust et al., 1983). The distribution function for probability of injury within the HHA method was defined with a mean value (Φ=0.5) equivalent to the ultimate strength of the L4/L5 spinal unit of young males (Porter, Adams and Hutton, 1989; and Hutton and Adams 1982). The regression of biomechanical model output against predicted spinal acceleration indicates that this corresponds to approximately a 17 g shock at the spine. Due to the limitations in the experimental data used to develop the model parameters, the biodynamic response model is restricted to a maximum spinal acceleration output of approximately 5 g. Hence, it cannot predict the spinal acceleration for a single shock of this magnitude. However, extrapolation of the regression of peak lumbar compressive force against peak spinal acceleration (Table 6) suggest that a repetitive shock dose equivalent to one single shock of this level will result in a 0.5 probability of injury.

The lower end point was evaluated using the ISO 2631 (1985) limits for steady state vibration, since less severe repetitive shock conditions are likely to fall close to the range of crest factors acceptable for analysis by ISO 2631 (1985). To analyze the HHA method for motion conditions near these levels, seat acceleration data from several Phase 3 and Phase 4 experiments were input to the HHA GUI. These data were used to evaluate the HHA method relative to ISO 2631 (1985), and also to compare to other existing knowledge of epidemiological data. The results of this analysis are provided in Table 19. The HHA results reported in Table 19 were calculated for a daily exposure duration of 6 hours. Results were also calculated for the equivalent exposure durations of one and ten years, assuming 240 working days in a year (i.e., 1,440 h and 14,400 h of exposure, respectively).

Chronic exposure (8 h per day) to vibration of approximately 0.63 $m \cdot s^{-2}$ rms is associated with the ISO 2631 (1985) limit for safe occupational exposure during a working lifetime. Two different motion conditions having an rms value of 0.63 $m \cdot s^{-2}$ were compared: Gaussian wide band vibration with no shocks; and a lower level of vibration with 0.3 g and 0.6 g shocks in the z axis. Gaussian wide band vibration at this level does not register a dose or probability of injury, since there are no acceleration peaks that exceed the minimum acceleration threshold of 3 $m \cdot s^{-2}$. However, the signal containing 0.3 and 0.6 g shocks with a 0.63 $m \cdot s^{-2}$ rms level (scaled data from Phase 4 ST1) registers a negligible probability of injury equivalent to a hazard severity of IV for either 6 hours or 1 year of exposure. However, hazard severity increases to level III if the working exposure is maintained for 10 years. This ranking is consistent with the ISO 2631 (1985) limit, given that daily exposure is considered safe, but indicating some caution for a lifetime of exposure. At this level of occupational motion exposure, epidemiological studies report an increased probability of low back pain, but are not able to establish a dose relationship (Figure 47) or radiological evidence of damage (Figure 48)(Village, Rylands and Morrison, 1993).

The relatively low probability of injury for a lifetime exposure to 0.63 $m \cdot s^{-2}$ rms vibration is confirmed by good quality epidemiological studies containing both control and exposed groups and exposure levels (Village, Rylands and Morrison, 1993). In contrast, the incidence of radiological damage in industrially exposed populations exceeded that for control groups when the vibration level exceeded 1.5 $m \cdot s^{-2}$ rms (Figure 48). The epidemiological literature does not adequately characterize the shocks in the motion environment, but rather relies on reporting rms vibration. Therefore, it is difficult to directly assess these data within the context of the present HHA method. Although only rms values are provided in most studies, it is highly improbable that vehicle rides having such high exposure levels would not contain significant repeated shocks. Therefore, a range of possible motion scenarios were evaluated from the measured seat acceleration data of Phase 3 and 4 experiments.

Seat acceleration signatures from the Phase 3 (LT2) steady state vibration condition and from the Phase 4 LT3 experiments (±2 g, z axis shocks at a rate of 32 per 5 min) were both approximately 1.6 $m \cdot s^{-2}$ rms, but contained different peak acceleration values (see Table 19). The probability of injury from a single day's exposure to either condition does not warrant

a high level of concern. However, the probability of injury becomes considerable after 1 year of exposure, when it is rated as a high hazard severity. The Phase 3 condition predicts approximately 50% injury after ten years, while the Phase 4 condition predicts greater than 90% injury after 10 years. Both of these estimates exceed the injury probability (30%) predicted by the epidemiological literature for similar levels of rms vibration exposure. However, the injury probability of 11% in response to the Phase 4 ST1 condition (1.1 $m \cdot s^{-2}$ rms) is lower than that predicted by epidemiological data. The Phase 4 ST1 motion profile is likely more similar to that experienced during the operation of a typical military vehicle on a daily basis, while the Phase 4 (LT3: single axis) condition represents a motion profile that would be unusual for routine vehicle operation, with large shocks (2 g at 6 Hz) presented at a rapid rate (1 shock per 10 s). Hence, it is not surprising that the ST1 data are more representative of the epidemiological literature. A more thorough validation against epidemiological data could be performed in future by performing an HHA on measured or synthesized seat acceleration signals from industrial or military vehicles for which there is corresponding clinical injury data.

It is encouraging that the relative risk of radiological damage reported in the epidemiological literature and health effects represented by the ISO 2631 (1985) limits appear to be consistent with that predicted by the HHA method for some vehicle ride conditions. The ability of the HHA to distinguish between the relative hazard associated with motion conditions at 0.63 $m \cdot s^{-2}$ rms and 1.6 $m \cdot s^{-2}$ rms demonstrates validity for this range of conditions. The results also demonstrate the ability of the HHA method to discern differences in the acceleration patterns that are not identified by the ISO 2631 (1985) method. It is interesting to note the distinction between the risk predicted for high level rms vibration and that predicted for vibration with repeated shocks. The shock content in the latter conditions would appear to increase the risk of injury.

In evaluating the application of the proposed HHA method to motion conditions that contain either high levels of vibration or small shocks, it is important to understand that the HHA method utilizes a minimum peak threshold of 3 $m \cdot s^{-2}$. This is approximately five times the daily rms level that is acceptable by ISO 2631 (1985), and represents a crest factor of approximately 5 for motion near the daily exposure limit. Therefore, the proposed HHA method will provide some overlap with

ISO 2631 in the analysis of the health effects of vehicles that generate vibration near, or in excess of, 0.63 $m \cdot s^{-2}$ rms, since the ISO 2631 (1985) vibration analysis is considered valid for a crest factor of 6 (ISO 2631, 1985) or more recently, 9 (ISO 2631, 1997). Where the crest factor falls between approximately 5 and 9, both the ISO 2631 vibration analysis and the proposed HHA method for repeated shocks could be applied to evaluate both the vibration content and the probability of injury. The HHA method is more sensitive to repeated low level shocks than the ISO 2631 (1985) method of analysis.

The HHA results of a more severe repeated shock condition (Phase 4 LT4) were generally supported by the experimental experience of Phases 3 and 4. The HHA predicted an injury probability of approximately 20% (hazard severity = II) for a single six hour exposure. This motion condition was utilized in two long duration experiments (LT3, 7 h;and LT4, 4 h per day for 5 consecutive days) which were reported to be near or at the limit of tolerance for the majority of volunteers. The projected tolerance time averaged 7 hours. However exposure was voluntarily terminated as early as 3 hours due to musculoskeletal soreness, and only two completed the 7 h experiment. All of the volunteers, but one, experienced musculoskeletal soreness, however none of the volunteers were injured by the experimental exposures. This lack of injury should not be interpreted as a contradiction of the 20% probability predicted by the HHA. The subjects in these experiments were carefully selected and clinically screened to exclude previous injury or existing conditions that may have predisposed them to injury. In addition, these subjects were encouraged to terminate exposure based on severe musculoskeletal soreness. The predicted injury probability of 20% does not appear to be unreasonable for the general military population, given the high level of fitness in experimental volunteers, their tolerance of discomfort, and the severity of musculoskeletal soreness reported.

Limitations of HHA method

The proposed HHA method is primarily limited by the range of available experimental data on which to base the model components, and by the lack of cohesive epidemiological data with which to validate the predicted probability of injury. Secondary limitations to the HHA method are inherent in the modeling approaches that were selected for inclusion in the method.

The HHA method is based on human response data from young male soldiers, ranging in age from approximately 20 to 40 years. These subjects were physically and medically fit, and were capable of tolerating higher levels of discomfort than would be expected of the general civilian population.

The biodynamic response models were developed with shock amplitudes which ranged from - 4 g to + 4 g, and 2 to 20 Hz. The linear response models applied to x and y axis seat data may be extrapolated beyond this range with some caution. However, the nonlinear nature of the z axis model prevents its applicability beyond the range of the data set used to train the recurrent neural network (- 2 g to + 4 g). Evaluation of the z axis model response to larger shocks confirmed that this model saturated for shocks greater than 5 g.

The biomechanical model was developed to calculate both compressive and shear forces. However, only the compressive forces have been incorporated into the present HHA method. There are very few good studies to quantify ultimate strength in shear, which would be required to incorporate a shear component in the dose model. The linear regressions for shear force against peak spinal acceleration have been included in Table 7 and could be incorporated into future modifications of the HHA method as new shear strength data become available. The predicted compressive and shear forces have not been directly confirmed using experimental methods on living subjects to measure the actual internal forces in response to shocks. Cadaveric data provide limited information. However, the forces associated with muscle activity in a living subject are considerable and will significantly influence both compression and shear responses. Due to the invasive nature of such measures and the high level of risk during experiments involving shocks, these measures were not included in the experiments and were not available in the literature.

The dose and injury models are based on ultimate strength and fatigue failure of the spinal unit and do not accomodate biological recovery processes such as bone remodeling or disc repair. The models do not specifically represent the effects of aging, which include loss of bone density and an associated reduction in strength. These two factors (biological recovery and aging) will tend to have opposite effects on the HHA predictions. However, the current model does not specifically address either issue. The effect of aging has been addressed to a limited extent by selecting a conservative exponent of 6

in the repetitive stress dose funtion. Methods of incorporating biological recovery and aging into the HHA method have been explored. These factors would add to the complexity of the model and were perceived as difficult to precisely define at the present time.

The dose model and injury risk are predicated on failure of the L4/L5 spinal unit. However, there is evidence in the literature that micro-fractures may occur at stress levels well below failure (Brinckmann, 1985). The long term significance of these micro-fractures is unknown. The biological recovery processes associated with repair of micro-fractures or other tissue damage are not likely to return the system to its original strength. Tissue damage and the biological recovery process may result in impaired nutrition of spinal tissues, leading to further degeneration. The role of biological recovery in the progressive degeneration of the spine was considered to be controversial. The added complexity of including biological recovery in the HHA method was not considered likely to improve the accuracy of the risk assessment.

Future modifications to the HHA could include biological recovery using the mathematical relationships described in Phase 2 (Roddan et al., 1995). The HHA method could include aging effects for evaluation of lifetime exposure by assigning a time dependent function to the ultimate compressive strength (dose equivalent to a 0.5 probability of injury). The necessary information for an aging effect could possibly be obtained from cadaver studies in the literature.

The HHA method is intended to represent the acute risk presented by short duration exposures (ranging from a few hours to a few weeks, as well as the long term chronic effects that may develop in response to a lifetime of exposure (e.g., degenerative joint disorders). A caution message has been included in the HHA GUI to indicate an excessive daily dose that is likely to result in musculoskeletal pain. A more comprehensive analysis of daily tolerance and recommendations for daily and weekly limits of exposure could be developed on the basis of Phase 4 data. However, these were not considered part of the deliverable for the HHA method in the current contract.

The proposed HHA method is based on theoretical and experimental knowledge, but requires validation in the field during typical military operations. The accuracy of the HHA predictions are presently limited by the current state of

knowledge of the human response to repeated mechanical shocks. Field validation should ideally detail the incidence and clinical characteristics of injury, the associated repeated shock environment, and the population demographics. Comparison of these epidemiological data with the HHA predictions of injury probability and the RAC of AR 40-10 would allow for a high level of confidence in the evaluation of vehicles and repetitive mechanical shock exposure.

Conclusions

This study reports the structure of a health hazard assessment (HHA) method for exposure to repeated mechanical shocks. The method introduces several innovative concepts that include the use of a biomechanical model, cadaver data, and a non-linear z axis acceleration response model. The biodynamic and biomechanical models were developed with the aid of experimental data obtained from soldiers exposed to repeated mechanical shocks in the range of 0.5 g to 4 g in the x,y and z axes. The HHA method includes a dose model based on peak compressive forces at the L4/L5 lumbar joint and material fatigue, and an injury risk model based on strength of the L4/L5 spinal unit and population variance. The HHA method has undergone a limited validation with existing experimental and epidemiological data, with acceptable results.

There are a number of limitations to the HHA method which will affect the accuracy of the hazard assessment. The probability of injury is based on a small amount of data describing vertebral fracture in the spinal units of cadavers. There is evidence in the literature that micro fractures may occur at stress levels well below failure (Brinckmann, 1985). The model needs to be more rigorously tested against chronic injury data due to long term exposures to WBV and repeated shocks. The model does not take account of either the ability of biological material to recover through the repair process, or the decline of vertebral strength with age. It is designed to represent male soldiers within an age range of approximately 20 to 40 years. However, it is proposed that this structure forms the basis of a HHA method, within which sub-components and parameters may be adjusted as the outputs are more rigorously tested against experimental and epidemiological data.

Appendix A

The project team

Dr. Anthony Brammer Principal Investigator, Consultant National Research Council	613-993-6160
Dr. Barbara Cameron Principal Investigator Project Manager, B.C. Research Inc.	604 224-4331
Dr. James Morrison Principal Investigator, Consultant Shearwater Engineering Ltd.	604 929-6589
Jordan Nicol Research Engineer, B.C. Research Inc.	604 224-4331
Dan Robinson Ergonomist, B.C. Research Inc.	604 224-4331
George Roddan Research Engineer, B.C. Research Inc.	604 224-4331
Julie Springer Research Engineer, B.C. Research Inc.	604 224-4331

Other B.C. Research personnel who worked on this project included: Dale Brown (Phase 2 and 3); Mark Garzone (Phase 4); Gillian Gibbs (Phase 4); Steve Martin (Phase 4); Brian Remedios (Phase 2 and 3); Laurel Ritmiller (Phase 4); Julia Rylands (Phase 1 and 3); Judy Village (Phase 1,2 and 3); and Alan Vukusic (Phase 4).

Appendix B

The project team biographies

Dr. Anthony Brammer, Ph.D. Physics (University of Exeter, 1967)

Dr. Brammer completed his undergraduate education and Ph.D. in Physics at the University of Exeter, England before completing a post-doctoral research fellowship in the division of Physics at the National Research Council of Canada. He has been a sessional lecturer in Physics at Carleton University, an adjunct professor in the Department of Mechanical Engineering at the University of Windsor, a lecturer for the National Research Council, and a graduate supervisor for the Department of Mechanical and Aeronautical Engineering at Carleton University. Presently he is the Senior Research Officer for the Institute for Microstructural Sciences, and has been the Senior Research Officer for the Division of Physics at the National Research Council of Canada. His research expertise includes: acoustic techniques and instrumentation, hand-arm vibration, biodynamics, machinery vibration, machinery noise, and noise exposure. Dr. Brammer has been a visiting scientist at the Institute of Occupational Health in Helsinki, Finland, the Department of Public Health at Kanazawa University in Japan, and at the Department of Health Care and Epidemiology at the University of British Columbia in Vancouver, Canada. He has extensive peer reviewed publications. Dr. Brammer has also received many awards and distinctions for his contributions in the area of vibration and acoustics. He is the Appointed Convenor in the current development of ISO standards for vibration. He is a member of numerous professional, learned, scientific, engineering, and technical societies as well as Canadian and international committees.

Dr. Barbara Cameron, Ph.D. Kinesiology (Simon Fraser University, 1992)

Dr. Cameron is Director of the Ergonomics and Human Factors Group at B.C. Research Inc. Prior to this appointment, she worked for 2 years as a consultant to the company. She has extensive experience in environmental ergonomics, pre-employment testing for job selection, and the physiological and biochemical characteristics of fatigue. In addition to her research expertise, Dr. Cameron has developed and delivered full education packages for university courses and for adult education workshops. At the University of Calgary, worked as a research

assistant studying thermoregulation in humans and animals. While completing her Ph.D. dissertation in work physiology at Simon Fraser University, she coordinated the Institute for Human Performance. She was responsible for performance testing and evaluation, and helped to coordinate a major collaborative research project between the University of Washington and Simon Fraser University in the hypobaric facility at SFU. She also assisted in the organization and implementation of regular pre-employment testing for firefighters, which included both physical and psychomotor evaluation of up to 1200 applicants. In her role as project manager for this study, Dr. Cameron coordinated a team of ergonomists, computer programmers, engineers, and consultants. She was responsible for all aspects of budget, administration, and timely delivery of reports. Dr. Cameron is also the project manager for a number of studies supported by Transport Canada and the Department of National Defence. Her project experience includes: effects of vessel motion on target detection in marine search and rescue; effects of extended crewing periods in Arctic icebreaking operations; evaluation of military tentage systems; and the development of occupationally based hearing and vision standards. Dr. Cameron completed a course in Industrial Ergonomics at the Harvard School of Public Health. She is a member of the B.C. Association of Kinesiologists, the Human Factors Association of Canada, the Human Factors and Ergonomics Society (U.S.), and the Ergonomics Society (U.K.).

Dr. James Morrison, Ph.D. Bioengineering (Strathclyde University, 1967)

Dr. Morrison has a B.Sc. in mechanical engineering and a postdoctoral research fellowship from Massachusetts Institute of Technology in Cambridge. Dr. Morrison is a Professor in Kinesiology and Associated Professor in Engineering Science at Simon Fraser University. He is also President of his consulting company, Shearwater Human Engineering Ltd. His areas of research include biomechanics, computer aided design, ergonomics and environmental ergonomics. Biomechanics research is centered on the modeling of human locomotion and analysis of muscle, joint and skeletal forces. Recently he has been investigating load transmission across long bone fractures. Computer Aided Design work involves automated manufacture of lower limb prostheses through computer generation of limb shapes from anthropometric data. Ergonomics research includes the measurement and analysis of WBV in humans and their interpretation in terms of acute and chronic health effects. Environmental ergonomics research includes thermal regulation, pressure physiology and design

of breathing apparatus. He is investigating the physiological consequences of hypoventilation, $C0_2$ retention, respiratory adaptation, the interaction of $C0_2$ and N_2 narcosis, and impaired performance directed towards defining the physiological requirements of underwater breathing apparatus and developing new concepts in apparatus design. Dr. Morrison's expertise in the area of human response to vibration and mechanical shock has been recognized by his appointment as a technical delegate to the Standards Council of Canada (SCC) and as a representative of SCC to the International Organization for Standardization (ISO) subcommittee on human response to vibration and mechanical shock (ISO SC4 TC108). Dr. Morrison has supervised 28 graduate students, is a member of three learned societies, is Subject Editor of Ergonomics Journal, and is the President of the B.C. Chapter of the Human Factors Association of Canada.

Jordan Nicol, M.Sc. Electrical Engineering (Simon Fraser University, 1996)

Mr. Nicol has a B.Sc. and M.Sc. in electrical engineering with a specialization in biomedical engineering. His Master's work was focused on modeling the dynamic response of the human spine to mechanical shock and vibration. This modeling involved the development of an artificial neural network and two linear difference models. The models developed by Mr. Nicol and his co-workers were also presented as a proposed annex to the International Organization of Standardization for inclusion in the ISO 2631. The annex presents the mathematical basis for a model to predict lumbar spine acceleration from measured seat acceleration, including shocks. Mr. Nicol's master's program was funded jointly by the B.C. Advanced Systems Institute, Simon Fraser University and B.C. Research Inc. During Mr. Nicol's work at Simon Fraser University he also contributed to the development of an alignment device for below knee amputees. Mr. Nicol programmed a microprocessor which controlled three motors used to power an adjustable alignment device required in the fitting of an amputee's prosthesis.

Dan Robinson, M.Sc. Kinesiology (Simon Fraser University, 1991)

Dan Robinson completed a B.Sc. in biochemistry at the University of British Columbia and an M.Sc. in Kinesiology at Simon Fraser University. His training has focused on evaluating human response to challenging work environments, using a wide range of physiological, biochemical and psychophysiological techniques. Mr. Robinson's project experience includes the

investigation of physiological and biochemical effects of altitude sickness and adaptation to altitude, the effects of extended work days on psychophysiological function and health in underground mine workers, and the influence of pesticide exposure on tree planters. In addition, he has experience with occupational task analyses, process flow, work organization and systematic layout planning. He has applied this knowledge to the design of control rooms, manufacturing facilities, office environments and libraries. His Master's thesis examined human response indices of low level exposure to organophosphate and carbamate pesticides while tree planting. Pesticide exposure indices included blood and tissue assay for cholinesterase isozyme inhibition, sensory and motor nerve conduction velocities, and physical symptom evaluation. While employed by B.C. Research Inc., Mr. Robinson is completing the requirements for a Ph.D. in Kinesiology. His dissertation examines the influence of spinal musculature and intra-abdominal pressure on the biodynamic response to mechanical shocks. This work is contributing to the development of a standard for the U.S. Army to evaluate health risk from exposure to repeated mechanical shocks. Mr. Robinson's experience in the evaluation of human response to vibration and impact has been recognized by his appointment as a technical delegate to the Standards Council of Canada (SCC) and as a representative of SCC to the International Organization for Standardization (ISO) subcommittee on human response to vibration and mechanical shock (ISO SC4 TC108). Mr. Robinson is a full member of the Human Factors Association of Canada and a student associate of the Human Factors and Ergonomics Society (U.S.).

George Roddan, B.Sc.(Hons) Mathematics and Physics (Simon Fraser University, 1977) P.Eng.

George Roddan has worked as Research Scientist at the Ocean Engineering Center (OEC) at B.C. Research Inc. since 1981. During this time he has participated as a technical expert in over 250 successfully completed projects. The projects have consisted mainly of scale model studies to evaluate the performance of various types of marine craft ranging from barges and fishing boats to the latest designs of planing yachts, fast catamarans, and advanced marine vehicles. Mr. Roddan possesses advanced skills in instrumentation and computerized data acquisition. Many of the hydrodynamic studies performed at the OEC require the use of specialized instrumentation such as force and torque gauges, pressure transducers, gyroscopes and wave probes. Data from these various sensors is acquired using a

variety of customized data acquisition programs. Mr. Roddan has overseen the development and implementation of both hardware and software elements of the current OEC data acquisition system. Mr. Roddan also has extensive experience in computer programming and data analysis. His programming abilities have been widely used in the OEC to develop custom analysis programs as well as numerical control programs (e.g., interfacing the computer to the hydraulic systems of the towing tank wave maker). In addition, Mr. Roddan has experience in computerized spectral analysis of vibration and shock phenomena, and has been a key contributor to the current study for the U.S. Army. Mr. Roddan was involved in the analysis of vibration data gathered in laboratory simulations of the vehicle environment. He also generated the digital control files which were used to control a three-axis shaker table used to simulate the vehicle environment. The control signals were based on a protocol developed by the principal investigator, and approved by an ethics review committee.

Julie Springer, M.Sc. Mechanical Engineering (University of Calgary, 1994)

Julie Springer's educational background includes a B.Sc. (U. of Calgary, 1990) in mechanical engineering and a minor in computer integrated manufacturing as well as an M.Sc. (U. of Calgary, 1994) in mechanical engineering with a focus on biomechanics and prosthetic design. Ms. Springer combined her education in engineering with anatomy and anthropometry. At the University of Calgary and Clynch Technologies Inc., she designed and developed supporting structures for computer-aided prosthetic socket design systems. She continued working in this field for two years at Simon Fraser University with Dr. J. Morrison, and also began contacts in ergonomics at wood processing mills. Ms. Springer has gained extensive expertise in computer aided design using AutoCAD. She has also conducted usability testing on the fit and comfort of lower limb prosthesis and worked in development of tools to aid in adjustability of prosthetic alignment devices. Currently employed by B.C. Research Inc. in the Ergonomics and Human Factors Group, Ms. Springer is working on a project with the U.S. Army on the development of an exposure standard for repeated impact in tactical ground vehicles. She has also worked on various industrial ergonomics contracts including: vibration assessment and ergonomic evaluation of seating in locomotive cabs; assessment of hand-arm segmental vibration and whole body vibration in mining operations; development and delivery of ergonomics training to hospital design groups; ergonomic input at a soderberg aluminum smelter;

ergonomic input in the laboratory design at a pulp and paper mill; ergonomic assessment of an MD6 compression tool; and ergonomic assessment of VDT workstations and laboratories at B.C.'s Women's and Children's Hospital. Ms. Springer is a full member of the International Society of Automotive Engineers (SAE), and is currently applying for her professional status in the Association of Professional Engineers, Geologists and Geophysicists of Alberta (APEGGA). Ms. Springer is also an associate member of the Human Factors Association of Canada (HFAC).

Appendix C

Tables

Table 1
Existing DRI and BS 6841 models

Model	Axis	Undamped f_n (Hz)	Damping ratio	Reference
W_d filter	x	na	na	BS 6841 (1987)
DRI	x	10	0.15	Payne (1984)
W_d filter	y	na	na	BS 6841 (1987)
DRI	y	7.2	0.15	Payne (1984)

Table 2
Single-degree-of-freedom model optimized to fit experimental ST1 data

Axis	Undamped f_n (Hz)	Damping Ratio (ζ)
x	2.125	0.22
y	2.125	0.22

Table 3
x axis linear model results

Model	rms error	rmd error
System identification model: linear difference equation (equation 25)	1.74	6.07
Lumped parameter model (Table 2)	2.06	7.27
BS 6841 filter	2.66	10.37

Table 4
y axis linear model results

Model	rms error	rmd error
System identification model: linear difference equation (equation 25)	1.97	7.26
Lumped parameter model (Table 2)	1.76	6.76
BS 6841 filter	2.33	9.88

Table 5
Segment characteristics

	Segment 1	Segment 2	Segment 3
Anatomical partition	above T6	T6 to T12	L1 to L5
Defining markers	C7 and T4	T8 and T10	L1 and L5
Spinal and soft tissue mass (% body mass)	20	13.2	14.7

Table 6
Regression equations relating compressive force (Cz) and predicted lumbar acceleration (a_x, a_y and a_z), in the x, y, and z axes.

Shock axis	Regression equation	Sample n	R^2
+x	$Cz = 28.0 \cdot a_x + 415.2$	80	0.65
-x	$Cz = 19.2 \cdot a_x + 446.7$	80	0.47
+y	$Cz = 64.9 \cdot a_y + 366.3$	80	0.83
±z	$Cz = 59.7 \cdot a_z + 461.6$	129	0.92

Table 7
Regression equations relating shear force (Cx and Cy) and lumbar acceleration (a_x, a_y and a_z), in the x, y, and z axes

Shock axis	Regression equation	Sample n	R^2
+x	$Cx = 13.5 \cdot a_x + 10.7$	80	0.83
-x	$Cx = 6.8 \cdot a_x + 18.3$	80	0.67
+y	$Cy = 15.9 \cdot a_y + 5.5$	80	0.92
±z	$Cx = 9.8 \cdot a_z + 9.2$	129	0.92

Table 8
Compressive strength measured during mechanical testing of lumbar spinal units (2 vertebrae and intervertebral disc)

Subject	Age	Compressive strength (N)				
		L1-L2	L2-L3	L3-L4	L4-L5	L5-S1
1	20		8500		11600	
2	18		10206		10330	
3	25		13954		10140	
4	20		8179		7631	
5	24		9460		9760	
6	19		7310		7710	
7	16		5120		8680	
8	23		7675		9206	
9	32		8404		11322	
10	32		6857		8088	
11	33		9024		10780	
12	46		10240		11237	
13	31				8710	
14	46	8553		9259		12981
15	31	11567		11895		10802
16	22			10780		12740
17	26					9987

* Subjects 1 - 9 from Porter, Adams and Hutton (1989). Subjects 10 - 17 from Hutton and Adams (1982).

Table 9
Compressive strength (N) estimated for the L4/L5 spinal unit from mechanical testing of lumbar spinal units

Subject	Age	Compressive strength (N)
1	20	9436
1	20	*11600
2	18	11330
2	18	*10330
3	25	15491
3	25	*10140
4	20	9080
4	20	*7631
5	24	10502
5	24	*9760
6	19	8115
6	19	*7710
7	16	5684
7	16	*8680
8	23	8520
8	23	*9206
9	32	9329
9	32	*11322

Table 9 cont'd
Compressive strength (N) estimated for the L4/L5 spinal unit from mechanical testing of lumbar spinal units

10	32	7612
10	32	*8088
11	33	10018
11	33	*10780
12	46	11368
12	46	*11237
13	31	*8710
14	46	10071
14	46	9755
14	46	12320
15	31	13620
15	31	10252
15	31	12533
16	22	11358
16	22	12092
17	26	9479
Mean	28	10093
Std dev.	9	1924

* Indicates data directly measured at the L4/L5 unit. All other data were calculated from that in Table 6.5.1 based on a scaling factor of 5.36% per vertebral level.(from Porter, Hutton and Adams, 1989; Hutton and Adams, 1982).

Table 10
Risk assessment code determination (AR 40-10, 1991)

Hazard severity	Hazard probability				
	A	B	C	D	E
I	1	1	1	2	3
II	1	1	2	3	4
III	2	3	3	4	5
IV	3	5	5	5	5

Table 11
General criteria for hazard probability level

Level	Descriptor	Fleet/inventory description	Probability (%)
A	Frequent	Continuously experienced	50 to 100
B	Probable	Will occur frequently	20 to 50
C	Occasional	Will occur several times	5 to 20
D	Remote	Unlikely, but can reasonably be expected to occur	1 to 5
E	Improbable	Unlikely, but possible	less than 1

Table 12
Assignment of hazard severity based on injury probability

Hazard severity	Injury probability(Φ)	Description
I	$\Phi \geq 0.5$	Catastrophic
II	$0.5 > \Phi \geq 0.1$	Critical
III	$0.1 > \Phi \geq 0.01$	Marginal
IV	$0.01 > \Phi$	Negligible

Table 13
General system description

Vehicle type:	Date:
Describe strategic use of vehicle: Include range of speeds, terrain conditions, arsenal type, loading conditions, and no. of occupants.	

Table 14
Machine description

Vehicle type	Date:
Weights	units -metric (Imp.)
Net:	
Ballast:	
Gross:	
Dimensions	
Wheelbase:	
Length:	
Width:	
Height:	
Engine	
Type:	
Cylinders:	
Horsepower:	
Drivetrain	
Transmission type:	
No. of gears:	
Suspension	
Front:	
Rear:	
Tire pressures:	
Front:	
Rear:	
No. of personnel:	
Noise levels:	
Temperature ranges:	
Fuel type, capacity and level	

Table 15
Vehicle performance parameters

Vehicle type:	Date:
Vehicle performance parameter	units -metric (Imp.)
Speed range:	
Acceleration:	
Turning rate:	
Breaking performance:	
Operating range	

Table 16
Mission Profile Assessment

Vehicle:	Loading condition:		Date:	
Terrain type	Speed range	Probability of encounter	Severity rating	RAC

Table 17
Typical ride courses at Aberdeen Proving Grounds

Test course	Course composition	Length
Paved	Bituminous concrete	2,235 ft.
Gravel	Compacted bank gravel	10,714 ft.
6-inch wash-board	Concrete	798 ft.
Radial wash-board	Concrete	243 ft.
Belgian block	Granite blocks in concrete	3940 ft.
Secondary A	Native soil	2.4 miles
Cross-country #1	Moderate: loam , gravel	5.2 miles
Cross-country #2	Moderate to rough	1.8 miles
Cross-country #3	Rough	3.3 miles
Cross-country #4	Severe	2.5 miles
Churchville B	Hilly, grades to 29%	5.0 miles

Table 18
Vehicle test data sheet

Date:

Vehicle description:

Load condition:

Instrumentation used:

Location and channel number of seatpad accelerometers:

Sampling frequency:

Filter settings:

Test no.	Speed (mph)	Course type	x axis filename	y axis filename	z axis filename	Comments

Table 19
Results of HHA using sample seat acceleration data measured during Phases 3 and 4

Motion description	rms	Exposure duration	Φ (injury)	HHA dose	Hazard severity
Gaussian Wide-band noise (0-40Hz)	0.63	6 hours 1 year 10 years	0 0 0	0 0 0	IV IV IV
Ph4 (ST1, scaled): 0.3 g shocks (32/5 min), 0.6 g shocks (32/5 min). 2 to 20 Hz	0.63	6 hours 1 year 10 years	0.000013 0.004 0.013	2001 4988 5811	IV IV III
Ph3 (LT2): steady state vibration	1.6	6 hours 1 year 10 years	0.00031 0.24 0.52	3503 8733 10173	IV II I
Ph4 (LT3, one axis): 2 g shocks (32/5 min) all shocks 6 Hz	1.6	6 hours 1 year 10 years	0.0065 0.95 0.98	5310 13237 15421	IV I I
Ph4 (ST1): 0.5 g shocks (32/5 min), 1 g shocks (32/5 min). 2 to 20 Hz	1.1	6 hours 1 year 10 years	0.00035 0.036 0.11	2657 6623 7716	IV III III
Ph4 (LT4): 2 g shocks (64/5 min), 4 g shocks (2/5 min). all shocks 6 Hz	2.65	6 hours 1 year 10 years	0.19 1 1	8447 21060 24532	II I I

Appendix D

Figures

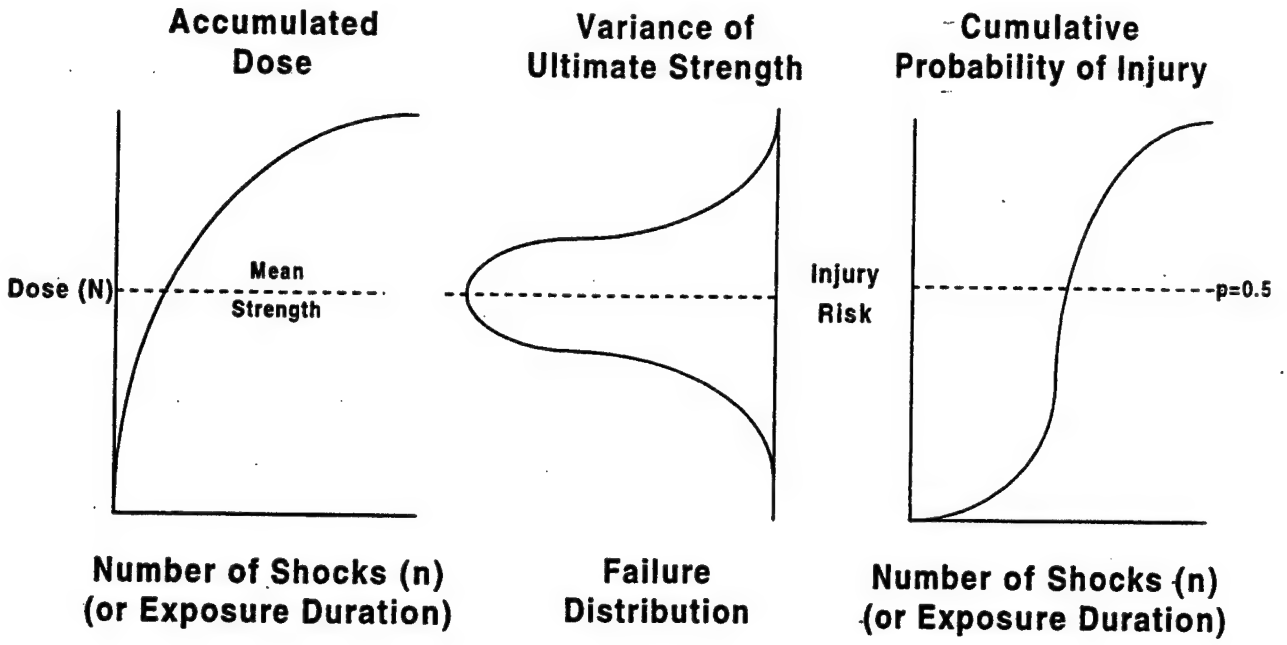

Figure 1. Conceptual illustration of the relationship between the computed dose value (N) and failure distribution function, which combine to estimate the risk of injury (cumulative probability function).

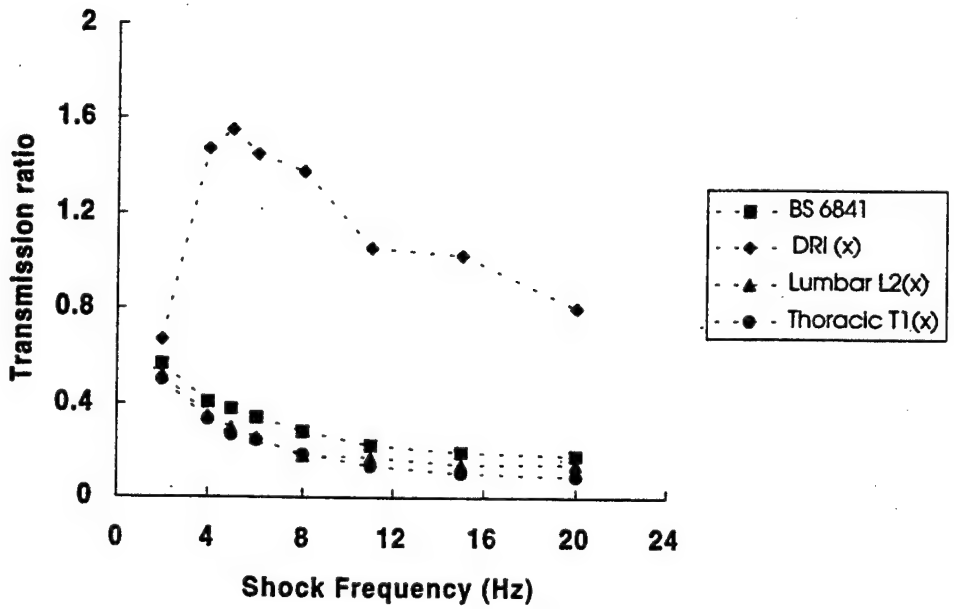

Figure 2. Comparison of the measured x axis seat to spine transmission ratio with predicted transmission ratios using the W_d filter (BS 6841) and the DRI (10 Hz) x axis model (shocks delivered in the negative x direction at the seat.

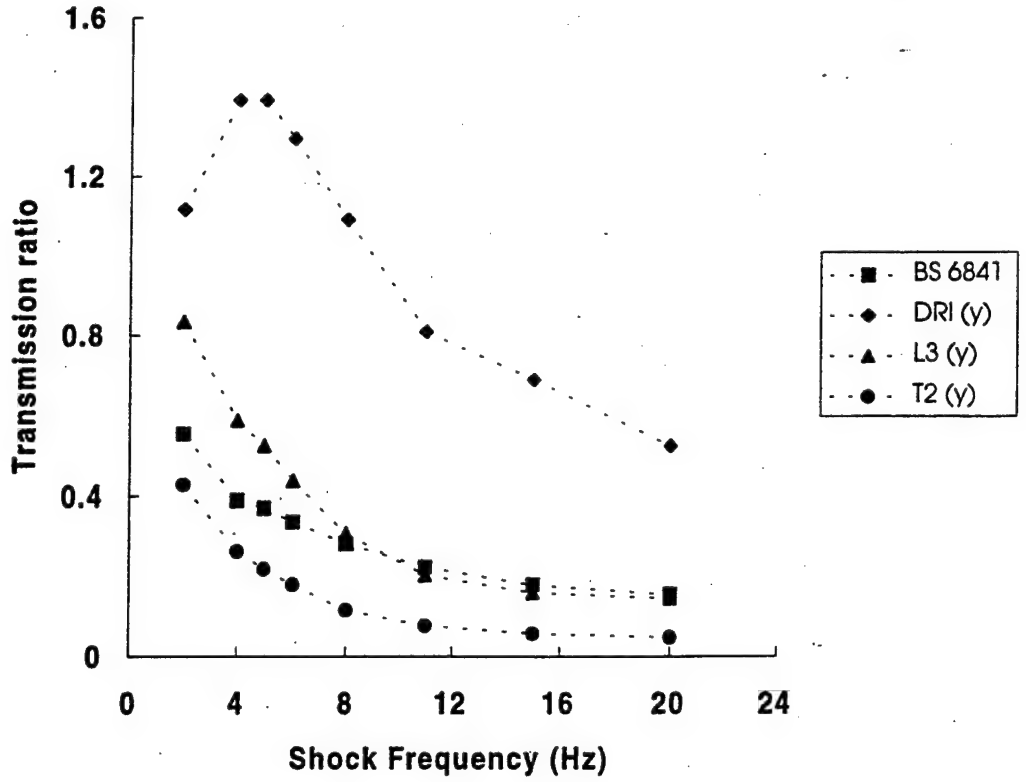

Figure 3: Comparison of the measured y axis seat to spine transmission ratio (positive shocks) with predicted transmission ratios using the W_d filter (BS 6841) and the DRI (7.2 Hz) y axis model.

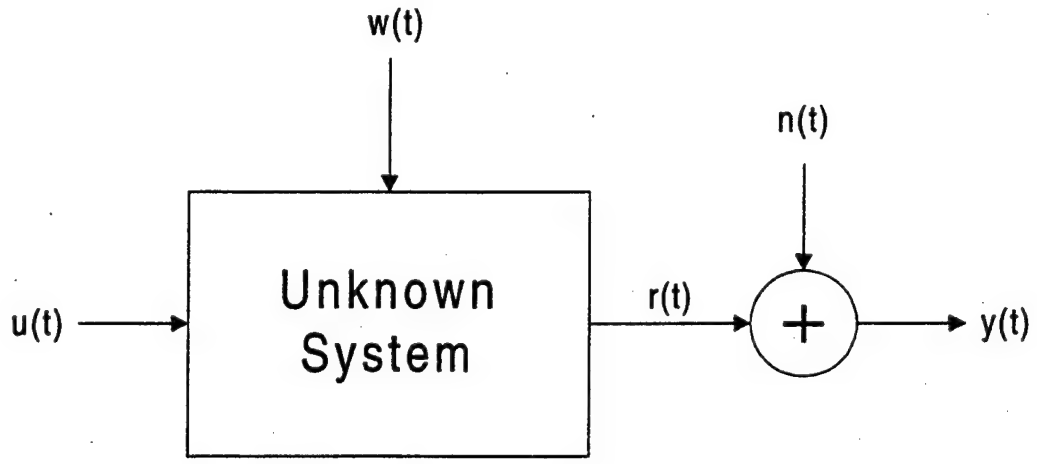

Figure 4: System Identification Approach

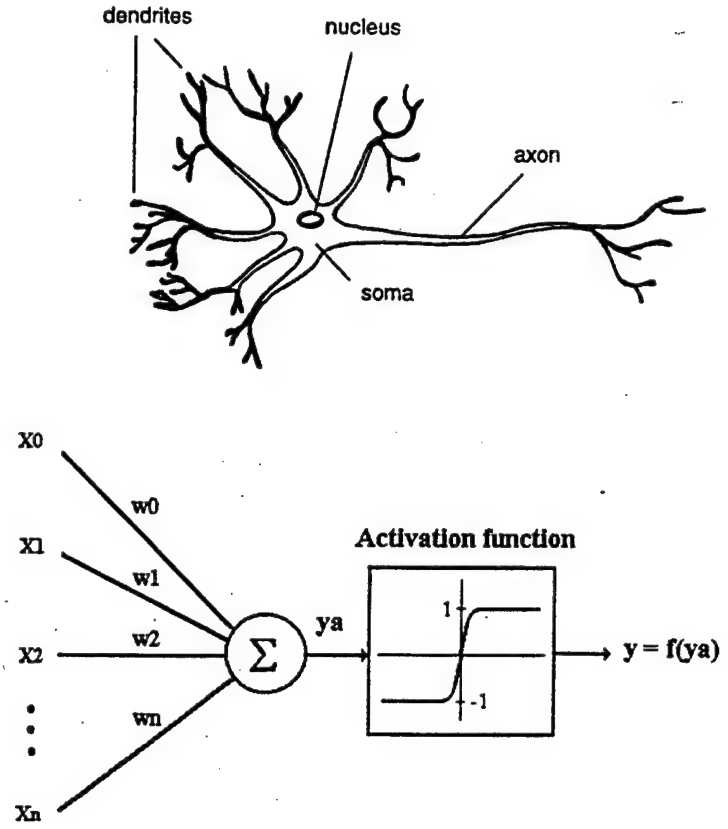

Figure 5. Biological Neuron (above) and Artificial Neuron (below), showing inputs X_o to X_n, weighting factors w_o to w_n, the hyperbolic tangent activation function, and the output y.

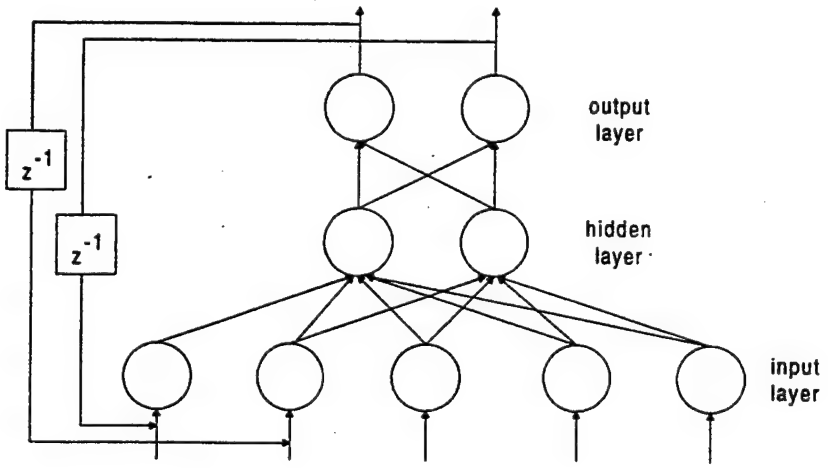

Figure 6. Externally-recurrent neural network.

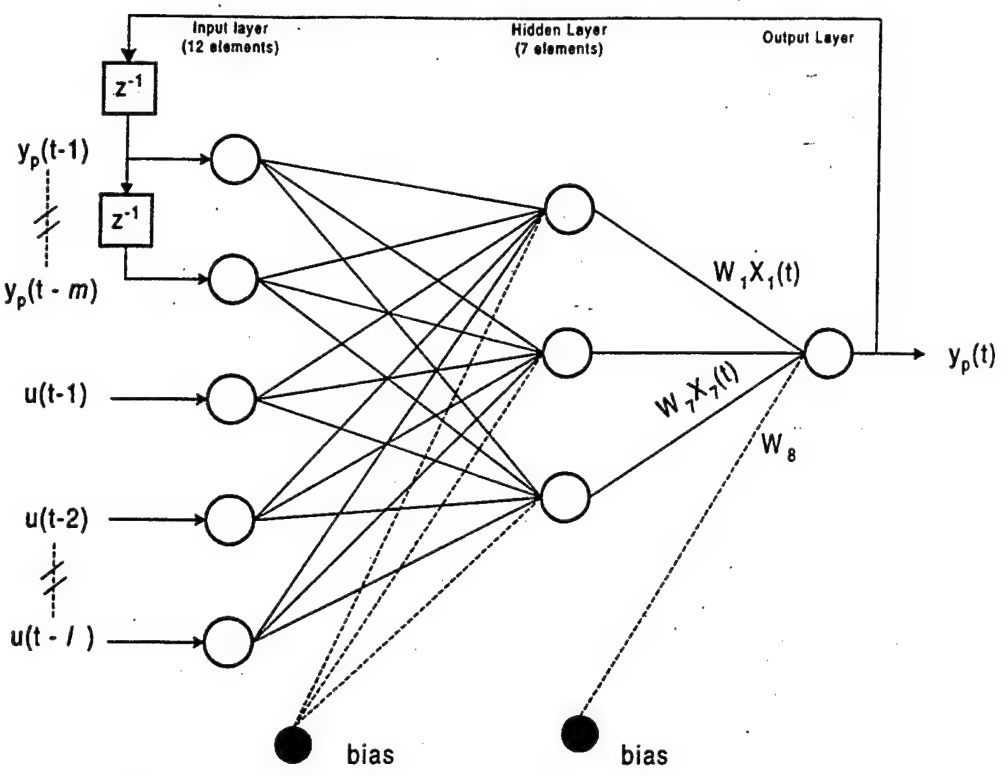

Figure 7. Finalized neural network structure.

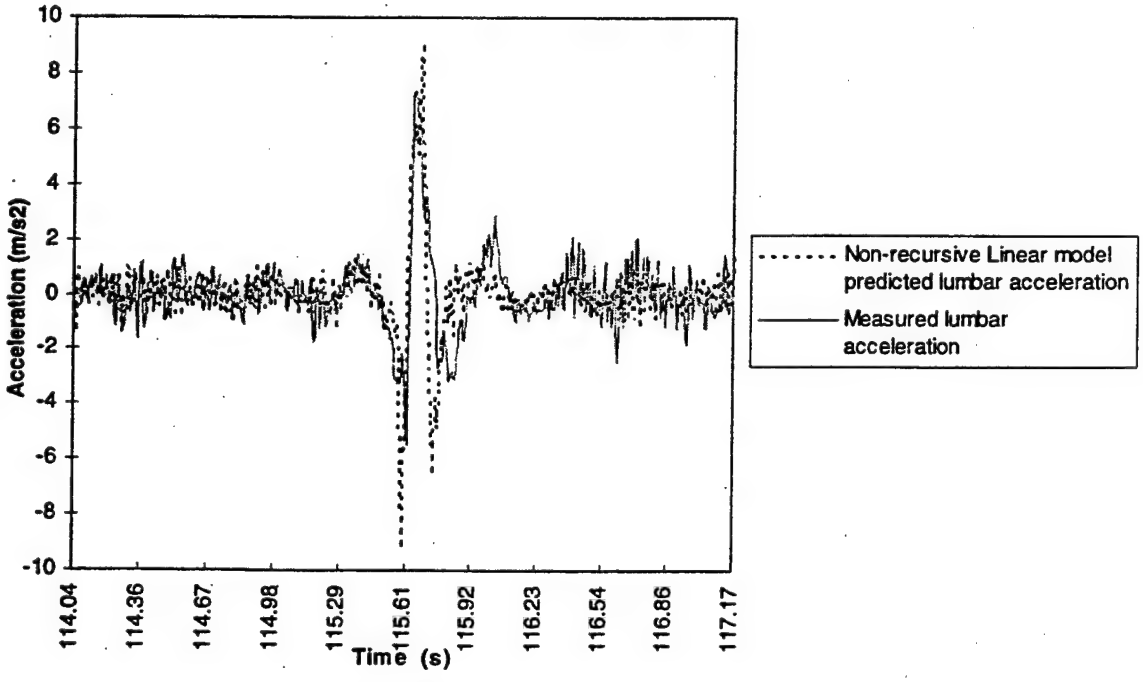

Figure 8. The measured lumbar response (in the x axis) to a +4 g, 8 Hz seat shock in the x axis, and the response predicted by a non-recursive linear model.

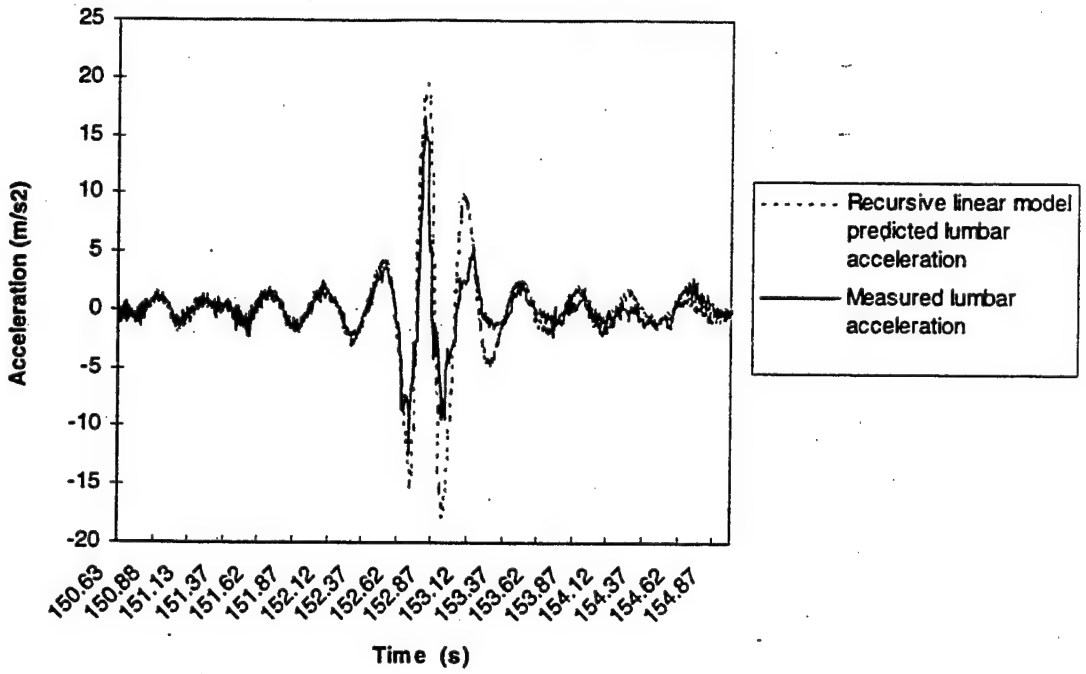

Figure 9. The measured lumbar response (in the y axis) to a +4 g, 4 Hz seat shock in the y axis, and the response predicted by a non-recursive linear model.

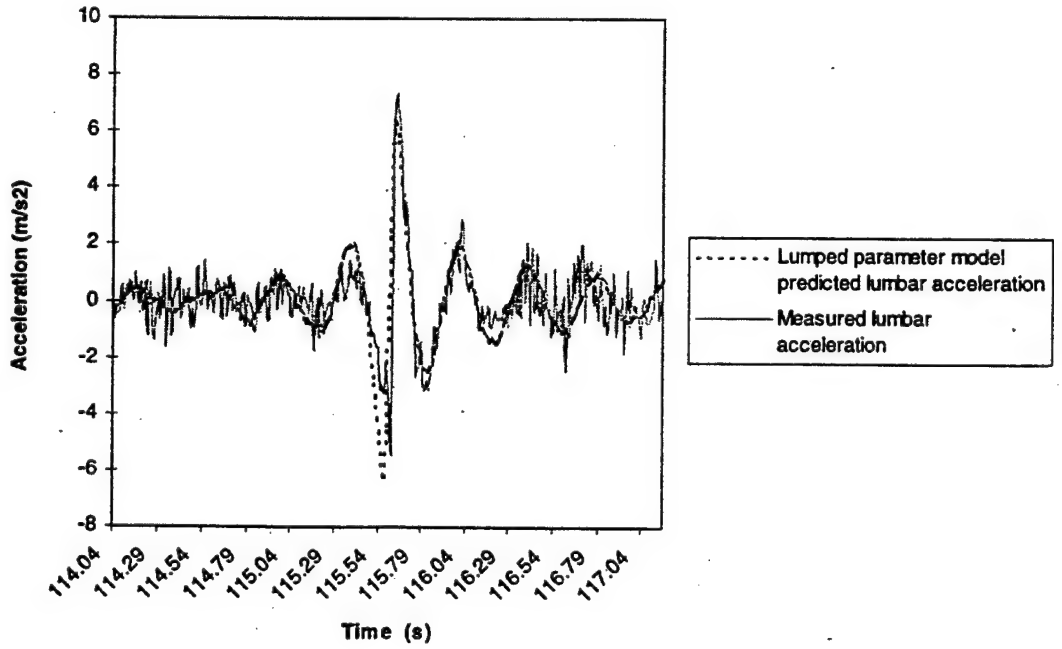

Figure 10 The measured lumbar response (in the x axis) to a +4 g, 8 Hz seat shock in the x axis, and the response predicted by a lumped parameter model (ζ=0.22, f_n=2.125 Hz).

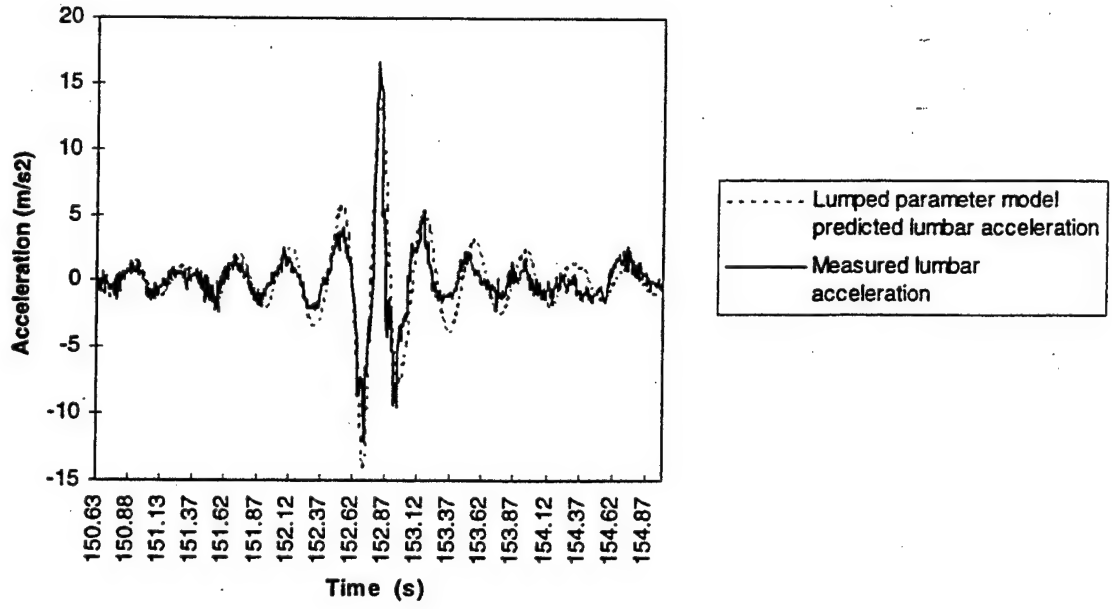

Figure 11 The measured lumbar response (in the y axis) to a +4 g, 4 Hz seat shock in the y axis, and the response predicted by a lumped parameter model (ζ=0.22, f_n=2.125 Hz).

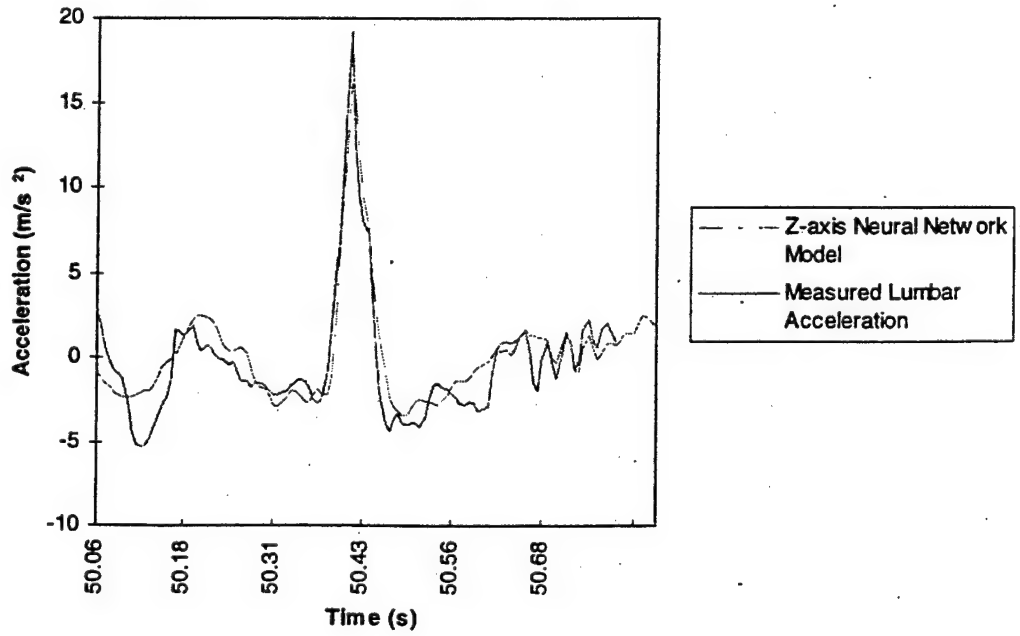

Figure 12. The measured lumbar response (in the z axis) to a +2 g, 8 Hz seat shock in the z axis and the response predicted by a neural network model.

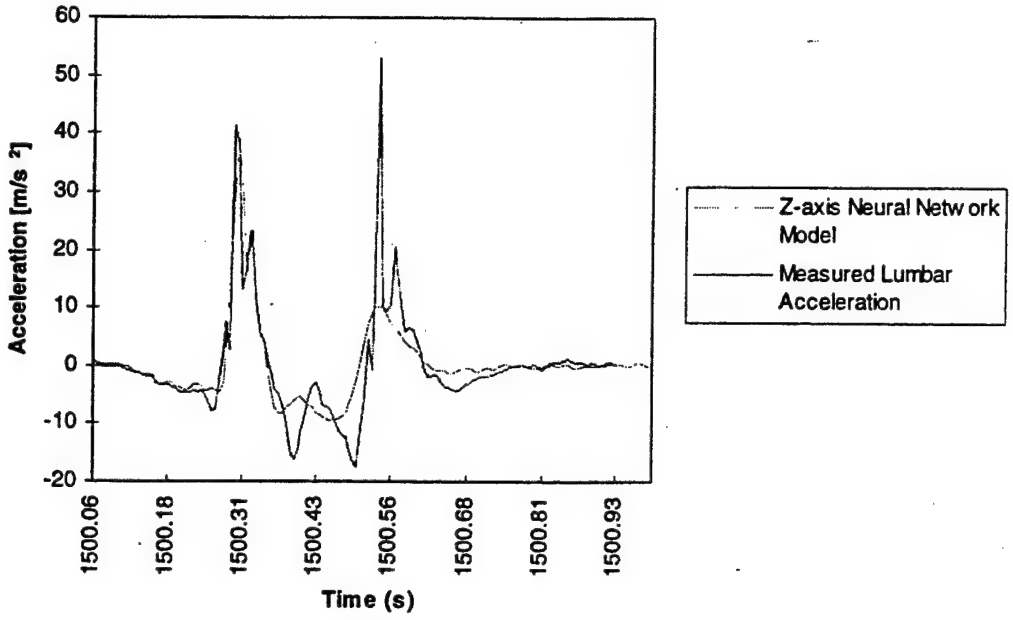

Figure 13. The measured lumbar response (in the z axis) to a +4 g, 8 Hz seat shock in the z axis and the response predicted by a neural network model.

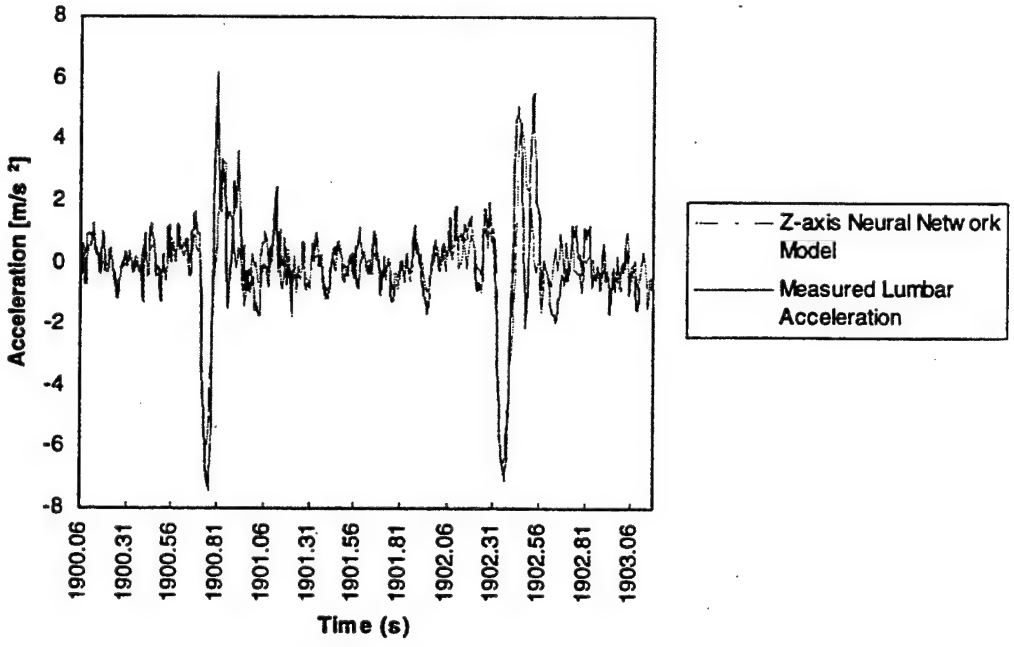

Figure 14. The measured lumbar responses (in the z axis) to a -1 g, 11 Hz and a -1 g, 8 Hz seat shock in the z axis and the response predicted by a neural network model.

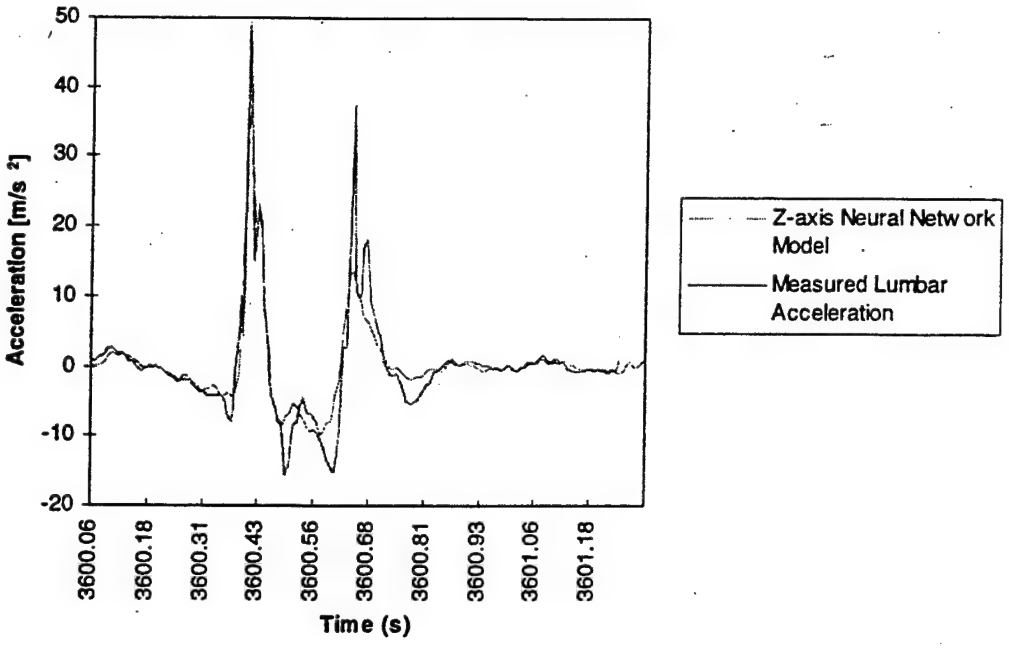

Figure 15. The measured lumbar response (in the z axis) to a +4 g, 4 Hz seat shock in the z axis and the response predicted by a neural network model.

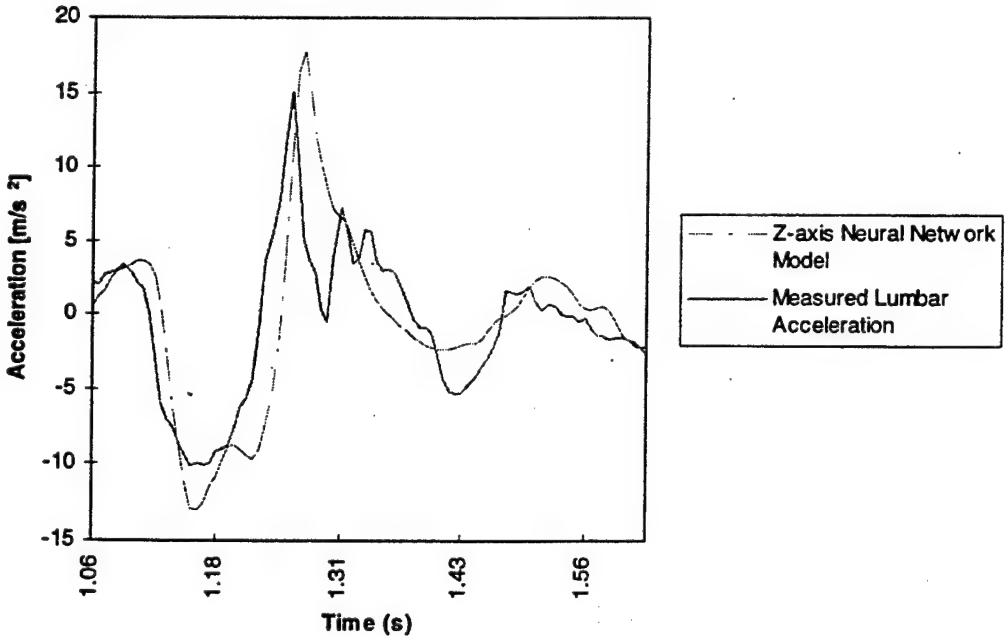

Figure 16. The measured lumbar response (in the z axis) to a -2 g, 5 Hz seat shock in the z axis and the response predicted by a neural network model.

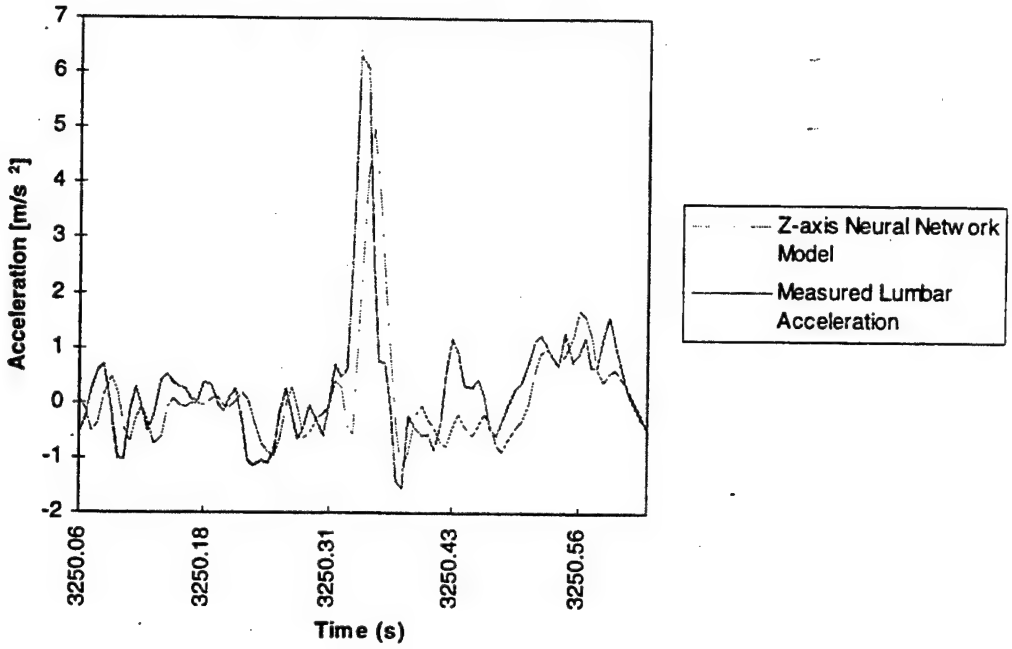

Figure 17. The measured lumbar response (in the z axis) to a +1 g, 8 Hz seat shock in the z axis and the response predicted by a neural network model.

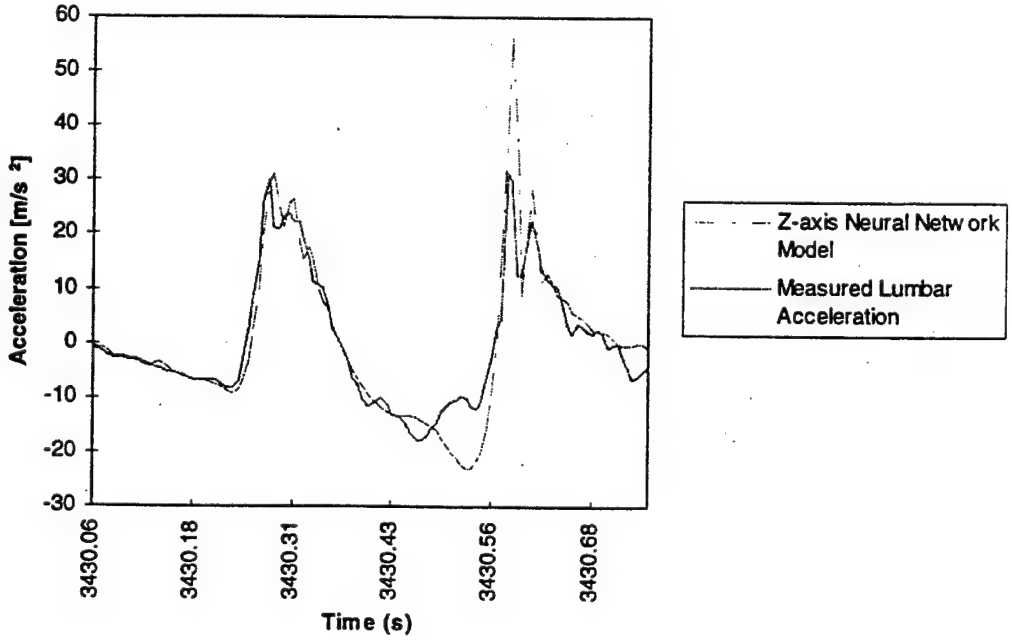

Figure 18. The measured lumbar response (in the z axis) to a +3 g, 5 Hz seat shock in the z axis and the response predicted by a neural network model.

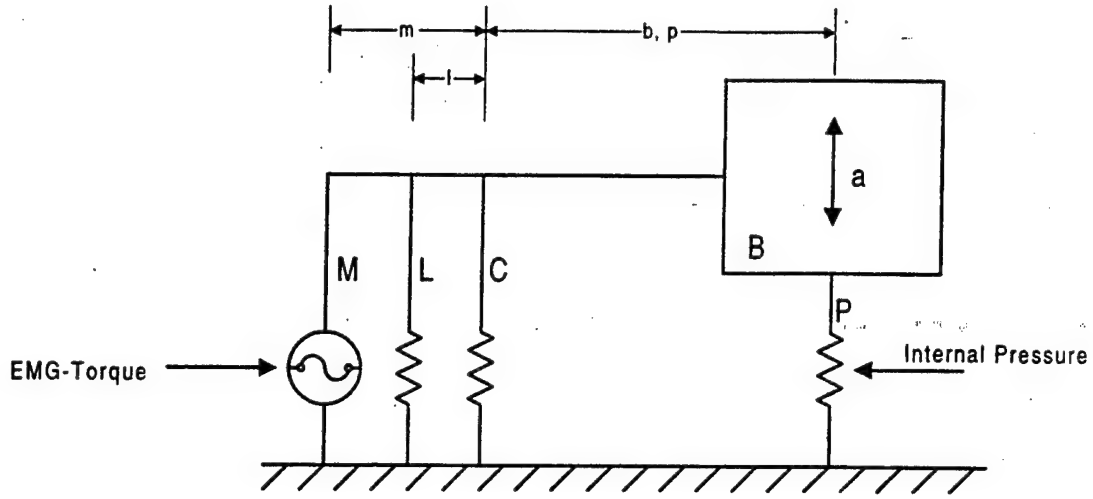

A)

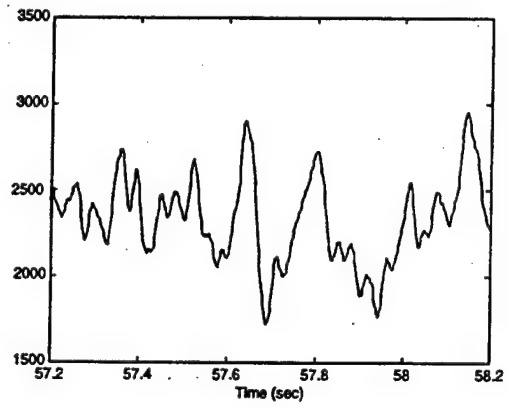

B)

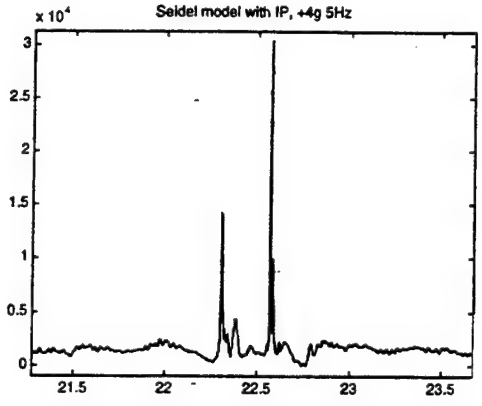

C)

Figure 19 (A) A schematic of the biomechanical model adapted from Seidel, Blüthner and Hinz, 1986; and (B) the compressive force response to a 0.5 g, 5 Hz, +z axis shock; and (C) a +4 g, 5 Hz, +z axis shock.

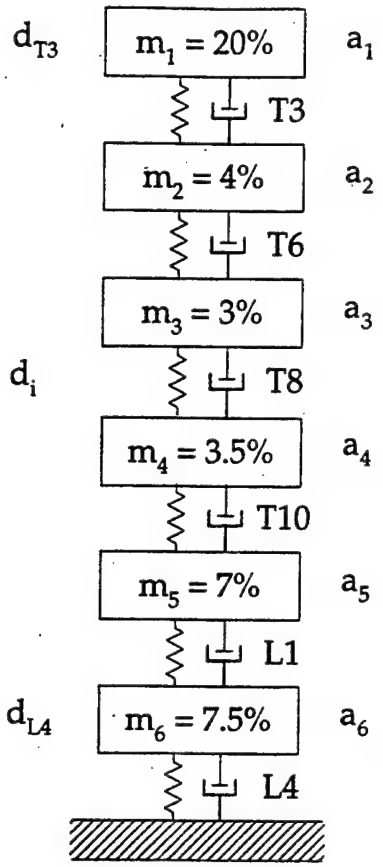

Figure 20. Segmented mass model. Segment masses (m_i) indicated as percent of total body mass. Acceleration of individual segments indicated as a partial sum of measured acceleration at T3 and L4.

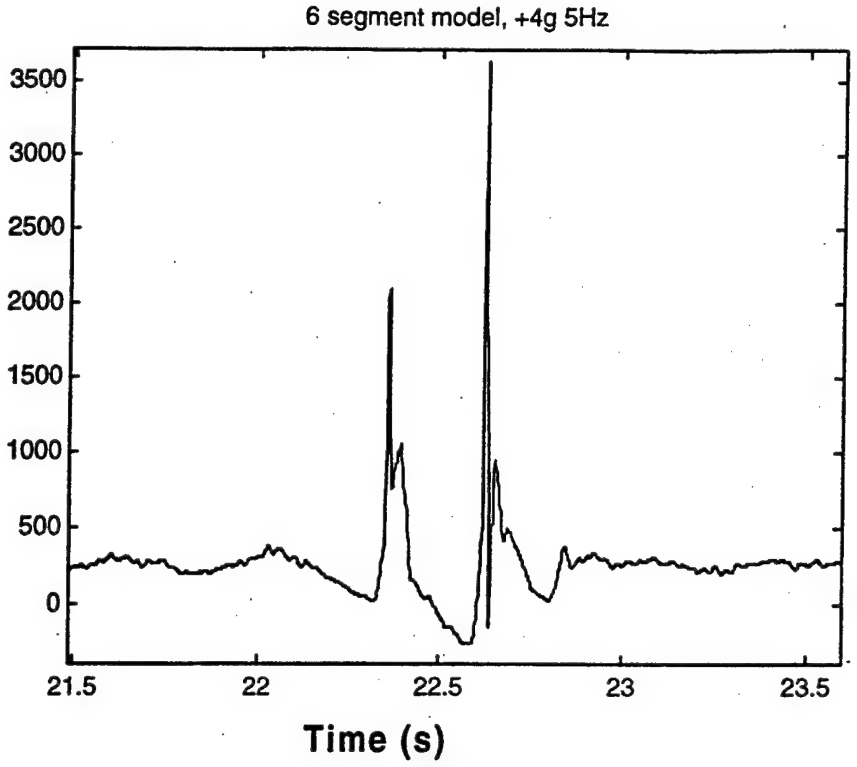

Figure 21. The spinal compression for a 4 g, 5 Hz +z axis shock at the seat, estimated using a six segment mass model.

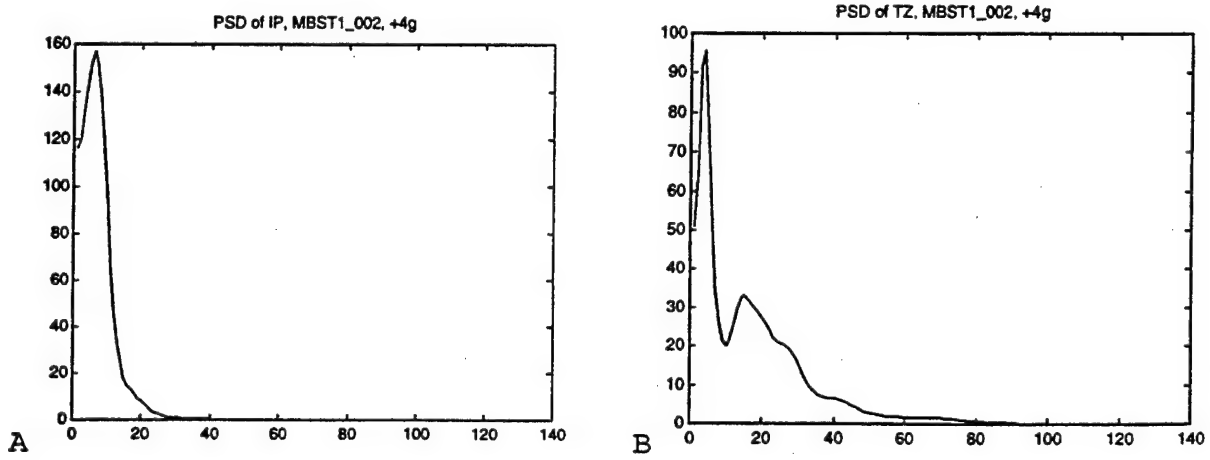

Figure 22. The power spectral density (PSD) of the internal pressure (A) and thoracic spinal acceleration response (B) to +4 g shocks at the seat in the z axis.

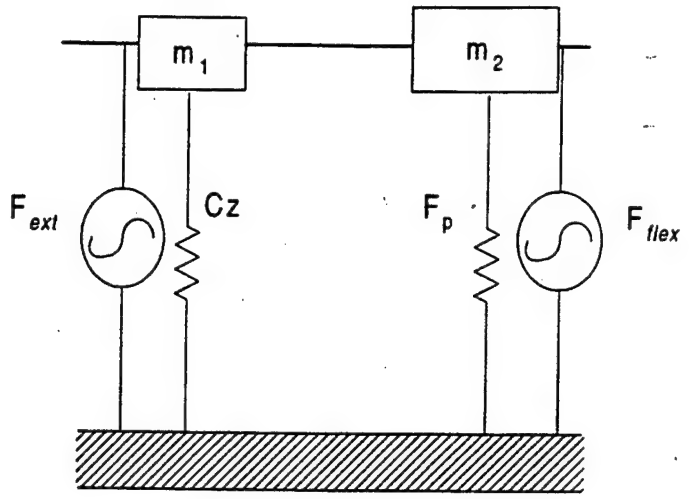

Figure 23. The eccentric segregated mass model (ESMM).

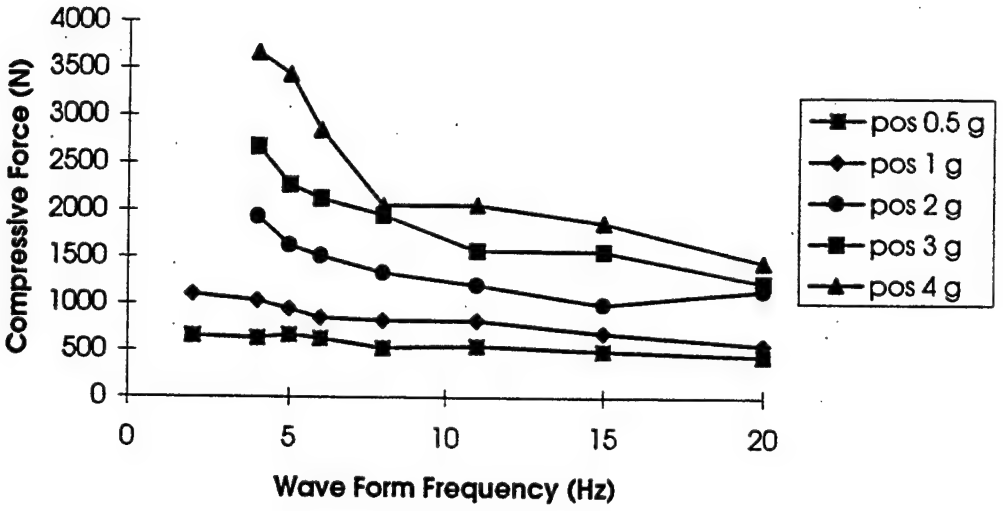

Figure 24. Frequency response curves for compressive force due to positive z axis shocks at the seat.

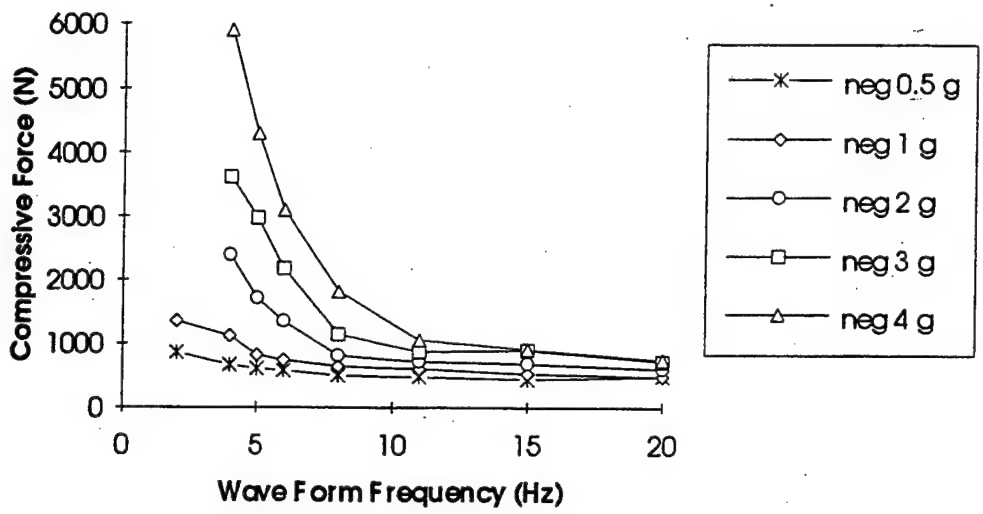

Figure 25. Frequency response curves for compressive force due to negative z axis shocks at the seat.

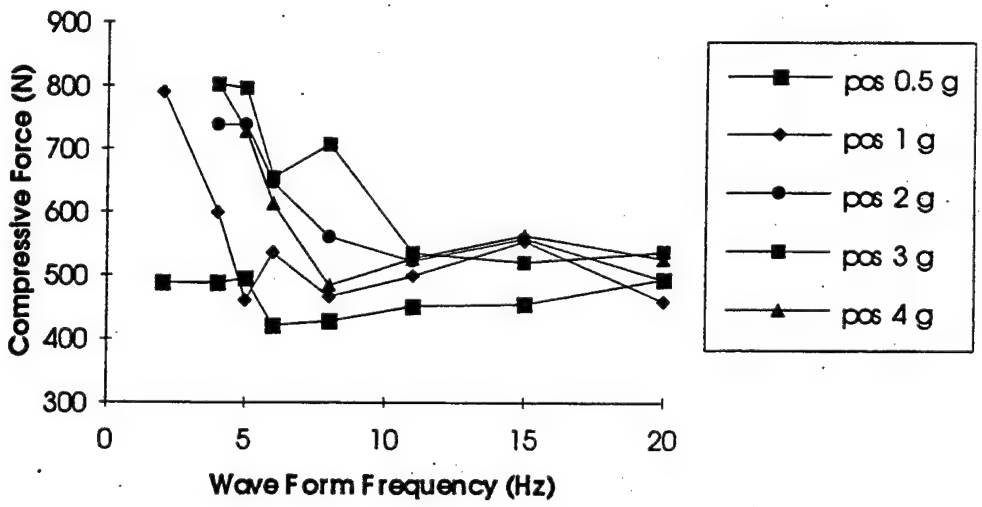

Figure 26. Frequency response curves for compressive force due to positive x axis shocks at the seat.

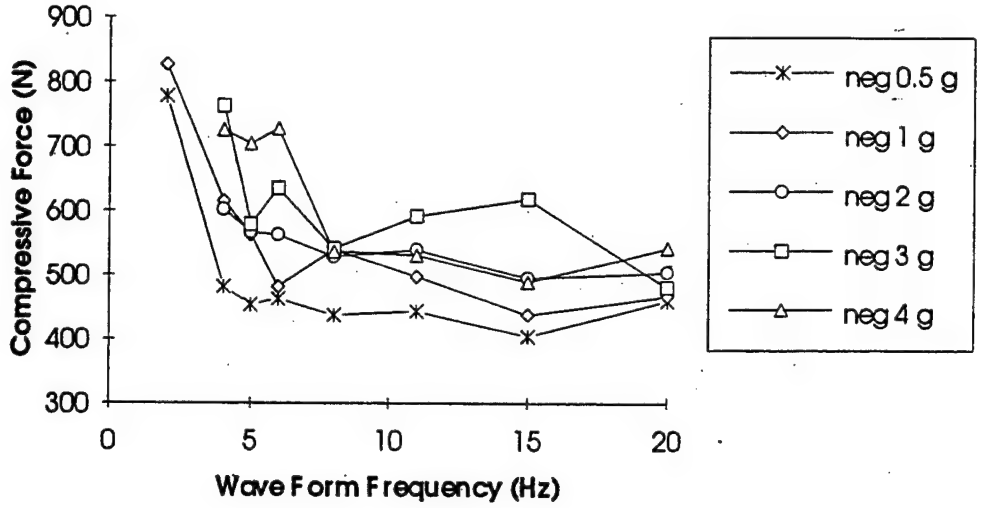

Figure 27 Frequency response curves for compressive force due to negative x axis shocks at the seat.

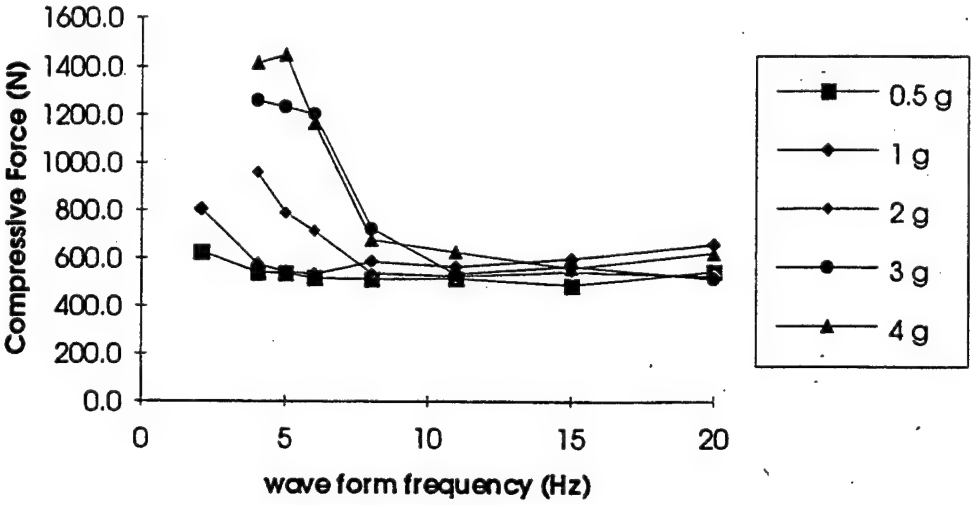

Figure 28. Frequency response curves for compressive force due to positive y axis shocks at the seat.

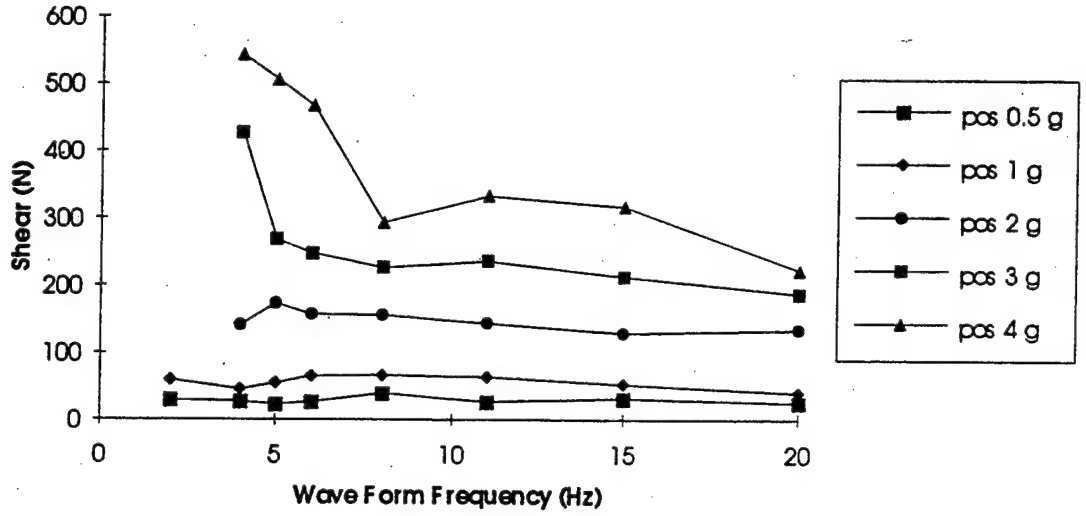

Figure 29. Frequency response curves for anterior-posterior shear force due to positive z axis shocks at the seat.

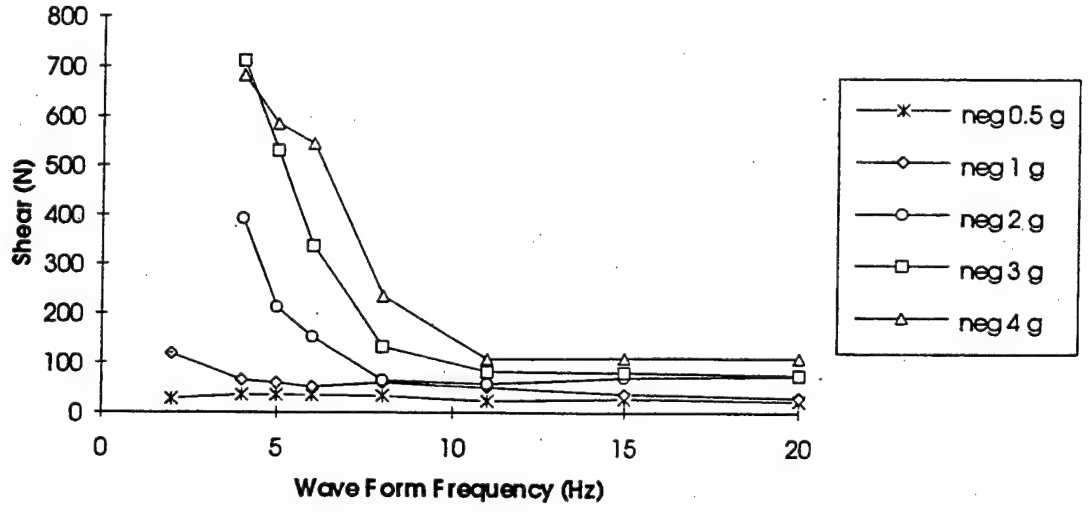

Figure 30. Frequency response curves for anterior-posterior shear force due to negative z axis shocks at the seat.

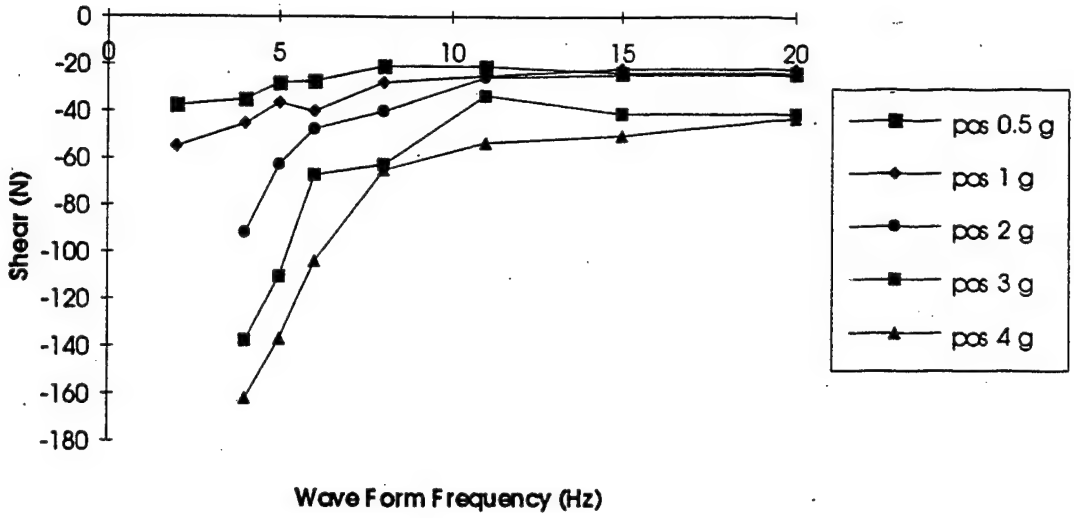

Figure 31. Frequency response curves for anterior-posterior shear force due to positive x axis shocks at the seat.

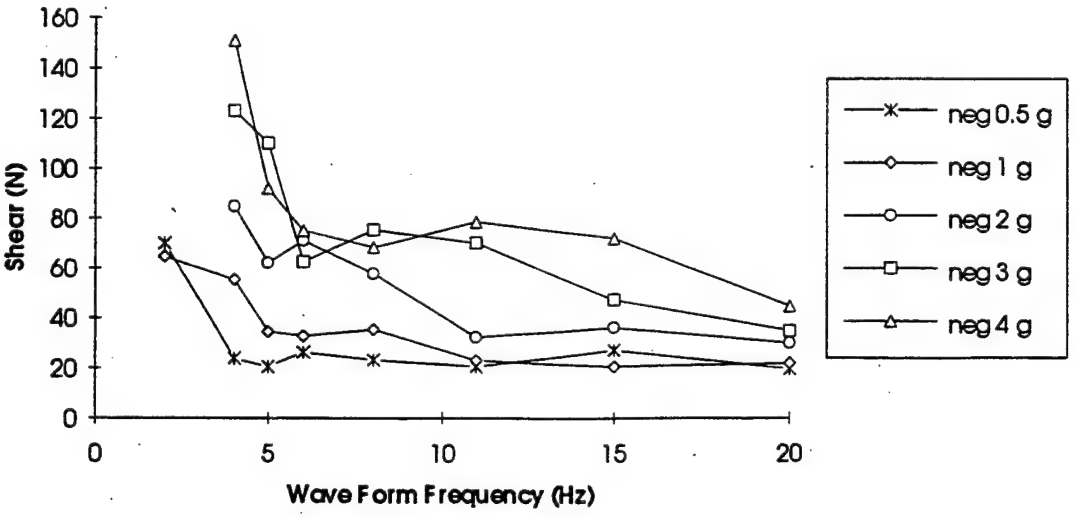

Figure 32. Frequency response curves for anterior-posterior shear force due to negative x axis shocks at the seat.

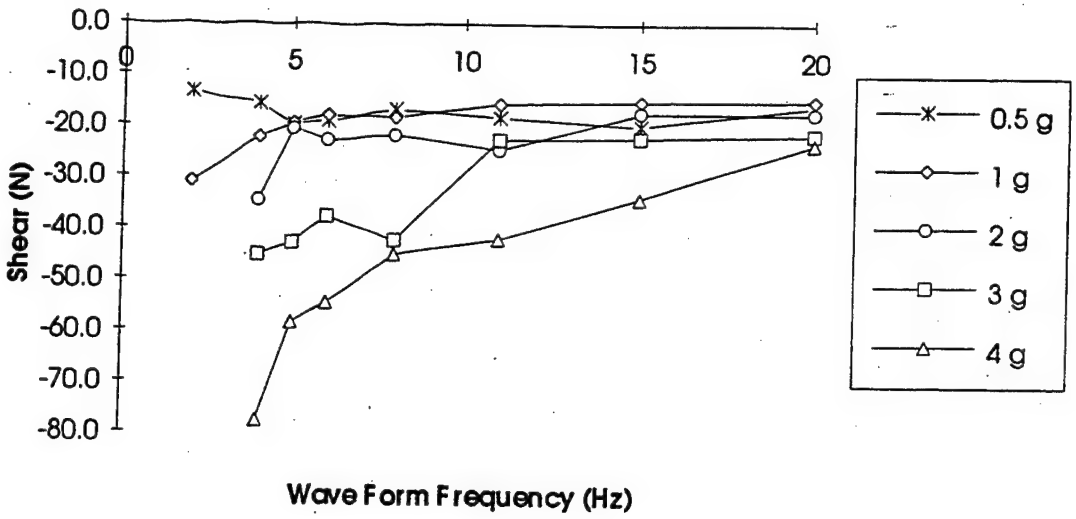

Figure 33. Frequency response curves for anterior-posterior shear force due to positive y axis shocks at the seat.

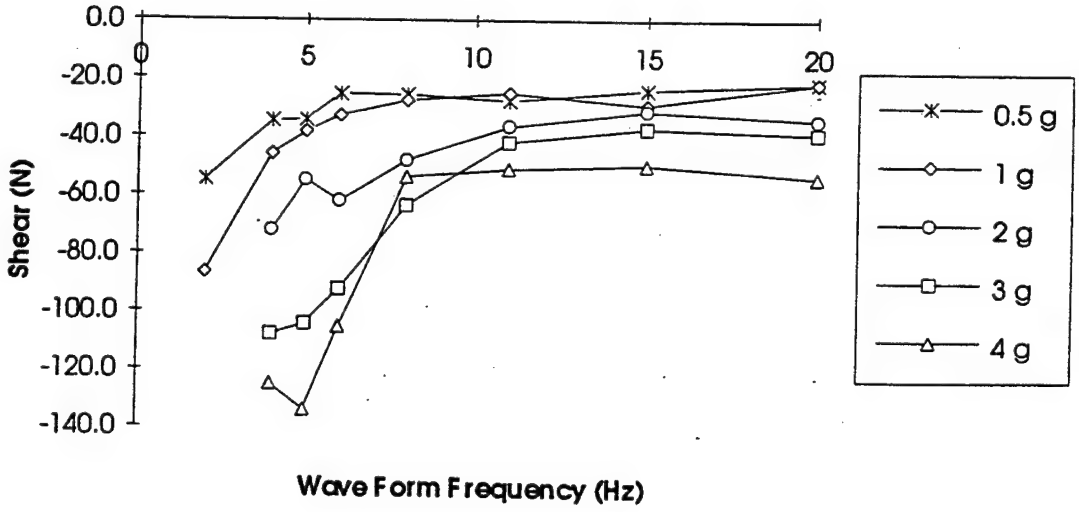

Figure 34. Frequency response curves for lateral shear force due to positive y axis shocks at the seat.

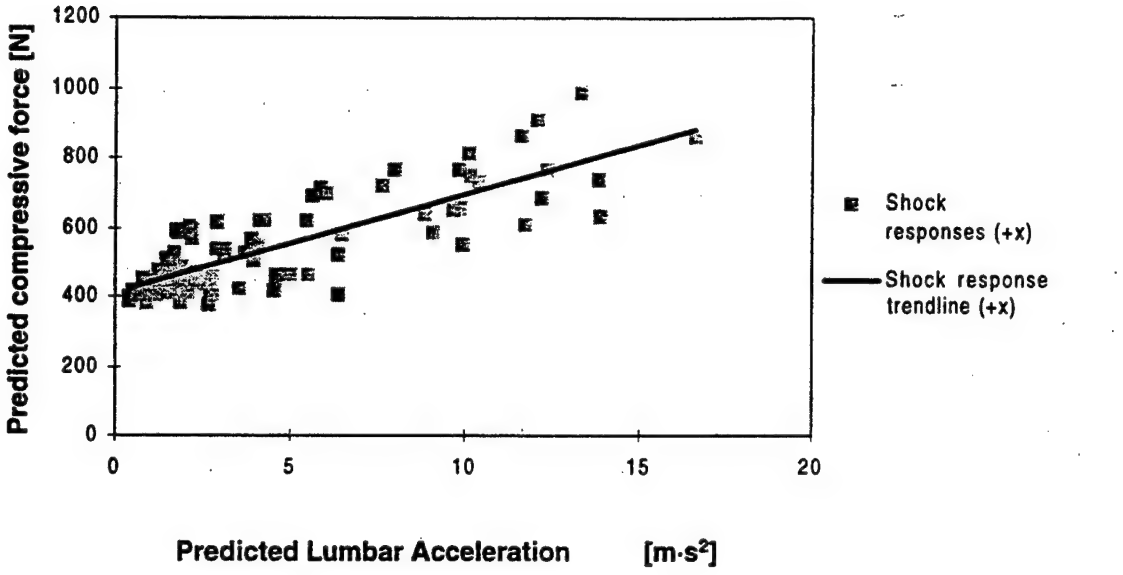

Figure 35. z axis lumbar compression versus lumbar acceleration for positive (0.5 to 4 g) x axis shocks at the seat.

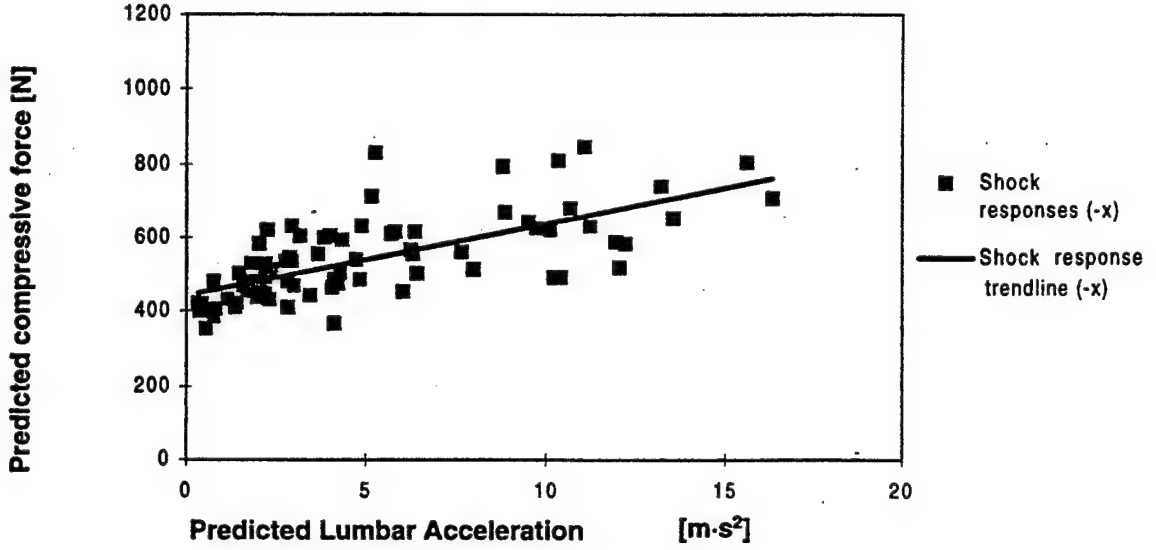

Figure 36. z axis lumbar compression versus lumbar acceleration for negative (0.5 to 4 g) x axis shocks at the seat.

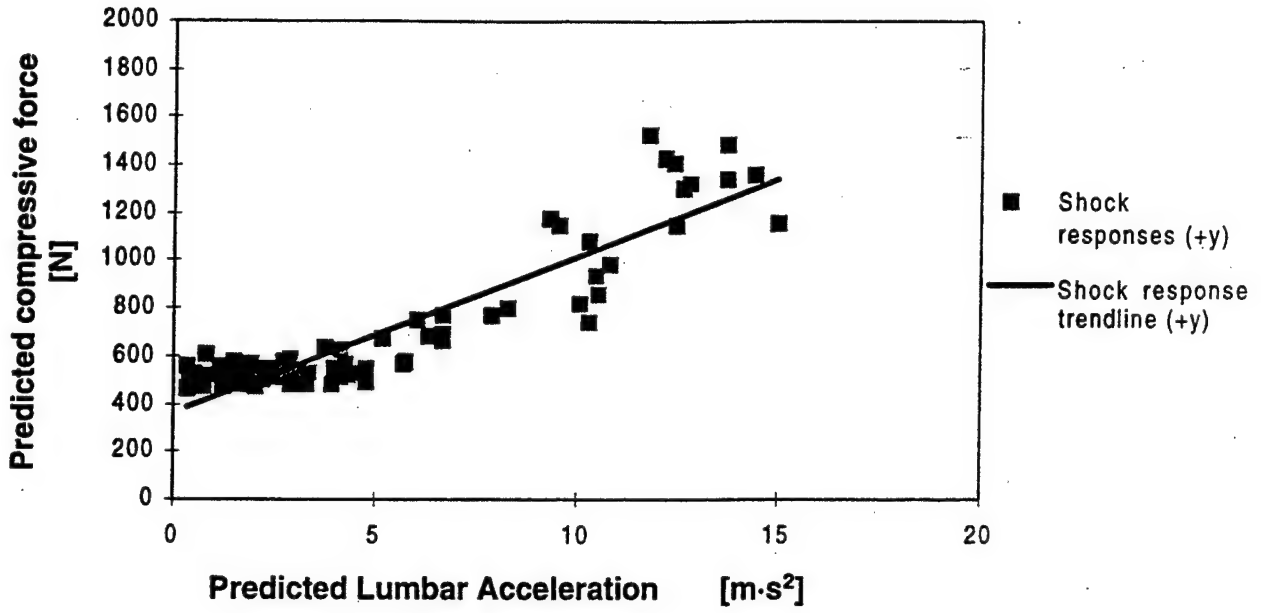

Figure 37. z axis lumbar compression versus lumbar acceleration for positive (0.5 to 4 g) y axis shocks at the seat.

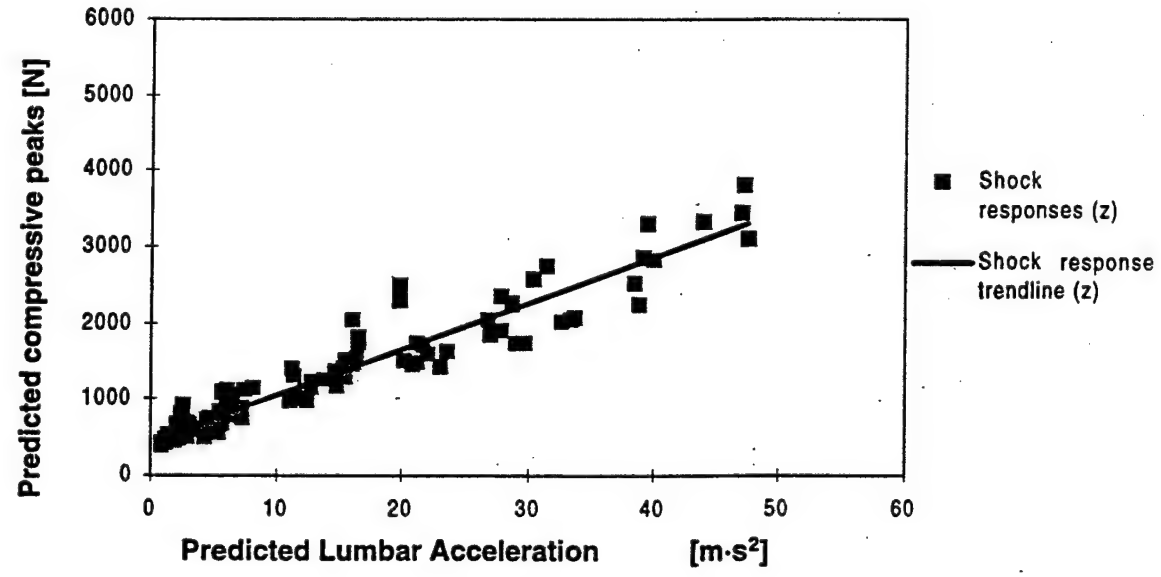

Figure 38. z axis lumbar compression versus lumbar acceleration for positive (0.5 to 4 g) and Negative (0.5 to 2 g)z axis shocks at the seat.

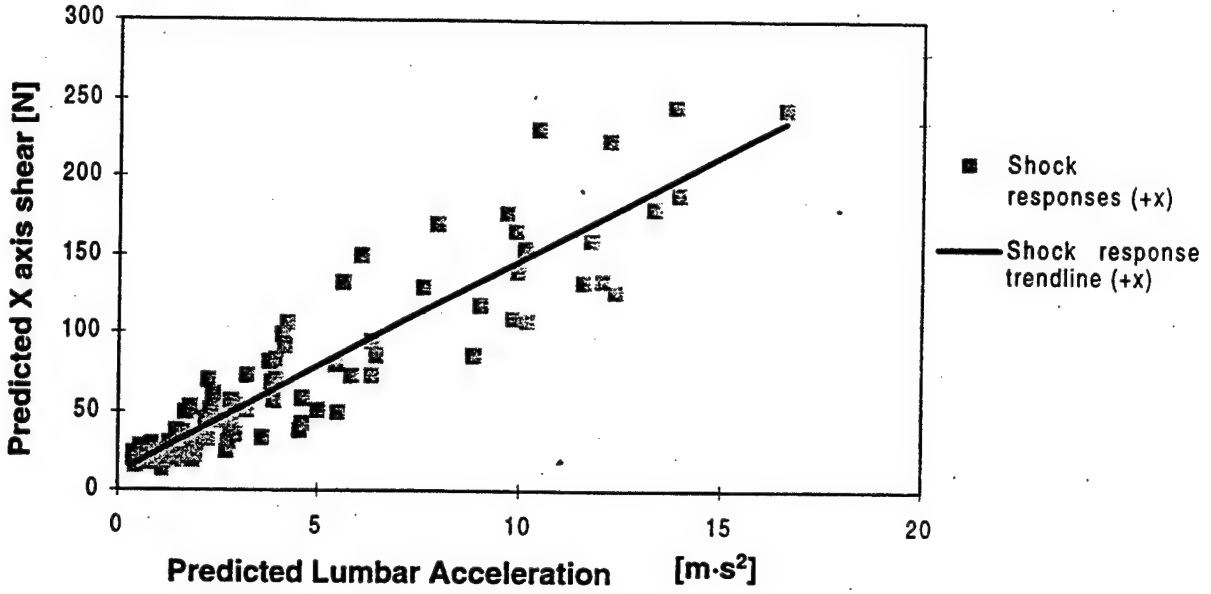

Figure 39. x axis lumbar shear force versus lumbar acceleration for positive (0.5 to 4 g) x axis shocks at the seat.

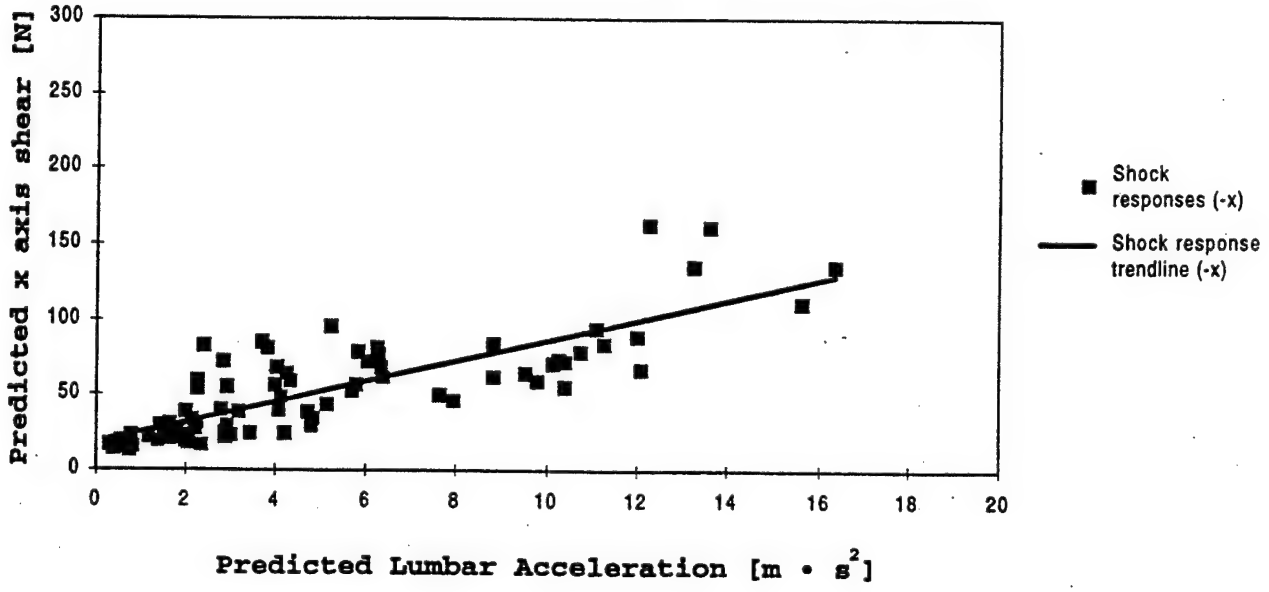

Figure 40. x axis lumbar shear force versus lumbar acceleration for negative (0.5 to 4 g) x axis shocks at the seat.

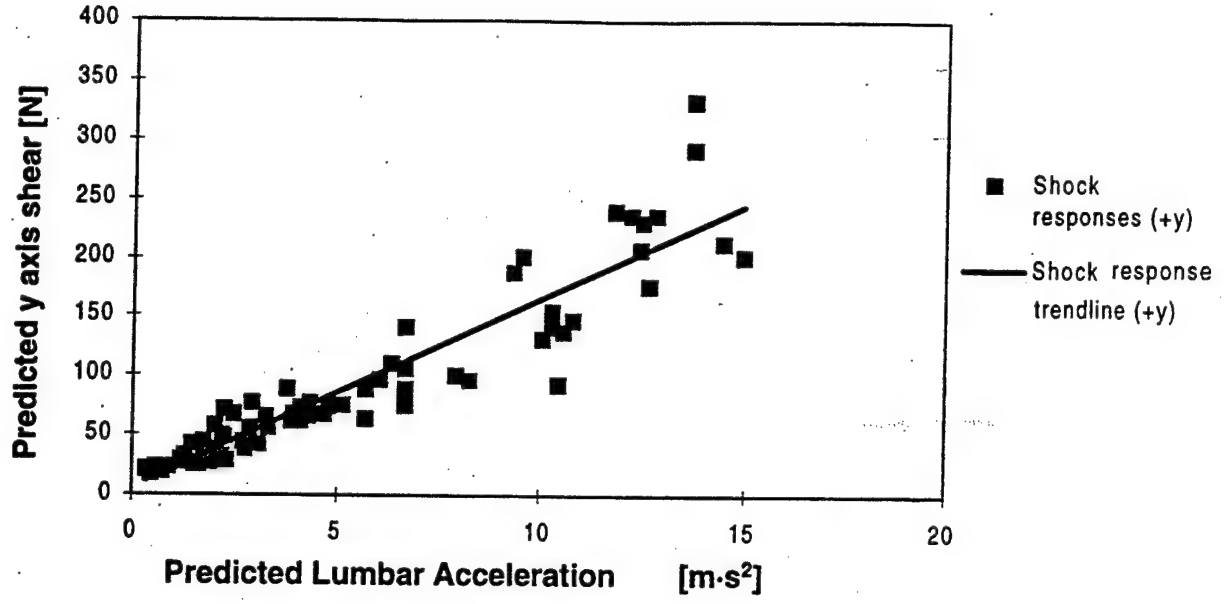

Figure 41. y axis lumbar shear force versus lumbar acceleration for positive (0.5 to 4 g) y axis shocks at the seat.

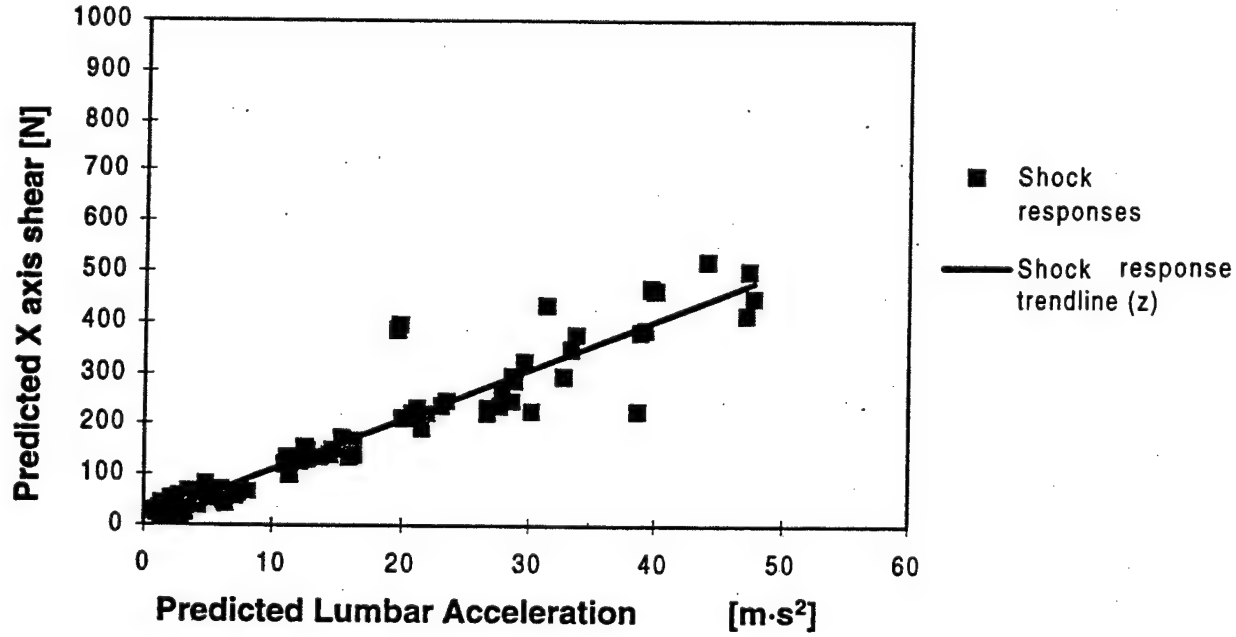

Figure 42. x axis lumbar shear force versus lumbar acceleration for positive (0.5 to 4 g) and negative (0.5 to 2 g)z axis shocks at the seat.

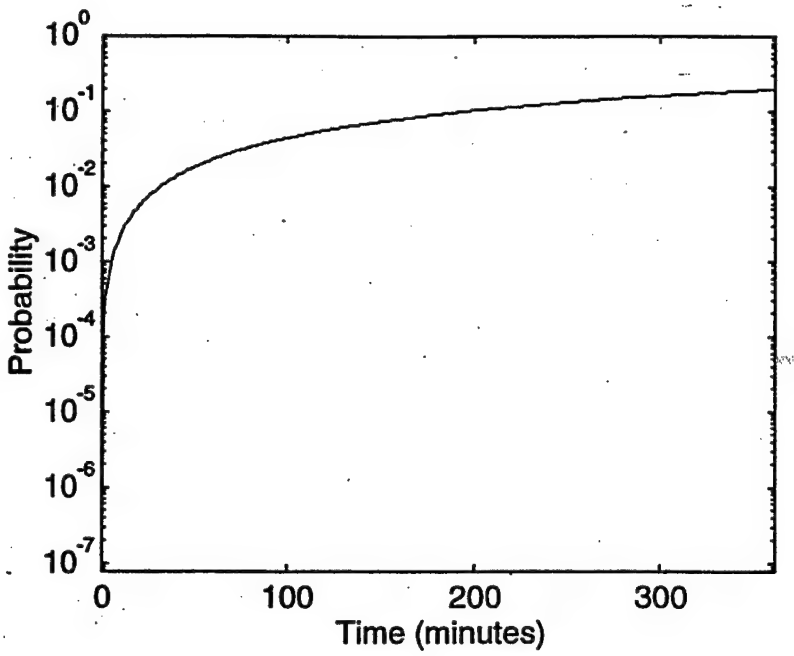

Figure 43. The risk of injury predicted in response to +2g and +4g shocks at the seat in the z axis. Exposure duration: 6 hours; shock rate: +2g at 32 per min. and +4g at 2 per 5min.

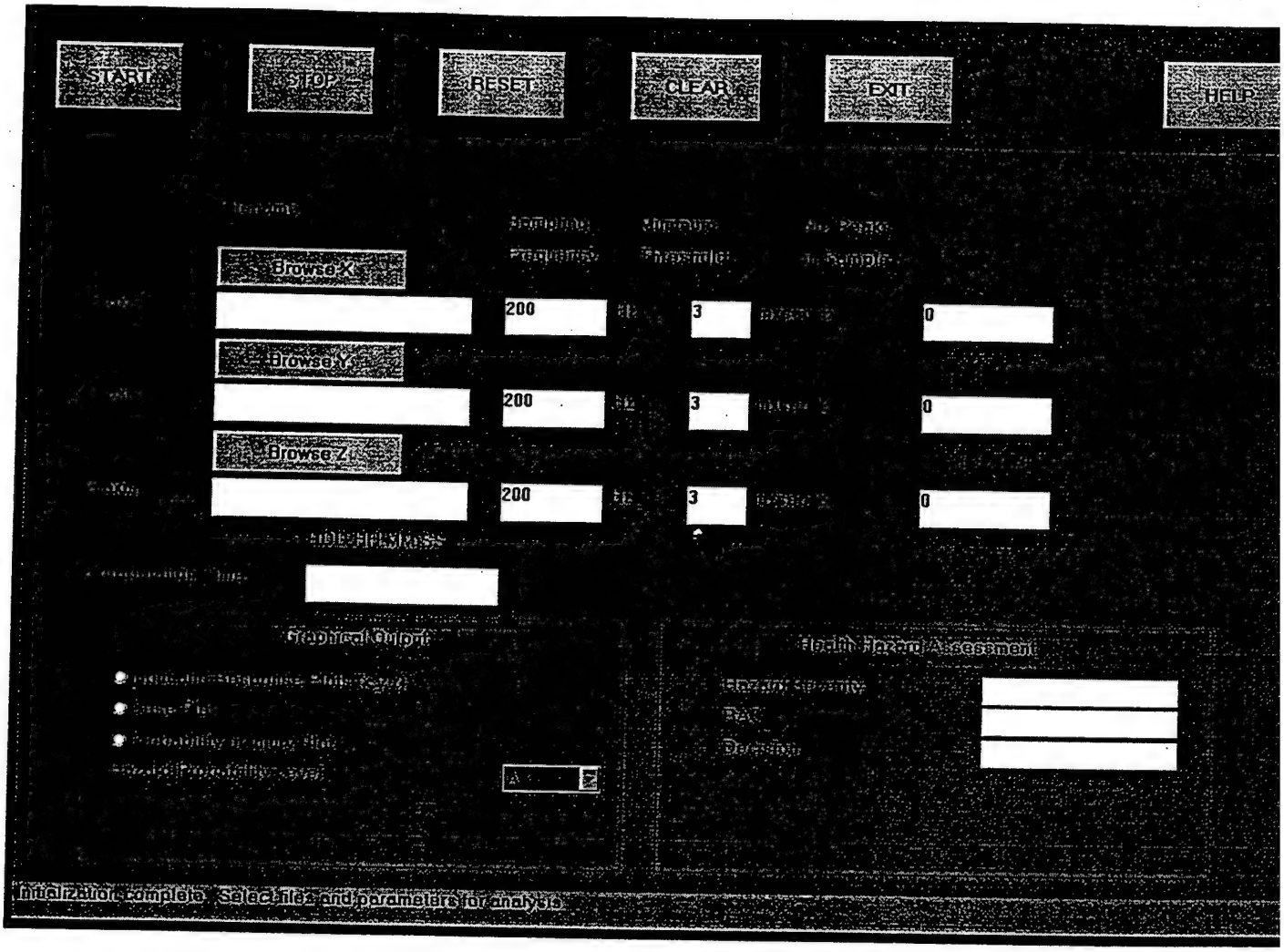

Figure 44. Health hazard assessment (HHA) method graphical user interface (GUI).

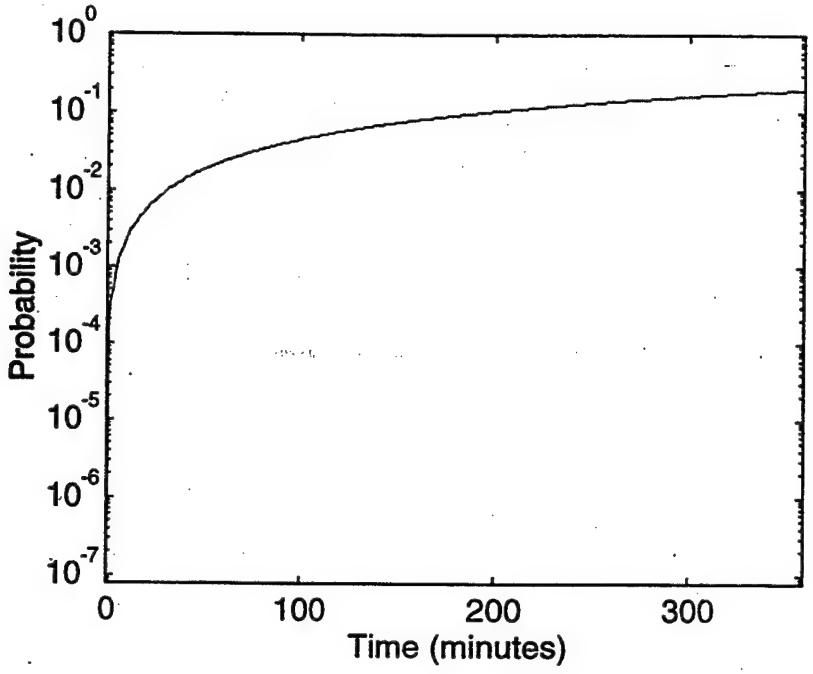

Figure 45. Probability of injury as a function of time (minutes) for the example outlined in the text (Final Probability of Injury = 0.1962)

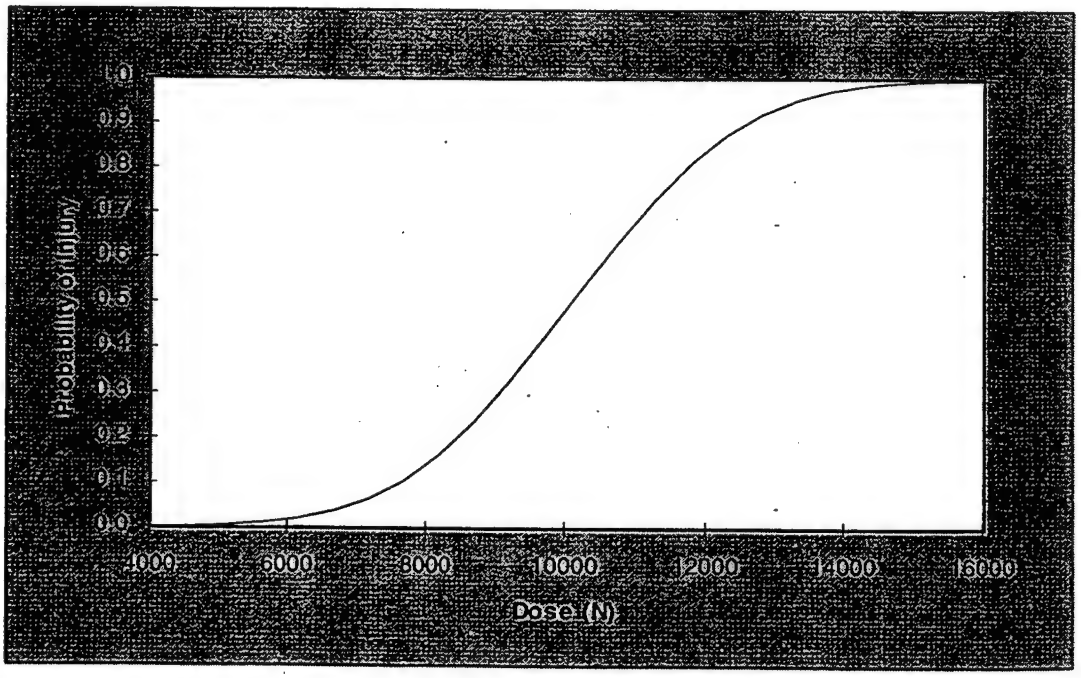

Figure 46. The relationship between compressive force dose value and the probability of injury.

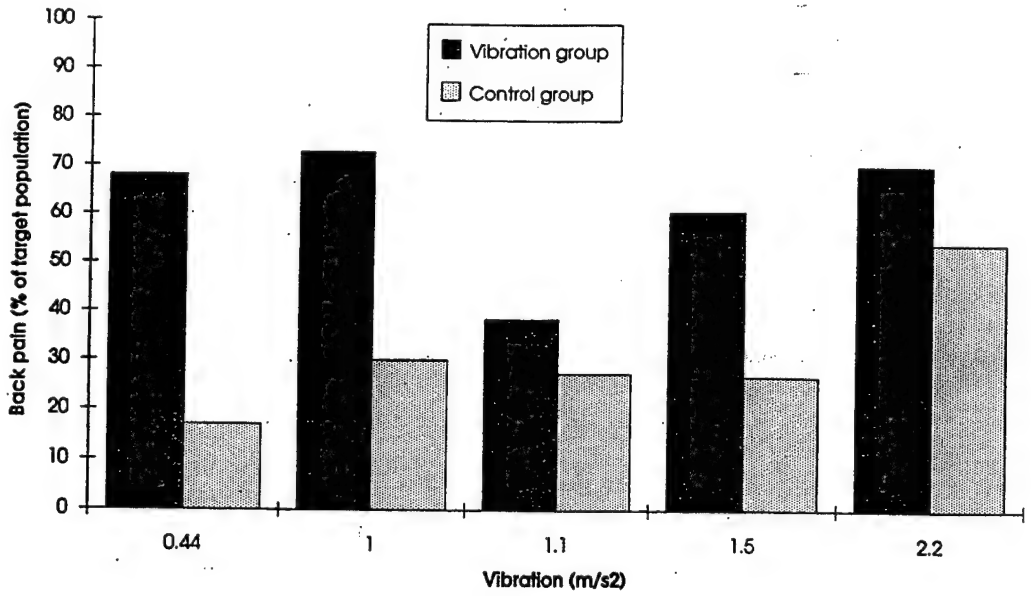

Figure 47. Incidence of low back pain in a vibration exposed group compared with a control group for several levels of vibration exposure. Data reported by different researchers and compiled by Village, Rylands and Morrison, 1993.

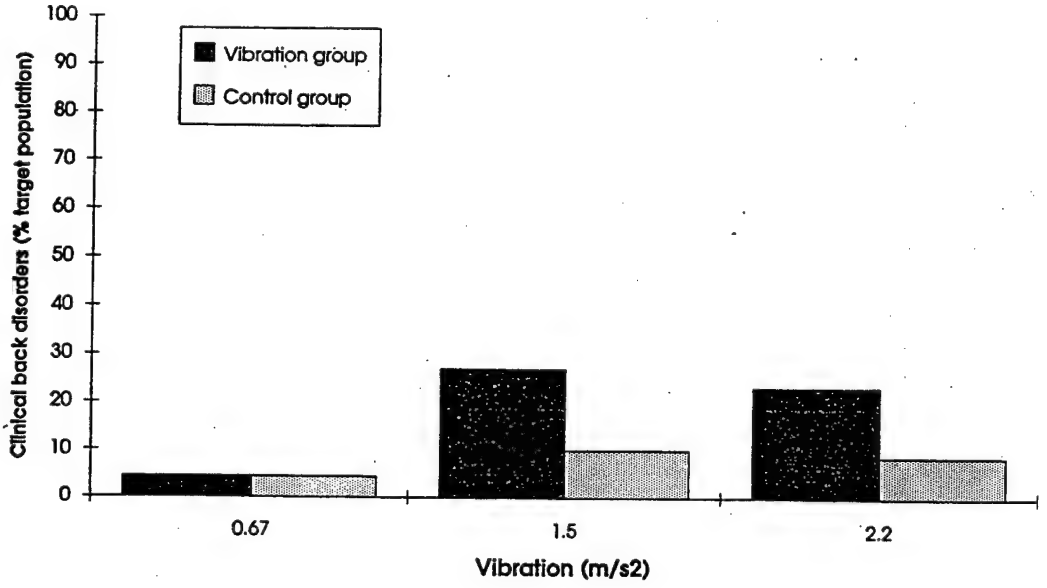

Figure 48. Comparison of the incidence of radiological damage in a control group relative to an occupational cohort exposed to vibration. Data reported by different researchers and compiled by Village, Rylands and Morrison, 1993.Village, Rylands and Morrison, 1993.

Appendix E

Publications based on Contract No. DAMD17-91-C-1115

To date, this work has resulted in a number of scholarly works which have been presented and published as papers in refereed journals, conference proceedings, post-graduate dissertations, and technical reports.

Journals

Nicol,J., Morrison, J.B., Roddan, G., and Rawicz, A. 1997. Modeling the Dynamic Response of the Human Spine to Shock and Vibration using a Recurrent Neural Network. International Journal of Vehicle Dynamics (in press).

Conference proceedings

Brammer, A.J., Roddan, G., Village, J., and Morrison, J.B. 1993. Machine identification of waveform characteristics, with application to seat motion. In Canadian Acoustical Association, October 8, Toronto, Canada.

Cameron, B.J., Robinson, D.G., Morrison, J.M., and Albano, J.P. 1995. Biochemical and EMG responses to extended exposure to mechanical shocks. In Human Response to Vibration, September 18-20, Bedford, England.

Morrison, J.B., Village, J., Roddan, G., Remedios, B., Robinson, D., Rylands, J., and Cameron, B. 1993. Analysis of spinal accelerations in response to 1, 2 and 3 g impacts at the seat. In Human Response to Vibration, September 20-22, Farnborough, England.

Morrison, J.B., Robinson, D., Roddan, G., Village, J., and Butler, B.P. 1994. Comparison of human response to impacts measured by infrared emitting diodes and accelerometers. In International Ergonomics Association (IEA), August 15-19, Toronto, Canada.

Morrison, J.B., Robinson, D.G., Roddan, G., Nicol, J.J., and Butler, B.P. 1995. Analysis of vertebra to skin transfer function in response to mechanical shock. In Human Response to Vibration, September 18-20, Bedford, England.

Morrison, J.B., Robinson, D.G., and Cameron, B.J. 1996. Human response to whole-body vibration and shock. In Canadian Society for Biomechanics 9th Biennial Conference, August 21-24, Burnaby, Canada.

Morrison, J.B., Martin, S.H., Robinson, D.G., Roddan, G., Nicol, J.J., Springer, M.J-N., Cameron, B.J., and Albano, J.P. 1996. Development of a comprehensive method of Health Hazard Assessment (HHA) for exposure to repeated mechanical shocks. In Human Response to Vibration, September 18-20, Nuneaton, England.

Nicol, J.J., Morrison, J., Roddan, G., and Rawicz, A. 1995. The application of an artificial neural network to modeling seat to spine transmission of acceleration. In Human Response to Vibration, September 18-20, Bedford, England.

Nicol, J.J., Morrison, J.M., and Roddan, G. 1996. An artificial neural network model of the dynamic response of the human spine to repeated mechanical shocks. In Human Response to Vibration, September 18-20, Nuneaton, England.

Robinson, D., Morrison, J.B., and Village, J. 1993. The pattern of electromyographic response to mechanical shocks. In Human Response to Vibration, September 20-22, Farnborough, England.

Robinson, D., Village, J., Roddan, G., Remedios, B., Morrison, J., and Brammer, J. 1993. The effect of mechanical shock frequency and amplitude on spinal transmission and internal pressure. In Canadian Acoustical Association, October 8, Toronto, Canada.

Robinson, D., Brown, D., Morrison, J.B., Cameron, B., and Village, J. 1994. A method to quantify the paraspinal muscle response to impacts at the seat. In International Ergonomics Association (IEA), August 15-19, Toronto, Canada.

Robinson, D.G., Morrison, J.M., and Cameron, B.J. 1995. The contribution of muscle response and internal pressure to estimation of spinal compression from mechanical shocks using a simple biomechanical model. In Human Response to Vibration, September 18-20, Bedford, England.

Rylands, J., Remedios, B., Morrison, J.B., and Village, J. 1993. A method for processing ECG signals to assess the instantaneous effects of mechanical shocks. In Human Response to Vibration, September 20-22, Farnborough, England.

Village, J., and Morrison, J.B. 1991. Development of a standard for the Health Hazard Assessment of mechanical shock and repeated impact. In Human Response to Vibration, September 25-27, Buxton, England.

Village, J., Rylands, J., and Morrison, J.B. 1993. Development of a dose-effect database for exposure to whole-body vibration: problems and assumptions. In Human Factors Association of Canada, August, Halifax.

Village, J., Morrison, J.B., and Robinson, D. 1993. Internal pressure response to mechanical shocks of varying frequency and amplitude. In Human Response to Vibration, September 20-22, Farnborough, England.

Vukusic, A., Morrison, J.B., Roddan, G., Robinson, D.G., and Cameron, B.J. 1995. The effect of continuous exposure on subjective responses to 1, 2 and 3 g shocks. In Human Response to Vibration, September 18-20, Bedford, England.

Vukusic, A.V., Morrison, J.M., Springer, M.J-N., Robinson, D.G., and Cameron, B.J. 1996. Comparison of subjective responses to repeated mechanical shocks with dose response functions and biodynamic models. In Human Response to Vibration, September 18-20, Nuneaton, England.

Technical reports

Cameron, B., Morrison, J., Robinson, D., Vukusic, A., Martin, S., and Roddan, G. 1996. Development of a Standard for the Health Hazard Assessment of Mechanical Shock and Repeated Impact in Army Vehicles, Phase 4 - Experimental Phase. Fort Rucker, AL: USAARL Contract Report No. CR 96-1.

Roddan, G., Brammer, T., Village, J., Morrison, J., Remedios, B., and Brown, D. 1995. Development of a Standard for the Health Hazard Assessment of Mechanical Shock and Repeated Impact in Army Vehicles, Phase 2. Fort Rucker, AL: USAARL Contract Report No. CR 95-2.

Village, J., Morrison, J., Smith, M., Roddan, G, Rylands, J., Robinson, D., Brammer, A., and Cameron, B. 1995a. Development of a Standard for the Health Hazard Assessment of Mechanical Shock and Repeated Impact in Army Vehicles, Phase 1. Fort Rucker, AL: USAARL Contract Report No. CR 95-1.

Village, J., Morrison, J., Robinson, D., Roddan, G, Rylands, J., Cameron, B., Remedios, B., and Brown, D. 1995b. Development of a Standard for the Health Hazard Assessment of Mechanical Shock and Repeated Impact in Army Vehicles, Phase 3 Pilot Tests. Fort Rucker, AL: USAARL Contract Report No. CR 95-3.

Theses

Nicol, J.J. 1996. Modeling the dynamic response of the human spine to mechanical shock and vibration using an artificial neural network. Master's thesis, Simon Fraser University.

Robinson, D.G. 1997. The Dynamic Human Response to Seated Shocks: The Influence of Muscle and Internal Pressure. Ph.D. dissertation, Simon Fraser University.

Vukusic, A.V. 1995. Subjective and associated objective response to repeated mechanical shocks in seated humans. Master's thesis, Simon Fraser University.

Appendix F

References

Air Standardization Coordinating Committee. 1982. Human tolerance to repeated shock. Air Standardization Coordinating Committee ADV PUB 61/25 : 1-6.

Allen, G.R. 1977. Human tolerance of repeated shocks. In Proceedings of the European Space Agency Life Sciences Research in Space, 343-349. Germany

Amirouche, F.M.L. 1987. Modeling of human reactions to whole-body vibration. Journal of Biomechanical Engineering. 109: 210-217.

Amirouche, F.M.L. and Ider, S.K. 1988. Simulation and analysis of a biodynamic human model subjected to low accelerations - A correlation study. Journal of Sound and Vibration. 123: 281-292.

Andersson, G.B.J., Örtengren, R., and Nachemson, A. 1977. Intradiscal pressure, intraabdominal pressure and myoelectric back muscle activity related to posture and loading. Clinical Orthopedics. 129: 156-164.

Anton, D.J. 1986. The influence of spinal fractures on Royal Airforce ejections. 1968-1983. Rep 529 Air crew equipment group, RAF Institute of Aviation Medicine, Farnborough, UK.

Begeman, P.C., Visarius, H., Nolte L.-P., and Prasad, P. 1994 Viscoelastic shear responses of the cadaver and Hybrid III lumbar spine. In 38th Stapp Car Crash Conference Proceedings, 1: 14. SAE 942205, Society of Automotive Engineers Inc., Warrendale, PA.

Belytschko, T. and Privitzer, E. 1978. Refinement and validation of a three-dimensional head-spine model. Wright-Patterson AF Base, OH: Aerospace Medical Research Laboratory. AMRL-TR-78-7.

Blüthner, R., Hinz, B., and Seidel, H. 1986. Zur Moglichkeit einer Abschatzung der Wirbelsaulenbeanspruchung durch Ganzkorpervibration unter experimentellen Bedingungen. On the possibility to estimate the mechanical strain of the lumbar spine caused by whole-body vibration under experimental conditions. Zeitschrift fur die Gesamte Hygiene. 2: 111-113.

Boileau, P.-E. 1988. Towards a new standard for evaluating exposure to whole-body vibration. In 12th Biennial Conference on Mechanical Vibration and Noise, 195-202. Montreal.

Boshuizen, H.C., Hulshof, C.T.J., and Bongers, P.M. 1990. Long-term sick leave and disability pensioning due to back disorders of tractor drivers exposed to whole-body vibration. International Archives of Occupational and Environmental Health. 62: 117-122.

Braunbeck, O.A. and Wilkinson, R.H. 1981. Simulation of human spine deformations for low amplitude sinusoidal excitation. Transactions of the American Society of Automotive Engineers, 76-1579: 9-13.

Brinkley J.W. 1971. Application of a biodynamic model to predict spinal injuries from use of aircraft ejection seats. AFSC Science and Engineering Symposium (Oct 5-7), Paper No. 711763.

Brinckmann, P. 1985. Pathology of the vertebral column. Ergonomics. 28: 77-80.

Brinckmann, P. 1988. Lumbar vertebrae. Clinical Biomechanics. 3(Suppl 1): S1-S23.

Brinckmann, P., Biggeman, M. and Hilweg, D. 1988. Fatigue fracture of juman lumbar vertebrae. Clinical Biomechanics. 4 (Supplement 2): S1-S23.

Brinckmann, P., Biggemann, M. and Hilweg, D. 1989. Prediction of the compressive strength of the human lumbar vertebrae. Clinical Biomechanics. 4(Supplement 2): S1-S27.

British Standards Institution. 1987. British Standards guide to measurement and evaluation of human exposure to whole-body mechanical vibration and repeated shock. London: British Standards Institution. BS 6841.

Cameron et al., 1995. Development of a Standard for the Health Hazard Assessment of Mechanical Shock and Repeated Impact in Army Vehicles: Phase 3. U.S. Army Aeromedical Research Laboratory, Contract Report No. CR-95-3.

Cameron, B., Morrison, J., Robinson, D., Vukusic, A., Martin, S., Roddan, G, and Albano, J.P. 1996. Development of a Standard for the Health Hazard Assessment of Mechanical Shock and Repeated Impact in Army Vehicles: Phase 4. U.S. Army Aeromedical Research Laboratory, Contract Report No. CR-96-1.

Carter, D.R., Caler, W.C., Spengler, D.M., and Frankel, V.H. 1981. Uniaxial Fatigue of Human Cortical Bone. The Influence of Tissue Physical Characteristics. Journal of Biomechanics. 14: 461-470.

Chaffin D.B. and Andersson, G.B.J. 1991. Occupational Biomechanics. 2nd Ed. John Wiley & Sons, Inc., New York.

Cholewicki, J., McGill, S., Norman, R.W. 1991. Lumbar spine load during the lifting of extremely heavy weights. Medical Science Sports Exercise. 23:1179-1186.

Coermann, R.R., Ziegenruecker, G.H., Wittwer, A.L., and Gierke, H.E. 1960. The passive dynamic mechanical properties of the human thorax-abdomen system and of the whole body system. Aerospace Medicine. 31: 443-455.

Demic, M. 1989. A contribution to identification of a non-linear biodynamic oscillatory model of man. International Journal of Vehicle Design. 10: 153-164.

Department of the Army. 1991. Health hazard assessment program in support of the army materiel acquisition decision process, Army Regulation 40-10, dated 15 September, 1983. Washington, DC.

Department of the Army. Basis of issue plans (BOIP). Qualitative and quantitative personnel reuirements information (QQPRI), Army Regulation 71-2, dated 15 June, 1982. Washington, DC.

Department of the Army. Army modernization training, Army Regulations 350-35, dated 3 September, 1985. Washington, DC.

Department of the Army. Systems safety engineering and management, Army Regulation 385-16, dated 3 September, 1985. Washington, DC:

Department of the Army. Manpower staffing standards system, Army Regulations 570-5, dated 15 April, 1984. Washington, DC.

Department of the Army. Human factors engineering program, Army Regulation 602-2, dated 17 April, 987. Washington, DC.

Donati, P., Grosjean, A., Mistrot, P., and Roure, L. 1983. The subjective equivalence of sinusoidal and random whole-body vibration in the sitting position (an experimental study using the 'floating reference vibration' method). Ergonomics. 26(3): 251-273.

Donati, P., and Bonthoux, C. 1983. Biodynamic response of the human body in the sitting position when subjected to vertical vibration. Journal of Sound and Vibration. 90 :423-442.

Dupuis, H. and Zerlett, G. 1987. Whole-body vibration and disorders of the spine. International Archives of Occupational and Environmental Health. 59: 323-336.

Fairley, T.E. and Griffin, J.J. 1989. The apparent mass of the seated human body: vertical vibration. Journal of Biomechanics. 22(2): 81-94.

Fairley, T.E. and Griffin, M.J. 1990. The apparent mass of the seated human body in the fore-and-aft and lateral directions. Journal of Sound and Vibration. 139: 299-306.

Fernandez, B., Parlos, A.G., and Tsai W.K. 1990. Nonlinear dynamic system identification using artificial neural networks (ANNs). International Joint Conference on Neural Networks, San Diego. 2: 133-141.

Fletcher, R. 1987 Practical Methods of Optimization. Wiley: New York.

Forshaw, S.E. and Ries, C. 1986. The assessment of transient vibration with respect to human exposure. Defence and Civil Institute of Environmental Medicine. DCIEM Report No. 86-R-07.

Fryer, D.I. 1961. Operational Experience with British Efection Seats. Flying Personnel Research Committee FPRC-1166.

Glaister, D.H. 1978. Human tolerance to impact acceleration. Injury. 9(3): 191-198.

Gozulov. S.A., Korzhen, Y., Skrupknik, V.G., and Sushkov, Y.N. 1966 Issledovaniye prochnosti poszonkov cheloveka na szhatiye. Arkiv Anatomii gistologii i empbiologii. 45-51.

Granhed, H., Jonson, R., Hansson, T. 1987. The loads on the lumbar spine during extreme weight lifting. Spine. 12(2): 146-149.

Griffin, M.J. 1990. Handbook of Human Vibration. London, England: Academic Press Ltd.

Griffin, M.J. and Whitham, E.M. 1980. Discomfort produced by impulsive whole-body vibration. Journal of the Acoustical Society of America. 68(5): 1277-1284.

Hall, L.C. 1987. Subjective response to combined random vibration and shock. Presented at UK Informal Group Meeting on Human Response to Vibration. Royal Military College of Science, Shrivenham.

Hansson, T. and Holm, S. 1991. Clinical implications of vibration-induced changes in the lumbar spine. Orthopedic Clinics of North America. 22: 247-253.

Hansson, T., Keller, T.S., and Spengler, D.M. 1987. Mechanical behavior of the human lumbar spine. II. Fatigue strength during dynamic compressive loading. Journal of Orthopedic Research. 5: 479-487.

Henzel, J.H., Mohr, G.C., and von Gierke, H.E. 1968. Reappaisal of biodynamic implications of human ejections. Aerospace Medicine. 39: 231-240.

Heselgrave, R.J., Frim, J., Bossi, L.L. and Popplow, J.R. 1990. The psychological, physilogical and performance impact of sustanined NB operations of fighter pilots. Defence and Civil Institute of Environmental Medicine. report 90-RR-08.

Hinz, B., Bluthner, R., Menzel, G., and Seidel, H. 1994. Estimation of disc compression during transient whole-body vibration. Clinical Biomechanics. 9: 263-271.

Hinz, B. and Seidel, H. 1989. The nonlinearity of the human body's dynamic response during sinusoidal whole body vibration. Industrial Health. 25: 169-181.

Hirsch, C. and Nachemson, A. 1961. Clinical observation of the spine in ejected pilot. Acta Orthopaedica Scandinavica 31.2.

Hoddinott, J.C. 1986. Investigation of the effect of duration on alternative methods of assessing human reponse to impulsive motion, 1-9. In United Kingdom Informal Group Meeting on Human Response to Vibration. Loughborough, University of Technology.

Holm, S. and Nachemson, A. 1983. Variations in the nutrition of the canine intervertebral disc induced by motion. Spine. 8(8): 866-873.

Hopfield, J.J. 1982. Neural Networks and physical systems with emergent collective computational abilities. In Proceedings of the National Academy of Science, U.S. 79: 2554-2558.

Hopkins, G.R. 1972. Nonlinear lumped parameter mathematical model of dynamic response of the human body. Wright-Patterson AF Base, OH: Aerospace Medical Research Laboratory. AMRL-TR-71-29:649-669.

Hulshof, C. and van Zanten, B.V. 1987. Whole-body vibration and low-back pain. International Archives of Occupational and Environmental Health. 59: 205-220.

Hutton, W.C., and Adams, M.A. 1982. Can the lumbar spine be crushed in heavy lifting? Spine. 7(6): 586-590.

International Organization for Standardization. 1974. ISO 2631 (1974): Guide to the evaluation of human exposure to whole-body vibration. ISO Standards 2631.

International Organization for Standardization. 1985. ISO 2631 1985. Guide for the evaluation of human exposure to whole-body vibration, Part 1. ISO 2631/1-1985

International Organization for Standardization. 1995. Mechanical Vibration and shock - Evaluation of human exposure to whole-body vibration - Part 1. Draft International Standard ISO/DIS 2631-1.2.

Jones, W.L., Madden, W.F., and Luedeman, G.W. 1964. Ejection seat accelerations and injuries. Aerospace Medicine. 35: 559-562.

Kanda, H., Murayama, Y., Tanaka, M., and Suzuki, K. 1982. Ergonomical Evaluation Methods of Repeated Shocks and Vibrations on High Speed Ships (Final Report). Journal of Japan Institute of Navigation. 67: 35-67.

Kazarian, L., and Graves, G.A. 1977. Compressive strength characteristics of the human vertebral centrum. Spine. 2: 1-14.

Kraemer, J., Kolditz, D., and Gowin, R. 1985. Water and electrolyte content of human intervertebral discs under variable load. Spine. 10(1): 69-71.

Lafferty, J.L. 1978. Analytical Model of the Fatigue Characteristics of Bone. Aviation Space and Environmental Medicine. 49: 170-174.

Larson, C., Well, B., and Kaplan, B. 1973. Study of flight environment effects on helicopter gunners. United States Army Aeromedical Research Laboratory. Report 73-15.

Laurell, L., and Nachemson, A. 1963. Some factors influencing spinal injuies in seated ejected pilots. Aerospoze Medicine. 34: 726.

Liebracht, B. 1990. Health hazard assessment primer. Fort Rucker, AL: U.S. Army Aeromedical research Laboratory. USAARL Report No. 90-5.

Markolf, K.L. 1970. Stiffness and damping characteristics of the thoracolumbar spine. In Proceedings of workshop on bioengineering approaches to problems of the spine, 87-143. Bethesda, Md: National Ministry of Health.

Markolf, K.L. and Steidel, R.F. Jr. 1970. The dynamic characteristics of the human intervertebral joint. Annual Meeting of the American Society of Mechanical Engineers. ASME, New York: 1-11.

Mil-Std 1472. Human engineering design criteria for military ststem, equipment and facilities. Washington, DC: Department of the Army.

Miner, M.A. 1945. Cumulative Damage in Fatigue. Journal of Applied Mechanics. 12: 159-164

Morrison, J.B., Robinson, D.G., Roddan, G., Nicol, J.J., Butler, B.P. 1995 Analysis of vertebra to skin transfer function in response to mechanical shocks. Proceedings of the United Kingdom Informal Group Meeting on Human Response to Vibration, Bedford, U.K.

Muksian, R. and Nash, C.D. 1974. A model for the response of seated humans to sinusoidal displacements of the seat. Journal of Biomechanics. 7: 209-215.

Myklebust, J., Sances, A., Maiman, D., Pintar, F., Chilbert, M., Rauschning, W., Larson, S., Cusick, J., Ewing, C., Thomas, D., and Saltzberg, B. 1983. Experimental spinal trauma studies in human and monkey cadaver. Society of Automotive Engineers. 831614: 149-161.

Narendra,K.S. and Parasarathy,K. 1990. Identification and control of dynamical systems using neural networks. IEEE Transactions on Neural Networks. 1(3): 4-27.

National Institute for Occupational Safety and Health 1981. Work practices guide for manual lifting. Technical Report 81-122, NIOSH, Cincinnati.

Nicol, J.J. 1996. Modeling the dynamic response of the human spine to mechanical shock and vibration using an artificial neural network. Master's thesis, Simon Fraser University.

Orne, D. 1969. A mathematical model of spinal response to impact. PhD Dissertation. University of Michigan.

Orne, D. and Liu, Y.K 1971. A mathematical model of spinal response to impact. Journal of Biomechanics. 4: 49-71.

Panjabi, M.M., Anderson, G.B.J., Jorneus, L., Hult, E., and Mattsson, L. 1986. In vivo measurements of spinal column vibrations. Journal of Bone and Joint Surgery. 68: 695-702.

Payne ,P., Brinkley, J.W., and Sandover J. 1994. Shock discomfort - a comparison of approaches. UK Group Meet on Human Response to Vibration. Alverstoke, Hants, UK: Institute of Naval Medicine.

Payne, P.R. 1965. Personnel restraint and support system dynamics. Wright-Patterson AF Base, OH: Aerospace Medical Research Laboratory. AMRL-TR-65-127: 1-112.

Payne, P. 1968. Injury Potential of Ejection Seats. Journal of Aircraft. 6(3): 273-278.

Payne, P. 1975. Spinal Injury in the Crash Environment. Aircraft Crashworthiness. 1: 273-298.

Payne, P. 1976. On quantitizing ride comfort and allowable acceleration, AIAA 76-873. Paper presented at the American Institue of Aeronatuics and Astronauts/Society of the Naval Architects and Marine Engineers Conference on Advanced Marine Vehicles, September, at Arlington, Virginia.

Payne, P. 1978. Method to Quantify Ride Comfort and Allowable Accelerations. Aviation Space and Environmental Medicine. 49: 262-269.

Payne, P.R. 1984. Linear and angular short duration acceleration allowables for the human body. Detron Inc., Arlington, VA: KTR 357-84.

Payne, P.R. 1991. A Unification of the ASCC and ISO Ride Comfort Methodologies, 1-24. Unpublished report, Payne Associates, Severna Park, Md.

Payne, P.R. 1992. A Unification of the ASCC and ISO Ride Comfort Methodologies, 377-3-R2. Unpublished report, Payne Associates, Severna Park, Md.

Payne, P.R. 1996. A ride comfort study. Unpublished report, Payne Associates, Severna Park, Md.

Pearsall, D.J., Reid, J.G., and Livingston, L.A. 1996. Segmental inertial parameters of the human trunk as determined from computed tomography. Annals of Biomedical Engineering. 24(2): 198-210.

Perey, O. 1957. Fracture of the vertebral end plate in the lumbar spine. Acta Orthopaedica Scandinavica. 25(Suppl):

Porter, R.W., Adams, M.A., and Hutton, W.C. 1989. Physical activity and the strength of the lumbar spine. Spine. 14(2): 201-203.

Prasad, P., King, A.I., and Ewing, C.L. 1974. The role of articular facets during +G_Z acceleration. Journal of Applied Mechanics. 41: 321-326.

Prasad, P., King, A.I. 1974. An experimental validated dynamic model of the spine. Jounal of Applied Mechanics. 41: 546-550.

Rizzi, M.A., Whitman, A.B., and DeSilva, C.N. 1975. A mathematical model of the spine based on mixture theory of directed cureves. Acta Mechanica. 21: 241-260.

Robinson, D.G., Morrison, J.M., and Cameron, B.J. 1995. The contribution of muscle response and internal pressure to estimation of spinal compression from mechanical shocks using a simple biomechanical model. In Human Response to Vibration, September 18-20, Bedford, England.

Roddan, G., Brammer, T., Village, J., Morrison, J., Remedios, B., Brown, D. 1995. Development of a Standard for the Health Hazard Assessment of Mechanical Shock and Repeated Impact in Army Vehicles: Phase 2. U.S. Army Aeromedical Research Laboratory, Contract Report No. CR-95-2.

Ruff, S. 1950, Brief Acceleration: Less than one second. pp. 584-597. In German Aviation Medicine, World War II. Washington, D.C.: U.S. Govt. Printing Office.

Sandover, J. 1979. A standard on human response to vibration - one of a new breed? Applied Ergonomics. 10(1):33-37.

Sandover, J. 1981. Vibration, posture and low-back disorders of professional drivers (part 1). Department of Health and Social Security DHS 402: 1-141.

Sandover, J. 1982. Measurement of the frequency response characteristics of man exposed to vibration. Department of Human Sciences,Loughborough University of Technology 1-138.

Sandover, J. 1983. Dynamic loading as a possible source of low-back disorders. Spine. 8: 652-658.

Sandover, J. 1986a. Vehicle vibration and back pain. pp. 13-1-13-8. In Advisory Group for Aerospace Research & Development Conference Proceedings No. 378 on Backache and Back Discomfort. Pozzuoli, Italy: North Atlantic Treaty Organisation.

Sandover, J. 1986b. Vibration and people. Clinical Biomechanics. 1: 150-159.

Sandover, J. 1988. Behaviour of the spine under shock and vibration: a review. Clinical Biomechanics. 3: 249-256.

Seidel, H., Blüthner, R., and Hinz, B. 1986. Effects of sinusoidal whole-body vibration on the lumbar spine: the stress-strain relationship. International Archives of Occupational and Environmental Health. 57: 207-223.

Shirazi-Adl, A. 1994. Biomechanics of the lumbar spine in sagittal/lateral moments. Spine. 19(21): 2407-2414.

Sinha, N.K. and Kuszta, B. 1983. Modeling and Identification of Dynamic Systems. New York, Van Nostrand Reinhold Company.

Smeathers, J.E. 1989. Measurement of transmissibility for the human spine during walking and running. Clinical Biomechanics. 4: 34-40.

Society of Automotive Engineers. 1974. Measurement of whole body vibration of the seated operator of agricultrural equipment (The Society of Automotive Engineers recommended practice). The Society of Automotive Engineers SAE J1013. Handbook part 11. 1404-1407. SAE, Detroit, Michigan.

Soechting, J.F. and Paslay, P.R. 1973. A model for the human spine during impact including musculature influence. Journal of Biomechanics. 6: 195-207.

Stech, E.L. 1963. The variability of human response to acceleration in the spinal direction. Frost Engineering Development Corporation. 122-109.

Stech, E.L., and Payne, P.R. 1963. Vertebral breaking strength, peinal frequency and tolerance to acceleration in human beings. Frost Engineering Development Corporation 122-101.

Village, J. and Morrison, J. 1989. Exposure of heavy equipment operators to whole body vibration and repeated shock. 89-96. In Proceedings of the Annual Conference of the Human Factors Association of Canada. Toronto.

Village, J., Rylands, J., and Morrison, J. 1993. Development of a dose-effect database for exposure to whole-body vibration: problems and assumptions. In Proceedings of the Human Factors Association of Canada. Halifax.

Village, J., Morrison, J., Robinson, D., Roddan, G, Rylands, J., Cameron, B., Remedios, B., Brown, D., and Butler, B.P. 1995. Development of a Standard for the Health Hazard Assessment of Mechanical Shock and Repeated Impact in Army Vehicles: Phase 3, Pilot Tests. U.S. Army Aeromedical Research Laboratory, Contract Report No. CR 95-3.

Vukusic, A.V., Morrison, J.B., Springer, M.J-N., Robinson, D.G., and Cameron, B.J. 1995. Comparison of subjective responses to repeated mechanical shocks with dose response functions and biodynamic models. Paper presented at Proceedings of the UK informal group meeting on Human Response to Vibration, September at Nuneaton, UK.

Weightman, B. 1976. Tensile fatigue of human articular cartilage. Journal of Biomechanics. 9: 193-200.

Wilkström, B-O., Kjellberg, A. and Landstrom, U. 1994. Health effects of long-term occupational exposure to whole-body vibration: A review. International Journal of Industrial Ergonomics. 14: 273-292.

Yamada, H. 1970. Strength of biological materials. Baltimore: Williams and Wilkins.

Appendix G

Glossary

$\ddot{\theta}_3$	angular acceleration at the lumbar segment
θ_3	flexion/extension angle of lumbar segment
Θ	set of model parameters
ϕ_3	lateral angle of lumbar segment
ζ	critical damping ratio
δ	peak spring deflection (DRI model)
ε	error
χ	calculated dose
Φ	probability of injury
τ	integration time variable
σ	standard deviation of Cz_u
ω	undamped natural frequency ($rad \cdot s^{-1}$)
$\in$	subset
Σ	summation
+x	positive x axis vibration or shock according to biodynamic convention: forward (ISO 2631,1985)
+y	positive y axis vibration or shock according to biodynamic convention: to left (ISO 2631,1985)
+z	positive z axis vibration or shock according to biodynamic convention: upward (ISO 2631,1985)
-x	negative x axis vibration or shock according to biodynamic convention: backward (ISO 2631,1985)

-y	negative y axis vibration or shock according to biodynamic convention: to right (ISO 2631,1985)
-z	negative z axis vibration or shock according to biodynamic convention: downward (ISO 2631,1985)
%	percent
>	greater than
<	less than
AFB	air force base
ANN	artificial neural networks
AR	Army Regulation
ARX	autoregressive model with exogenous inputs
ASCC	Air Standardization Coordinating Committee
a	acceleration
a(t)	BS 6841 frequency weighted acceleration
a_i, and b_i	system model coefficients
$a_{w\,1}$, $a_{w\,2}$	ISO 2631-1 weighted rms magnitude of vibration for periods 1 and 2
a_w (t)	frequency weighted rms acceleration in $m \cdot s^{-2}$
a_w (t)	ISO 2631-1 weighted instantaneous acceleration
b	horizontal distance from L3/L4 joint
B	upper body mass
BS	British Standard (associated with the British Standard Institution)
BSI	British Standards Institution
BCRI	B.C. Research Inc.
C	compressive load

C1	first cervical vertebrae
C7	seventh cervical vertebrae
Cx	antero-posterior shear forces at the L4/L5 joint
Cy	lateral shear forces at the L4/L5 joint
Cz	compressive forces at the L4/L5 joint
Cz_i	compressive force obtained from biomechanical model in response to the i^{th} shock
Cz_u	ultimate compressive strength of lumbar L4/L5 joint, mean of dose distribution
Cz_e	accumulated compressive force dose
Δ	fractional degree of fatigue of a material
di	vertical position of segment i
DIS	Draft International Standard
DRI	Dynamic Response Index; a prediction of spinal stress
DRI_e	Dynamic Response Index dose function
DSE	duration of safe exposure
EMG	electromyography
erf	error function
ESMM	Eccentric Segregated Mass Model
eVDV	estimated Vibration Dose Value
F_c	lumbar spine compressive force
F_{ext}	extensor muscle force
F_{flex}	flexor muscle force
f	frequency

fn	natural frequency
FIR	finite impulse response
F_n	compressive force at segment n in a multi-segment model
F_p	force exerted by abdominal pressure
FFNN	feed forward neural networks
g	acceleration due to gravity (9.81 $m \cdot s^{-2}$)
GUI	graphical user interface
G(x)	non-linear transformation of x
Gz	vertical acceleration
h	hours
HHA	health hazard assessment
HHAM	health hazard assessment method
HHAR	Health Hazard Assessment Report
Hz	Hertz
i	shock
IEMG	integrated electromyography
IIR	infinite impulse response
IHHAR	Initial Health Hazard Assessment Report
IMP	imperial units
IRED	infra-red emitting diodes
ISO	International Organization for Standardization
kN	kilonewtons
L	ligament tension (anterior or posterior)

l	estimated moment arm of anterior and posterior ligaments
L1	first lumbar vertebrae
L2	second lumbar vertebrae
L3	third lumbar vertebrae
L4	fourth lumbar vertebrae
L5	fifth lumbar vertebrae
l and m	in system identification theory, the input and output model orders (the number of previous inputs and outputs used to predict a given output)
LT2	long term experiment 2, Phase 4
LT3	long term experiment 3, Phase 4
LT4	long term experiment 4, Phase 4
M	muscle force
m	meters
m_i	soft tissue masses
m_{app}	apparent mass
$M_{L4/L5}$	net muscle moment at L4/L5 joint
M_x	moment in sagittal plane relative to L4/L5 joint center
M_p	moment associated with intra abdominal pressure
M_y	moment in coronal plane relative to L4/L5 joint center
MA	moving average
MANPRINT	Manpower and Personnel Integration
MARS	Multi Axis Ride Simulator, Fort Rucker, Alabama

MB	megabytes
MIL-STD	Military Standard
min	minutes
mph	miles per hour
MRI	magnetic resonance imaging
$m.s^{-2}$	meters per second squared; units of acceleration
msec	milliseconds
N	number of data samples
N	Newtons, unit of force
No.	number
n(t)	measurement noise
n_I	number of cycles completed at stress level Si
N_I	number of cycles required to cause failure at stress level Si
NIOSH	National Institute for Occupational Safety and Health
P	intra-abdominal pressure
p	equivalent moment arm for intra-abdominal pressure
P	a mathematical operator describing system behavior
$\hat{P}$	a mathematical operator predicting system behavior
PEs	processing elements
r(t)	unobservable system output
RAC	Risk Assessment Code as per AR 40-10
rad	radians
rmd	tenth power root mean

rms	root mean squared
rmse	root mean squared error
rmq	root mean quad
RNN	recurrent neural network
$R_{x,y,z}$	force at the L4/L5 joint in absolute coordinates
R^2	correlation coefficient squared
s	seconds
S_e	equivalent static stress level
S_u	static failure stress
S_i	applied cyclic stress level
S1	first sacral vertebrae
SA	cross-sectional area of abdomen
SAE	Society of Automotive Engineers
SISO	single input, single output
ST1	Short Term 1
Std. dev.	standard deviation
t	time
T_1, T_2	exposure time for periods 1 and 2
T1	first thoracic vertebrae
T2	second thoracic vertebrae
T3	third thoracic vertebrae
T4	fourth thoracic vertebrae
T5	fifth thoracic vertebrae
T6	sixth thoracic vertebrae

T8	eighth thoracic vertebrae
T9	ninth thoracic vertebrae
T10	tenth thoracic vertebrae
T12	eleventh thoracic vertebrae
tanh	hyperbolic target
TGVs	tactical ground vehicles
TOP	test operations procedures
u(t)	input signal (measured)
U	input space mapped by P
USAARL	United States Army Aeromedical Research Laboratory
v	angle between spinal axis and vertical at L3/L4 level
VDV	Vibration Dose Value; defined in BS 6841 (1987)
$W_{b, c, d, e, f, g}$	ISO and BS frequency weighting factors
W_j/w_j	weighting factor
w(t)	system noise
w0 … wn	scalar gain factors (weighting factors) in a neural network
WBV	whole-body vibration
y(t)	output data (measured from a system)
y(t), y_p	output data (predicted from a system)
yr	year